Reversion of Taxane Resistance through PRMT5 Inhibition in Castration-Resistant Prostate Cancer

by

Naz Uzunalioğlu

A Dissertation Submitted to the
Graduate School of Health Sciences
in Partial Fulfillment of the Requirements for
the Degree of

Master of Science

in

Cellular and Molecular Medicine

August 25, 2023

ABSTRACT

Reversion of Taxane Resistance through PRMT5 in Castration-Resistant Prostate Cancer

NAZ UZUNALİOĞLU

Master of Science in Cellular and Molecular Medicine

August 25, 2022

The most common cancer in men is prostate cancer (PCa), and the first-line treatment for PCa is the surgical intervention of the tumor and/or chemical castration and radiotherapy. Despite the initial efficacy of this treatment, a stage known as castration-resistant prostate cancer (CRPCa) is eventually reached by a majority of patients within 2 to 3 years. At this stage, chemotherapeutic drugs like taxanes (such as Docetaxel and Cabazitaxel) are considered as treatment options. However, a significant clinical challenge emerges withathe development of drug resistance over time. Epigenetic regulation in cancer has a significant impact on tumor development and progression, as well as chemotherapy resistance. Therefore, targeting epigenetic mechanisms emerges as a promising strategy to prevent drug resistance.

Previously, CRPCa cell lines resistant to Dtx and Cbz were generated to identify potential epigenetic targets that could overcome resistance. The Epigenetic Drug Library screen was conducted to uncover the reversing effects of epigenetic modifiers on resistance mechanism. In this thesis, the screen revealed Protein Arginine Methyltransferase 5 (PRMT5) as a re-sensitizer to taxane treatment. RNA sequencing analyses revealed that PRMT5 silencing led to the negative enrichment of four signaling pathways, including MYC, E2F, and G_2/M. Indeed, MYC inhibition led to a stronger suppression of growth in resistant cells contrast to parental cells. Furthermore, the treatment of resistant cell lines with PRMT5 inhibitors induced cell cycle arrest in the G_2/M phase, suggesting the restoration of taxane susceptibility. This effect was accompanied by an increase in apoptotic markers (Caspase 3/7 activation and Annexin-V staining). Pharmacological inhibition of PRMT5 reduced ABCB1 activity, as determined by the Calcein efflux assay, indicating that PRMT5 may be involved in an efflux-related mechanism. These results offered valuable insights into potential avenues

for addressing taxane resistance in CRPCa treatment, paving the way for the development of more effective therapeutic strategies.

Anahtar Kelimeler: PRMT5, taxane resistance, castration resistant prostate cancer, epigenetics

ÖZETÇE

PRTM5 Proteininin Prostat Kanserinde Taksan Direncine Karşı Etkinin İncelenmesi

NAZ UZUNALİOĞLU

Hücresel ve Moleküler Tıp, Yüksek Lisans

25 Ağustos 2023

Erkeklerde en yaygın kanser prostat kanseri (PCa) olup ilk tercih edilen tedavi yöntemleri arasında, cerrahi müdahale, kastrasyon ve radyoterapi yer almaktadır. Bu tedaviler başlangıçta bir etkinliğine sahip olmasına rağmen, çoğu hasta 2 ila 3 yıl içerisinde kastrasyon direnci prostat kanseri (CRPCa) olarak adlandırılan prostat kanserinin en agresif aşamasına ilerler. Bu aşamada, Dosetaksel ve Kabazitaksel gibi kemoterapötik ilaçlar tedavi seçenekleri olarak düşünülür. Ancak, zamanla ilaç direncinin gelişmesiyle de tedavi yöntemleri kısıtlanmaktadır. Kanserde epigenetik düzenlemenin, tümör gelişimi ve ilerlemesinin yanı sıra kemoterapi direnci üzerinde de önemli bir etkisi vardır. Bu nedenle epigenetik mekanizmaların hedeflenmesi, ilaç direncinin önlenmesi için umut verici bir strateji olarak ortaya çıkmaktadır.

Daha önceki çalışmalarda dirence karşı gelebilecek potansiyel epigenetik hedefleri belirlemek amacıyla Dosetaksel ve Kabazitaksel'e dirençli CRPCa hücre hatları oluşturulmuş olup Epigenetik İlaç Kütüphanesi epigenetik modülatörlerin direnç mekanizması üzerindeki ters etkilerini ortaya çıkarmak için uygulanmıştır. Bu tezde, Epigenetik ilaç kütüphanesi Protein Arjinin Metiltransferaz 5 (PRMT5)'in taksana dirençli hücre hatlarını tekrardan taksan tedavisine duyarlı hale getirildiği ortaya koyulmuştur. Kullanılan PRMT5 inhibitörleri CRPCa hücre hatlarında direnci geri çevirici özellikleri başarılı bir şekilde koloni oluşturma özellikleri ile vurgulanmış olup RNA dizileme analizleri ile de PRMT5 ekspresyonunun azalması MYC, E2F ve G2/M dahil olmak üzere üç sinyal yolunun negatif zenginleşmesine yol açtığı gösterilmiştir. Daha sonrasında MYC inhibisyonunun, dirençli hücrelerin büyümesini parental hücrelere kıyasla daha güçlü bir şekilde bastırdığı gözlemlenmiştir. Ayrıca, PRMT5 inhibitörleri ile dirençli hücre hatlarının tedavisi, G2/M fazında hücre bölünmesininde durdurucu etki göstererek taksana duyarlılığını yeniden sağlandığı düşünülmüştür. Bu etki, apoptotik

belirteçlerin artışıyla (Kaspaz 3/7 aktivasyonu ve Annexin-V boyaması) birlikte desteklenmiştir. Ek olarak, PRMT5'in farmakolojik inhibisyonu, Calcein-AM deneyi ile ABCB1 aktivitesini azalttığını, bunun da PRMT5'in hücre membranında akış pompa mekanizmasında yer alabileceğini göstermektedir. Bu sonuçlar, CRPCa tedavisinde taksan direnciyle başa çıkmak için potansiyel olanaklar hakkında değerli öngörüler sunarak, daha etkili terapötik stratejilerin geliştirilmesinin yolunu açmaktadır.

Anahtar Kelimeler: PRMT5, taxane resistance, castration resistant prostate cancer, epigenetics

ACKNOWLEDGEMENTS

I would like to convey my heartfelt appreciation to all who have provided their support and contributions towards the successful culmination of my thesis. Foremost, I extend my gratitude to Prof. Ceyda Açılan Ayhan, my advisor, for her guidance, mentorship, and unwavering backing throughout this research endeavor. Additionally, I would like to express my profound thanks to Dr. Buse Cevatemre, whose expertise, encouragement, and invaluable feedback have significantly influenced this study of my scholarly pursuits.

I extend profound gratitude to Professor Tuğba Bağcı Önder, Asst. Prof. Nihal Terzi Cizmecioğlu, and all esteemed faculty members and professors whose invaluable expertise and profound insights have played a pivotal role in the advancement and refinement of my research endeavors. Additionally, this master thesis was funded by Koç University Seed Funding supported by Buse Cevatemre, Ph.D. Thus, I would like to present deepest gratitude to her during this project once again.

I express my heartfelt gratitude to Hande Özkan and Barış Sergi for embellishing my university experience with their invaluable support and guidance during the laboratory activities. Their attentive listening, delightful companionship, and timely assistance during challenging times have been truly instrumental in making my time in the laboratory a pleasurable and fruitful journey.

I extend profound gratitude to my family, whose unwavering presence, unwavering support, and invaluable guidance have been constant pillars of strength throughout my journey. They have generously shared their wisdom and experiences, and their unwavering belief in me has continuously propelled me forward, even in times of adversity. Moreover, I wish to express my sincere appreciation to Ayşe Berfin Güney, whose unyielding faith in me has been a driving force, inspiring me to strive for higher achievements. Finally, I would like to express my highest gratitude to Serap Özer for her sponsorship, along with my colleagues at Analitik Kimya company for providing me a supportive environment.

Naz Uzunalioğlu

TABLE OF CONTENTS

List of Tables 9
List of Figures 10
Abbreviations 12
Chapter 1: Introduction 1
1.1. Prostate Cancer 1
1.2. Castration Resistant Prostate Cancer (CRPCa) 1
1.3. The Therapeutic Drugs: Taxanes 2
1.3.1. Docetaxel 3
1.3.2 Cabazitaxel 3
1.4. Drug Resistance in PCa 4
1.4.1 Taxane Resistance 5
1.4.2. Taxane Resistance Reversal in CRPCa 7
1.5. Epigenetics 7
1.5.1. Epigenetic Writers: PRMTs 8
1.5.2. Association between PRMTs and Cancer 8
1.6. The Role of PRMT5 9
1.6.1. Association between PRMT5 and Cancer 10
1.7. Aim of this thesis 12
Chapter 2: Material and Method 13
2.1. Cell Culture and Reagents 13
2.4. Crystal Violet Colony Formation Assay 14
2.5. Doubling Time Assay 14
2.6. Epigenetic Drug Library Screening 15
2.7. siRNA-mediated Gene Knock-out 15
2.8. CRISPR-mediated Gene Knock-Out 15
2.9. RNA Isolation 17
2.10. cDNA Synthesis 17
2.11. Quantitative Real Time PCR (qRT-PCR) 17
2.12. Protein Isolation and Quantification of Protein Concentration (BCA Assay)
2.13. Histon extraction 19
2.14. Nuclear/Cytosolic Isolation 19
2.15. Western Blotting 20
2.16. Cellular Thermal Shift Assay (CETSA) 20
2.17. Calcein-AM Assay 20
2.18. RNA sequencing and Analysis 22
2.19. Annexin-V Staining Flow Cytometry Assay 23
2.20. Caspase 3/7 Activation Flow Cytometry Assay 23
2.21. Cell Cycle Analysis 24
2.22. Immunofluorescence (IF) Staining 24
2.23. Cell Cycle Arrest 25
2.24. Statistical Analysis 25
Chapter 3: Results 23
3.1. Generation of Taxane Resistant CRPCa Cell Models 23

3.2. The Effect of Taxane Resistance on Cell Proliferation 25
3.3. The Reversion of Resistance via PRMT5 Inhibition in CRPCa 26
3.3.1. Epigenetic drug library screening identifies PRMT5 as a re-sensitizer to taxanes 26
3.3.2. The effect of PRMT5 knock-down on clonogenic capacity of cells 31
3.3.3. The effect of PRMT5 Silencing on the Proliferation of Taxane-Sensitive and Resistant Cells 35
3.4. Characterization of PRMT5 Inhibitors 36
3.4.1. The effect of PRMT5 inhibitors on sDMA 36
3.4.2. Evaluation of Target Engagement of PRMT5 Inhibitors by CETSA 37
3.5. The Underlying Cause of Resistance: ABCB1 39
3.6. Transcriptomic Changes upon PRMT5 Inhibition 44
3.6.1. RNA Sequencing after PRMT5 knock-down 44
3.6.2. Validation of RNA Sequencing 49
3.7. Cell Cycle Arrest Caused by The Pharmacological Inhibition of PRMT5 53
3.8. PRMT5 Inhibition with Taxanes Induced Apoptosis in Du145 Resistant Cell Lines 56
3.8.1 Annexin V Staining 56
3.8.2 Caspase 3/7 Staining 59
3.9. Cellular Localization of PRMT5 in Du145 Parental and Taxane Resistant Cells 67
3.9.1. PRMT5 Selectively Localizes to Cytosol in Both Parental and Taxane Resistant Du145 Cells 67
3.9.2 PRMT5 Co-Localizes to Centrosomes in a Cell Cycle-Dependent Manner 68
Chapter 4: Discussion and Conclusion **76**
4.1. Summary of Principal Discoveries 77
4.2. Contrasting Findings with Prior Research 81
4.3. Contribution of Results for Drug Resistance in CRPCa 82
4.4 Future Perspectives 83
4.5. Conclusion 84
Bibliography 86

LIST OF TABLES

Table 2.1. Oligonucleotide sequences used for this study.

Table 2.2. qRT-PCR primers specific to PRMT5 and housekeeping genes GAPDH and ACTB.

Table 2.3. DEGs from RNA-seq hit and specific primer sequences

Table 3.1. Comparison of the IC50 values and relative resistance of Dtx/Cbz resistant cells.

Table 3.2. The identification of DEGs from RNA Sequencing.

LIST OF FIGURES

Figure 1.1. A schematic illustration of the taxane's mechanism of action.
Figure 1.2. The chemical structures of (A) Docetaxel, and (B) Cabazitaxel.
Figure 1.3. Illustration of development of taxane resistance in PCa.
Figure 1.4. A schematic illustration of PRMT5 symmetrically dimethylates histones.
Figure 1.5. Functional domains of PRMT5.
Figure 1.6. PRMT5 overexpression led to the development of cancer.
Figure 3.1. Establishment and characterization of taxane resistant cells.
Figure 3.2. Difference in proliferation capacities of Du145-P and Du145-DtxR cells.
Figure 3.3. Epigenetic drug library screening on Du145-DtxR cells.
Figure 3.4. Inhibition of PRMT5 exerts an effect of overcomed taxane resistance.
Figure 3.5. Pharmacological inhibition of PRMT5 affects the clonogenic capacity of taxane-resistant cells.
Figure 3.6. Colony formation capacity of Du145 cells after PRMT5 knock-down.
Figure 3.7. Quantification clonogenic capacity of cells after PRMT5 knock-down.
Figure 3.8. Clonogenic capacity of cells after CRISPR-Cas9-mediated knock-out of PRMT5.
Figure 3.9. The effect of PRMT5 knock-down on cell proliferation in taxane sensitive and resistant cells.
Figure 3.10. The sDMA modified target protein levels upon treatment with the PRMT5 inhibitors in Du145 parental and taxane resistant cells.
Figure 3.11. The sDMA modified histone levels upon treatment with the PRMT5 inhibitors in Du145 parental and taxane resistant cells.
Figure 3.12. The sDMA modified target protein expression levels upon siRNA-mediated PRMT5 knock-down on Du145-P and Du145-DtxR cells.
Figure 3.13. The effect of PRMT5 inhibitor GSK591 on target engagement and PRMT5 expression in Du145 cells.
Figure 3.14. ABCB1 overexpression in taxane resistant cells.
Figure 3.15. Calcein uptake assay in parental and resistant cells upon PRMT5i treatment.
Figure 3.16. The change in ABCB1 expression after PRMT5 silencing.
Figure 3.17. RNA sequencing analysis revealed the top enriched GSEA pathways.
Figure 3.18. RNA sequencing analysis confirms the knock-down of PRMT5.

Figure 3.19. Analysis of shared genes between Du145-DtxR/Du145-P and siPRMT5/siCtrl on Du145 DtxR cells.
Figure 3.20. Heatmap of validation of down-regulated genes in siPRMT5/siCtrl on Du145-DtxR cells.
Figure 3.21. Change in MYC and PRMT5 expressions after siPRMT5 in Du145-DtxR.
Figure 3.22. The effect of MYC silencing on clonogenic capacity of Du145-P and Du145-DtxR cells.
Figure 3.23. The distribution of cell cycle phases upon PRMT5 inhibition by flow cytometry.
Figure 3.24. Annexin V staining flow cytometry on Du145 resistant cells shows an increased apoptosis after combinatorial treatment.
Figure 3.25. Annexin V staining flow cytometry on Du145 resistant cells shows an increased apoptosis after combinatorial treatment.
Figure 3.26. Nuclear and cytosolic localization of PRMT5 protein in Du145-P and Du145-DtxR cells.
Figure 3.27. PRMT5 localizes centrosomes in cell cycle specific manner.
Figure 3.28. PRMT5 localizes centrosomes in metaphase in various cancer cells.
Figure 3.29. The confirmation of cell cycle arrest upon double thymidine block (DTB), STLC, and colcemid treatments by flow cytometry.
Figure 3.30. PRMT5 localizes centrosomes on cell cycle arrested U2OS cells.
Figure 3.31. Localization of PRMT5 to centrosomes after PRMT5 overexpression on U2OS cancer cells.
Figure 3.32. Co-staining of PRMT5 and y-tubulin and evaluation of PRMT5 localization after PRMT5 siRNA silencing.
Figure 4.1. A schematic model of PRMT5 inhibition effect on taxane resistant CRPCa.

ABBREVIATIONS

ABC	Atp Binding Cassette
ADT	Androgen Deprivation Therapy
AR	Androgen Receptor
ATP	Adenosine Triphosphate
AUC	Area Under The Curve
BCA	Bicinchoninic Acid
BSA	Bovine Serum Albumin
CBP	CREB-Binding Protein
CBZ	Cabazitaxel
CBZ-R	Cabazitaxel-Resistant
CR	Castration Resistance
CREB	Camp-Response Element Binding Protein
CRISPR	Clustered Regularly Interspaced Short Palindromic Repeats
CRPCa	Castration Resistant Prostate Cancer
DEG	Differentially Expressed Gene
DMEM	Dulbecco's Modified Eagle Medium
DMSO	Dimethyl Sulfoxide
DNA	Deoxyribonucleic Acid
DNMT	DNA (Cytosine-5)-Methyltransferase
DTX	Docetaxel
DTX-R	Docetaxel-Resistant
EGF	Epidermal Growth Factor
EMT	Epithelial-Mesenchymal-Transition
EPC	Enhancer Of Polycomb
ES	Enrichment Scores
EZH	Enhancer Of Zeste Homolog
FBS	Fetal Bovine Serum
FC	Fold Change
FDR	False Discovery Rate
FOSL	Fos-Related Antigen
FRET	Fluorescence Resonance Energy Transfer
GAPDH	Glyceraldehyde-3-Phosphate Dehydrogenase
GFP	Green Fluorescence Protein
GGPPS	Geranylgeranyl Diphosphate Synthases
Non-targeting guide RNA	gNT
PRMT5 guide RNA	gPrmt5
GREAT	Genomic Regions Enrichment of Annotations Tool

GSEA	Gene Set Enrichment Analysis
GTP	Guanosine-5'-Triphosphate
HA	Hemagglutinin
HAT	Histone Acetyltransferases
HCC	Hepatocellular Carcinoma
HDAC	Histone Deacetylases
HEPES	4-(2-Hydroxyethyl)-1-Piperazineethanesulfonic Acid
HIV	Human Immunodeficiency Virus
HMT	Histone Methyltransferases
HRP	Horseradish Peroxidase
HSPA	Heat Shock Protein
IC50	Half-Maximal Inhibitory Concentration
KMT	Lysine methyltransferases
MDR	Multidrug Resistance
MLL	Mixed Lineage Leukemia
M-MLV	Moloney Murine Leukemia Virus
NFDM	Nonfat Dry Milk
PCA	Principal Component Analysis
PCR	Polymerase Chain Reaction
PMSF	Phenylmethylsulfonyl Fluoride
PNK	Polynucleotide Kinase
PRMT	Protein Arginine Methyltransferase
PRMT5	Protein Arginine Methyltransferase 5
PTM	Post-Translational Modifications
PVDF	Polyvinylidene Fluoride
RIPA	Radioimmunoprecipitation Assay
RNA	Ribonucleic Acid
RPMI	Roswell Park Memorial Institute
SEM	Standard Error of The Mean
SDS	Sodium Dodecyl Sulfate
SIRT	Sirtuin
siCntrl	Control siRNA
siPRMT5	siRNA of PRMT5
SRB	Sulforhodamine B
StDev	Standard Deviation
TBST	Tris Buffered Saline Tween-20
TCA	Trichloroacetic Acid
TNFA	Tumor Necrosis Factor Alpha
UNT	Untreated
UPR	Unfolded Protein Response
UTR	Untranslated Region
WB	Western Blot

Chapter 1:

INTRODUCTION

1.1. Prostate Cancer

Prostate cancer (PCa) is the second leading cause of death and most frequent cancer in men overall, following skin cancer (W. Krause 2023; McGuire 2016; Siegel et al. 2011). It is reported in 15% of males globally at some time in their lives (Maluf et al. 2021). Risk factors include genetic susceptibility, genetic aberration, or family background of prostate cancer, obesity, hypertension, and high testosterone levels in the blood (Steinberg et al. 1990; Zeegers, Jellema, and Ostrer 2003; Calle et al. 2003; Martin et al. 2010; Gann et al. 1996).

PCa was primarily regarded as a disease resistant to treatment (Yagoda and Petrylak 1993). This explains why, for a certain medicine, data from various researchers varied considerably and lacked repeatability. For this reason, many studies involving the combination of two or more medications were conducted. None of the combinations had a significant effect on survival or reaction (Eisenberger et al. 1985). Indeed, patients initially demonstrate a favorable prognosis (Belkahla et al. 2022). While Androgen Deprivation Therapy (ADT) is commonly used as the initial treatment approach, it has demonstrated a significant reduction in Prostate-Specific Antigen (PSA) levels (Y. Huang et al. 2018). While it is often complemented by surgical interventions and radiation therapy, regrettably, ADT is a transient treatment method. Regrettably, notwithstanding the mentioned treatment modalities, mortality remains an inescapable outcome for individuals afflicted by advanced PCa (Y. Huang et al. 2018; Lian et al. 2015).

1.2. Castration Resistant Prostate Cancer (CRPCa)

Nearly all patients with advanced prostate cancer develop metastasis and invasion within 18–24 months of starting hormone therapy (Y. Huang et al. 2018). This form of the disease, which is resistant to hormone therapy, is the most aggressive and lethal form of prostate cancer. It is also known as castration-resistant prostate cancer (Y. Huang et al.

2018; Davies et al. 2019). A considerable number of patients experience the development of CRPCa. In managing CRPCa, the utilization of cytotoxic chemotherapy with taxanes, such as docetaxel and cabazitaxel, represents a crucial therapeutic option (Maloney et al. 2020).

1.3 The Therapeutic Drugs: Taxanes

Taxanes function by binding to the free β-tubulin subunit within the cytoplasm, preventing microtubule depolymerization (Figure 1.1). The mitotic spindle is a structure that is essential for cell division. It is composed of microtubules that help to segregate chromosomes during mitosis. When the mitotic spindle is disrupted, the cell cannot pass from metaphase to anaphase. This blocking mechanism can also trigger apoptosis by activating a number of signaling pathways (Fojo and Menefee 2007). This, in turn, induces mitotic arrest, cell death, and impedes cellular trafficking (Chandrasekar et al. 2015).

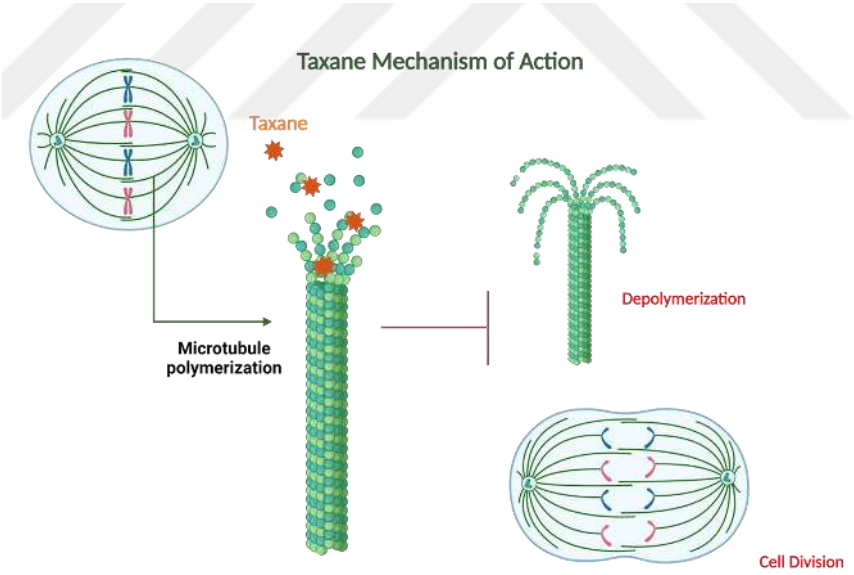

Figure 1.1. A schematic illustration of the taxane's mechanism of action. This figure was created using Biorender.

1.3.1. Docetaxel

Docetaxel is a taxane chemotherapeutic agent that induces apoptosis in prostate cancer cells by phosphorylating Bcl-2 and inhibiting nuclear translocation of AR (Pienta 2001). However, when used alone or in combination with other agents, the vast majority of patients (approximately 69% of patients) have a poor prognosis and experience a decrease in PSA levels (Picus and Schultz 1999; Berry et al. 2001). In order to increase the efficacy of docetaxel, many trials have been conducted, but no benefit has been seen (Nader, El Amm, and Aragon-Ching 2018). Although, cancer frequently recurs within a few years. In light of the limited efficacy of docetaxel as a first-line treatment for prostate cancer, second-line treatment options are being evaluated. Cabazitaxel, a taxane derivative with a distinct mechanism of action from docetaxel, has emerged as a preferred treatment option (Oudard et al. 2017).

1.3.2 Cabazitaxel

Cabazitaxel is a type of chemotherapy drug that was developed after resistance to other taxane (i.e., docetaxel) drugs was observed. It is a taxane that binds to tubulin, a protein that is essential for cell division. This binding prevents cells from dividing and eventually kills them (Mita et al. 2009).

Cabazitaxel exhibits a slight variance in its chemical composition compared to docetaxel. This disparity is attributed to the presence of methyl groups at the 7th and 10th positions on the taxane ring (Figure 1.2). This structural distinction contributes to a decreased affinity of cabazitaxel towards MDR1, a protein recognized for its role in drug efflux. Consequently, cabazitaxel displays an extended cellular retention duration, thereby impeding the depolymerization of microtubules. This effectuates a notably enhanced G2/M arrest and apoptosis induction by cabazitaxel (Maloney et al. 2020).

A. **B.**

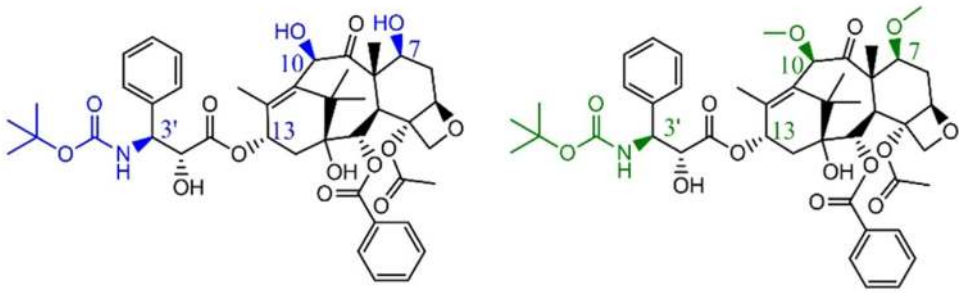

Docetaxel (Dtx) Cabazitaxel (Cbz)

Figure 1.2. The chemical structures of (A) Docetaxel, and (B) Cabazitaxel.

Additionally, cabazitaxel has been shown to be effective in patients who have developed resistance to docetaxel over time (de Bono et al. 2010). The distinct mechanism of action of cabazitaxel makes it more effective against cancer cells that have become resistant to docetaxel. A number of clinical trials have demonstrated that cabazitaxel is effective in prolonging the survival of patients with prostate cancer that has progressed after docetaxel treatment. As a result, cabazitaxel is now considered to be the preferred second-line treatment for prostate cancer (Nader, El Amm, and Aragon-Ching 2018). However, CRPCa patients can also show the recurrence to cabazitaxel over time (Oudard et al. 2017).

1.4. Drug Resistance in PCa

Drug resistance is the ability of tumor cells to survive and grow despite being exposed to chemotherapeutic drugs. Drug resistance can arise through diverse mechanisms, prominently including enhanced efflux pump activity and genetic mutations that attenuate the efficacy of the therapeutic agent. These adaptations often serve the primary purpose of impeding the intracellular accumulation of the drug. The accumulation of mutations in tumor cells allows them to survive despite exposure to drugs and to evade mechanisms that trigger cell death (Semenas et al. 2012). Tumor cells develop various mechanisms to become insensitive to drugs, including the activation of

cell proliferation-enhancing pathways such as the EGFR/VEGFR (Mahon et al. 2011) pathways, as well as other pathways such as the PI3K/Akt, MAPK/ERK (Zelivianski et al. 2003; Mahon et al. 2011), mTOR (Wu, Birle, and Tannock 2005), and NFκB pathways (Domingo-Domenech et al. 2006).

1.4.1 Taxane Resistance

The development of new treatments is essential, especially for CRPCa. Drug resistance is a major concern, and the treatment methods have been limited. Post-castration chemotherapy is an effective treatment, but patients eventually develop resistance to drugs. As a result, they become unresponsive to treatment and have an average survival time of 18 months. In most cases, the disease progresses rapidly after patients develop resistance to taxanes (Sella et al. 2007). Despite advances in treatment methods for prostate cancer (PCa), such as surgical intervention, chemotherapy, and radiotherapy, the mechanism of drug resistance remains a major obstacle to successful treatment (Semenas et al. 2012).

In the last decade, significant efforts have been made to study the genomic and transcriptomic profiles of castration-resistant prostate cancer (CRPCa). However, the epigenetic landscape of taxane-resistant CRPCa remains largely unexplored. Drug resistance is a complex phenomenon that is controlled by a variety of mechanisms. Epigenetic factors play a significant role in drug resistance, by enabling cancer cells to escape apoptosis and increase proliferation. These changes in gene expression can lead to the development of more aggressive and metastatic cancer cells (Y.-P. Liu et al. 2021). A summary of development of the taxane resistance mechanisms in PCa is illustrated as in Figure 1.3.

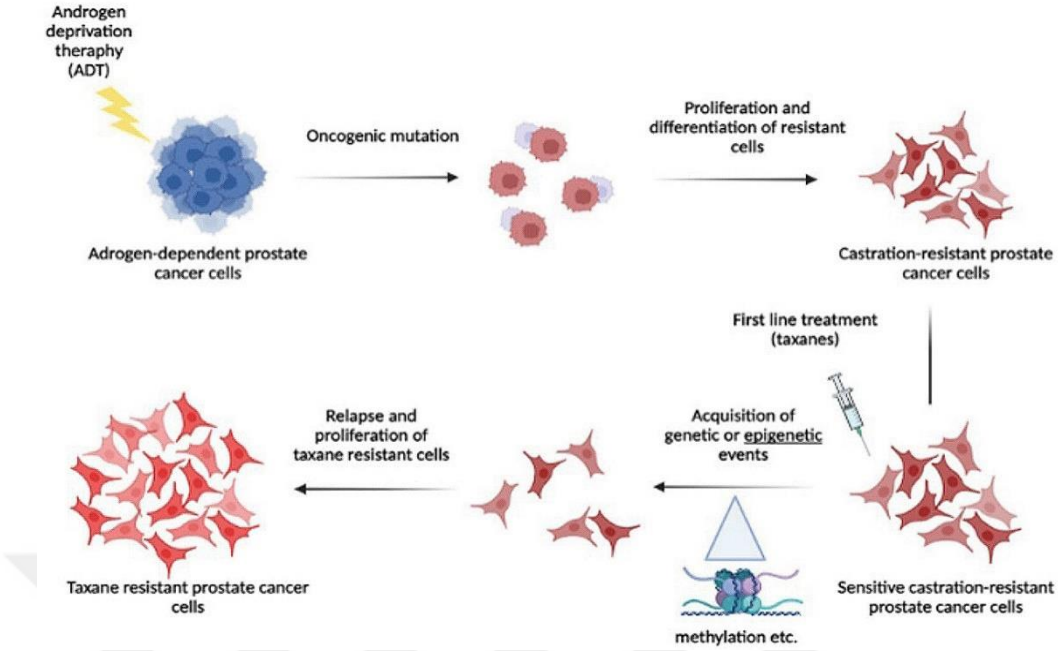

Figure 1.3. Illustration of development of taxane resistance in PCa. This figure was created using Biorender. Androgen deprivation therapy is used for first line treatment. Over time, numerous oncogenic mutations may accumulate, enabling these cells to both survive and proliferate, as well as differentiate into castration-resistant cells. At this juncture, taxanes are the predominant therapeutic agents used to address these cells. However, resistance to these drugs can also developed. Furthermore, the emergence of drug resistance in cancer is facilitated by several mechanisms. One such mechanism is epigenetic changes, which significantly influence tumor growth and metastasis. Subsequently, cancer may also recur and progress to a stage referred to as CRPCa.

The mechanisms of taxane resistance are still under investigation, but many ongoing studies have made significant progress in identifying the key factors involved. These factors include the ATP efflux pump, the activation of apoptosis-inducing pathways, and the dysregulation of proliferation-promoting mechanisms (Maloney et al. 2020). Among the activated signaling pathways, there are several that are involved in cell proliferation, such as the Bcl-2, Hedgehog, p53, PI3K, STAT3, and NF-κB pathways (Duronio and Xiong 2013; Yip and Papa 2021).

ATP efflux pumps control the cellular uptake of drugs, such as taxanes. The overexpression or downregulation of these pumps can have a significant impact on the efficacy of taxanes in cancer cells (J.-Q. Wang et al. 2021). ABC transporters are a major

class of ATP efflux pumps that play a key role in multidrug resistance (MDR) (Choi and Yu 2014). The ABCB1 gene, which encodes one of the ABC transporters, is highly expressed in prostate cancer cells and is associated with resistance to taxanes (Lombard et al. 2021).

1.4.2. Taxane Resistance Reversal in CRPCa

Recent studies have focused on reversing drug resistance caused by cancer recurrence. This drug resistance to taxanes, especially in prostate cancer, has not been fully resolved and limits treatment options. Therefore, new strategies are being investigated. It is believed that patients can be cured by achieving synergy with combination therapy and overcoming drug resistance. With the advancement of technology, clinical studies are prioritizing personalized treatments that are specifically tailored to prostate cancer (PCa). In recent years, the importance of epigenetic mechanisms in taxane-resistant cells has been highlighted by transcriptomic analyses of castration-resistant prostate cancer (CRPC). However, the underlying mechanisms are still largely unknown.

1.5. Epigenetics

Nucleosomes are the fundamental structural units of chromatin, the complex of DNA and proteins that constitute chromosomes (Lund and van Lohuizen 2004). They are composed of an octamer of histone proteins, two molecules each of H2A, H2B, H3, and H4 (Khorasanizadeh 2004). The N-terminal tails of histones protrude from the nucleosome core, as a sign of epigenetic modifications. Epigenetic modifications are covalent changes to DNA or histone proteins that do not change the underlying DNA sequence. These changes can affect gene expression, which is the process by which genes are turned activated or inactivated (Strahl and Allis 2000).

Histone modifications are recognized by proteins called bromodomains and chromodomains. These proteins bind to chromatin and initiate such biological processes, as chromatin folding, regulation of transcription, and DNA damage repair mechanism. Histone acetylation is often associated with gene activation, while histone methylation can function as a site for both activator and repressor. Epigenetic inheritance is the passing

down of epigenetic marks from one cell generation to the next. This can be important for cell differentiation and function (Lund and van Lohuizen 2004).

Histone methylation is an epigenetic modification that can occur on the amino groups of lysine or arginine residues. It can be mono-, di-, or trimethylated. Histone methylation is thought to be a marker of chromatin regulation, along with other epigenetic modifications such as acetylation and phosphorylation. Histone methylation can greatly affect gene expression. Lysine Methyltransferases (KMTs) and Protein Arginine Methyltransferases (PRMTs) are the two largest groups of histone methyltransferases (Dawson and Kouzarides 2012).

1.5.1. Epigenetic Writers: PRMTs

Arginine methylation is a frequent post-transcriptional modification (PTM) implicated in several physiological activities, including signal transmission, DNA repair, activator or repressor of transcription, protein folding, and mRNA level control mechanism (Yang and Bedford 2013; Bedford and Clarke 2009; Bedford and Richard 2005). In general, for cells, arginine methylation is utilized by an enzyme family known as PRMTs. In higher eukaryotes, this family presently consists of nine members. Based on the kind of methyl mark formed on the arginine residue, these enzymes are sub grouped into three classes; Type I, II and III (Zurita-Lopez et al. 2012; Feng et al. 2013).

It is predicted that insights into the unique functions of the many PRMTs will lead to novel techniques for cancer prevention, diagnosis, and therapy (Yang and Bedford 2013). There are now around 120 methylated proteins identified in arginine residues, including histone and non-histone proteins (Boisvert, Chénard, and Richard 2005; A. Guo et al. 2014). The number of arginine-methylated protein substrates continues to expand, as do the identification of new functional functions and the participation of various regulatory processes (Boisvert, Chénard, and Richard 2005; Ong, Mittler, and Mann 2004; Boisvert et al. 2003). PRMTs are normally ubiquitously expressed and regulate crucial cellular processes affecting cell growth, proliferation, and differentiation. Deregulation of these enzymes is likely to have a role in the pathogenesis of several illnesses, including cancer (Yang and Bedford 2013).

1.5.2. Association between PRMTs and Cancer

Accumulating data suggests that methylation of arginine residues may have an important role in the formation, invasion, and aggressiveness of various forms of malignancies (such as cancer). Although the correlation between methylation of arginine residues and cancer is a relatively recent field of study, the functions that PRMTs demonstrated their importance in the development of cancer. Several human tumors, such as breast, prostate and lung, have dysregulated PRMT expression (Baldwin, Morettin, and Côté 2014; Hong et al. 2004; Cheung et al. 2007; Y.-R. Kim et al. 2010).

Contrary to expectations, most cancer cells express alternative isoforms of the PRMT family. This suggests that these isoforms play a role in the mechanism of cancer development. The expression levels and functional properties of these isoforms vary between different cancer types. Unfortunately, these isoforms have not been well-characterized. The PRMT family is a promising target for cancer therapy (Cha and Jho 2012).

In addition, these various PRMT isoforms must be considered when devising and assessing prospective treatment candidate techniques or drugs. This is crucial so that the specific mechanism of action may be comprehended. Although revealing the functions of PRMTs are limited, the available information clearly suggests that they have a special role in cancer. Therefore, they might have some overlapping duties, they clearly have separate responsibilities (Baldwin, Morettin, and Côté 2014).

1.6. The Role of PRMT5

PRMT5, a type II enzyme (Yang and Bedford 2013; Branscombe et al. 2001) within the expanding family of PRMTs, is known for methylating arginine residues on both histones and non-histone substrates (Baldwin, Morettin, and Côté 2014; Beketova et al. 2022). PRMT5 has been studied the most. Biochemical and structural studies have shown that PRMT5 forms a complex with the MEP50 protein to catalyze the symmetric dimethylation of the arginine residues of histones H4R3, H3R8, and H2AR3. This process is thought to regulate gene transcription. Other studies have shown that some dimethylations of histones (H3R2, H3R8, and H4R3) can also affect gene transcription

(Figure 1.4). PRMT5 forms a hetero-octameric complex with four PRMT5 proteins and four cofactors, MEP50 and WDR77 (Antonysamy et al. 2012; Ho et al. 2013).

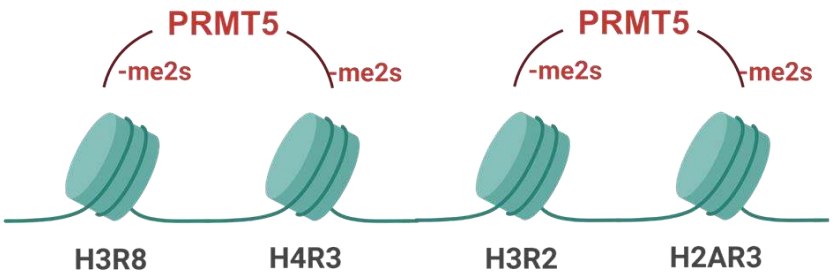

Figure 1.4. A schematic illustration of symmetrically dimethylates histones by PRMT5. This figure was created using Biorender. PRMT5 is responsible for methylating four specific arginine residues in histone tails, which are H4R3, H2AR3, H3R8, and H3R2. Among them, H4R3me2s and H3R8me2s typically correlate with the suppression of transcription (Kim and Ronai 2020).

The protein PRMT5 is structurally composed of three main parts. the N-terminal TIM barrel domain is responsible for the assembly of the PRMT5-MEP50 complex. It also contains the Rossmann fold, which is responsible for protein catalysis and activates its catalytic activity. The C-terminal β-barrel domain helps dimerization of PRMT5 to form the tetramer in the complex (Figure 1.5) (Antonysamy et al. 2012; Ho et al. 2013).

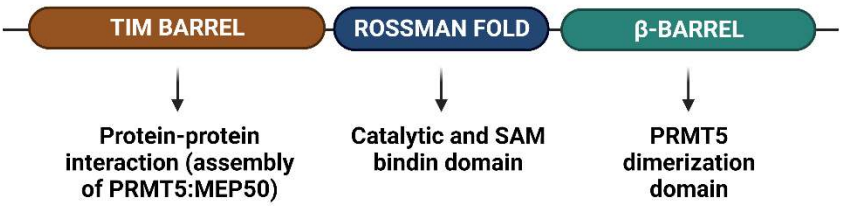

Figure 1.5. Functional domains of PRMT5. This figure was created using Biorender. The PRMT5 structure comprises an N-terminal TIM barrel domain that assists in forming the PRMT5:MEP50 complex. Next, there's a central Rossman fold domain, which binds to SAM and undertakes catalysis. This domain also possesses a typical methyltransferase structure that supports PRMT5's catalytic function (Antonysamy et al. 2012). Lastly, the C-terminal β-barrel domain helps PRMT5 dimerize, creating the inner core tetramer within the PRMT5:MEP50 complex (Sun et al. 2011).

Apart from the epigenetic regulation of gene transcription, PRMT5 by using PTM for methylation NF-B, EGFR, p53, and other signaling molecules (Shailesh et al. 2018). The majority of PRMT5's substrates are histones, and methylation has a substantial influence on the expression of downstream genes. Arginine dimethylations of H2AR3me2s, H4R3me2s, H3R8me2s and H3R2me2s can alter chromatin structure and lead to gene-level silencing. Methylation of H4R3 and H3R8 generated by PRMT5 is often connected with transcriptional repression (Blanc and Richard 2017; Tarighat et al. 2016; Stopa, Krebs, and Shechter 2015; Jing, Zhao, et al. 2018), although PRMT5-induced methylation of H3R8me2s is occasionally associated with transcriptional activation (Tarighat et al. 2016).

PRMT5 therefore has a function in controlling cell proliferation, differentiation, cell division and control mechanism, DDR, and apoptosis (Stopa, Krebs, and Shechter 2015; Karkhanis et al. 2011; Shailesh et al. 2018). PRMT5, a crucial regulatory protein, is overexpressed in several malignancies (Stopa, Krebs, and Shechter 2015).

1.6.1. Association between PRMT5 and Cancer

Chemical studies suggest that PRMT5 could function as a cancer-causing gene through two possible mechanisms: firstly, by suppressing tumor suppressor genes or cell cycle regulators through epigenetic processes, and secondly, by modifying signaling molecules after translation. Broadly, PRMT5 is highly expressed in different types of cancers, including PCa (Figure 1.6) (Beketova et al. 2022).

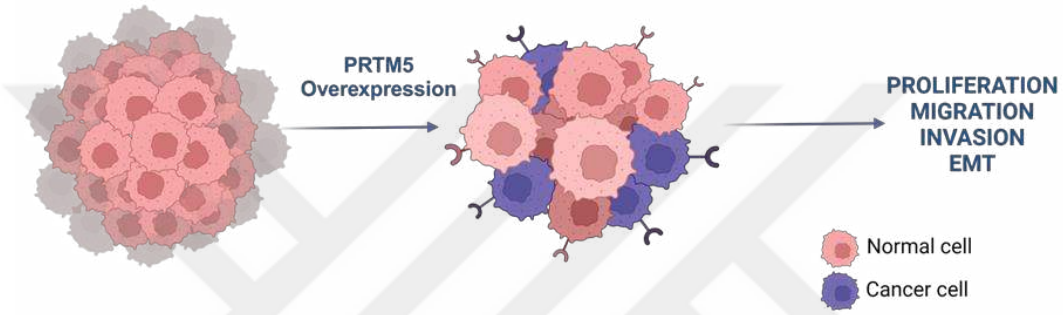

Figure 1.6. PRMT5 overexpression led to the development of cancer. This figure was created using Biorender. Overexpression of PRMT5 significantly increases cell proliferation and directly correlates with migration and EMT mechanisms.

PRMT5 symmetrically dimethylates a wide range of transcription factors, including RAD9, p53, FEN1, E2F1, and proteins involved in chromatin regulation (Z. Guo et al. 2010; Bandyopadhyay et al. 2012; Cho et al. 2012). p53 is one of the most well-known genes and is responsible for the transcription of the TP53 gene. This gene encodes a protein that plays a critical role in regulating the cell cycle and apoptosis (Jansson et al. 2008). A specific mutation in p53, converting three arginine residues (R333, R335, R337) to lysine, hinders its ability to induce G1 phase arrest, yet the apoptotic functionality remains unaltered. By inducing apoptosis, PRMT5 suppression may sensitize tumor cells to chemotherapy and/or radiotherapy, according to this theory (Durant, Cho, and La Thangue 2009). PRMT5 regulates the EGFR–RAS–ERK signaling pathway at two distinct nodes. First, the Hung group (Hsu et al. 2011) demonstrated that R1175 of EGFR is methylated by PRMT5 (Andreu-Pérez et al. 2011).

1.7. Subcellular Localization of PRMT5

In numerous somatic cells, PRMT5 is primarily found in the cytoplasm (Hou et al. 2008, Pal et al. 2007). The movement of PRMT5 seems to be important in managing pluripotency during the early stages of mouse embryo development (Tee et al. 2010). PRMT5 possesses three unique nuclear exclusion signals (NES) that differ from the typical leucine-rich NES (Gu et al. 2012, Stopa et al. 2015).

In various cells, PRMT5 constitutes a complex with p44/MEP40/WD45/WDR77 (Guderian et al. 2011, Kroiss et al. 2009, Hou et al. 2008). Furthermore, during mouse development, the location of PRMT5 within the cell changes (Tee et al. 2010). Recent research revealed that PRMT5 in the cytoplasm is crucial for the proliferation of prostate cancer cells, but when in the nucleus, it suppresses their growth. Supporting this, benign prostate epithelial cells have PRMT5 in the nucleus, while premalignant and malignant prostate tissues show their presence in the cytoplasm. This suggests that the role of PRMT5 is influenced by its location within the cell, and its movement between the nucleus and cytoplasm might be pivotal in the development of prostate cancer. Yet, the specific function of PRMT5 in both the cytoplasm and nucleus, as well as how its location within the cell relates to prostate cancer, remains unexplored (Gu et al. 2012).

1.8. Aim of this thesis

This research aimed at epigenetic alterations associated with taxane resistance and their growing recognition as potential modulators for overcoming taxane resistance in PCa. The recurrence of drug resistance poses a significant challenge in cancer therapy, particularly when employing taxane-based treatments. Nonetheless, the efficacy of taxane therapy is impeded by the development of resistance mechanisms, necessitating a thorough exploration of alternative strategies to surmount this resistance phenomenon.

Chapter 2:

MATERIALS AND METHODS

2.1. Cell Culture and Reagents

The PCa cell lines DU-145 and 22Rv1, HEK293T, U2OS, MDA-MB-231, MIA-Paca-2 and RPE-1 cell lines were obtained from ATCC. Cell lines were sustained in a standard procedure at 37°C maintained in a 5% CO_2 humidified environment. Du145 and 22Rv1 cell lines were grown with in RPMI-1640 (Sigma Aldrich, R8758) with supplemented heat-inactivated 10% FBS (Biowest, S160H), 100 U/mL of penicillin, and 100 g/mL of streptomycin (Life Technologies, 15140122. DMEM (Sigma Aldrich, 51434C) was used to culture HEK293T cells with heat-inactivated 10% FBS, 2 mM L-glutamine, 100 U/mL penicillin, and 100 g/mL streptomycin.

In this study, in addition to the PRMT5 inhibitor (HLCL-61, Cayman, 19897) present in the epigenetic drug library, several additional PRMT5 inhibitors were also tested. Other inhibitors that were tested include GSK591 (Cayman, 18354), GSK3326595 (Cayman, 27305), LLY-283 (Cayman, 21596), JNJ-63619178 (Cayman, 29231), and EPZ015666 (Cayman, 17285).

2.2. Generation of Taxane Resistant Cell Lines

The Docetaxel and Cabazitaxel resistant Du145 and 22Rv1 cell lines (Du145-DtxR, Du145-CbzR and 22Rv1-DtxR, 22Rv1-CbzR) was generated by Buse Cevatemre Yıldırım, PhD and İpek Bulut, MSc. Briefly, the dose-escalation method was used to establish resistant cells. In this approach, taxane-sensitive cells, Du145 and 22Rv1, were cultured with IC_{50} doses of the taxanes (Dtx/Cbz) for 72 h. After the cells recovered, this cycle was repeated using newly determined IC_{50} doses, and this process took an overall duration of 8-12 months.

2.3. Sulforhodamine B (SRB) Cell Viability Assay

Du145/22Rv1 parental ($4 \times 10^3/7.5 \times 10^3$) and resistant ($7.5 \times 10^3$) cells were seeded into 96-well plates overnight, then treated with an increasing dose of Dtx/Cbz for 72 h. To assess cell viability, 50 µL of 50% (w/v) trichloroacetic acid (TCA) (Sigma Aldrich, T6399) was added to the wells containing 200 µL volume (with a final concentration of 10%) of culture medium (final concentration of 10% TCA) and allowed fixation at +4°C for 1 h. Afterwards, the wells were washed five times with dH_2O and 50 µL of SRB (Santa Cruz, sc-253615) dye was added and incubated at RT for 30 mins. Wells were then washed five times with 1% acetic acid (v/v) and the dye was dissolved by adding 150 µL of 10 mM Tris Base (Sigma Aldrich, T1503). The colorimetric measurements were taken at 570 nm absorbance (Synergy H1 Hybrid reader, BioTek). Blank measurement was subtracted in all samples and % cell viability was shown after division of each absorbance value by the absorbance of the non-treated group.

2.4. Crystal Violet Colony Formation Assay

Du145/22Rv1 parental ($3 \times 10^2/2 \times 10^3$) and resistant ($1 \times 10^3/2 \times 10^3$) cells were seeded into 12-well plates, then treated with increasing doses of Dtx/Cbz for 72 h treatment. Cells were further cultured with fresh medium and allowed for colony formation for 14 days. The medium was removed, and all groups were fixed with 1 ml of ice-cold methanol (Merck, 1.06009) at -20°C for 10 min. After methanol removal and PBS wash two times, 0.5 ml of 0.01% crystal violet solution (Merck, 1.09218) was added for 30 min. After washing out the excessive dye using dH_2O and allowing dry-out, colonies were visualized and quantified by the ImageJ program (Schneider et al., 2012).

2.5. Measurement of Cell Doubling Time

Du145-P/R cells (1×10^5 cells) were seeded in 6-well plates. From day 1 to day 6, cells counted every 48 h with trypan blue dye (Ecotech, B100). The doubling time was quantified using the following formula below.

(t=time, N=cell number)

$$\text{Doubling time } T_d = (t2 - t1) \frac{* \ln(2)}{2\ln(N2/N1)}$$

2.6. Epigenetic Drug Library Screening

Epigenetic Drug Library (Cayman, 11076) was screened to identify potential epigenetic regulators for overcoming taxane resistance, and the screen was performed by İpek Bulut, MSc., and Buse Cevatemre Yıldırım, Ph.D. The Du145-DtxR cells were treated with a collection of 145 epigenetic inhibitors at a constant concentration of 5 μM, along with the IC_{25} value of Dtx, for 72 h. The viability of cells was assessed using the SRB viability assay, as described in Chapter 2.3.

2.7. siRNA-mediated Gene Knock-out

Lipofectamine 3000 (Invitrogen, L3000015) was used to transfect siRNA into both parental and taxane-resistant Du145 and 22Rv1 cells, following the manufacturer's instructions. The parental cells (12×10^4) and resistant cells (17×10^4) were seeded for transfection. 100 pmol of siRNA (*siControl*, Thermo Scientific, 4390844; *siPRMT5*, Thermo Scientific, s20377; *siMyc*, Fisher Scientific, s9129) was mixed with 7.5 μL of Lipofectamine 3000 Reagent in Opti-MEM (Invitrogen, 31985062). After incubating the mixture for 15 min at room temperature (RT), it was added dropwise to the wells. The siRNA mixture was removed, and medium was refreshed on the following day Samples were further collected at the indicated endpoints for evaluation of knock-down efficiency via qRT-PCR and Western Blotting.

2.8. CRISPR-mediated Gene Knock-Out

The pLentiCRISPR-v2 plasmid (Addgene, 52961) was digested using BsmBI enzyme (NEB, R0580), and the backbone was then dephosphorylated with Antarctic Phosphatase enzyme (NEB, M0289) according to the manufacturer's protocol. gRNA oligos were phosphorylated and annealed using T4 PNK enzyme (Thermo Fisher, M0201S). The ligation reaction was performed using T4 Ligase (Thermo Fisher, M0202S) according to the manufacturer's protocol. For transformation of ligation products, competent *E.coli* Stbl3 bacterial cells were mixed with ligation products and competent cells were incubated for 30 sec at 42°C and immediately on ice for 2 min (heat-shock method). Then, cells were further allowed to grow at 37°C for 1 h in SOC medium (NEB, B9020S). Finally, transformed cells were centrifuged at 400 g for 5 min, and the resuspended cells were spread onto agar plates. Ligation colonies were grown in LB

overnight and plasmid isolation was performed for PCR to confirm successful cloning of the gRNA sequence into backbone. The oligonucleotide sequences for the non-targeting and targeting guides for PRMT5 are listed in Table 2.3.

Lentivirus production was performed with HEK293T cells with 2500 ng of the target plasmid, 2250 ng of psPAX2 (Addgene, 12260), and 225 ng of VSV-G (Addgene, 8454) using Fugene 6 (Promega, E2311). HEK293T cells (2×10^6) were seeded into 10-cm plates overnight, and next day they were transfected with the plasmids that mixed in 380 µL of serum-free DMEM and 20 µL of Fugene. The transfection mixture was added dropwise onto the cells and allowed transfect cells for 16 h. The medium was refreshed the next day and was collected after 48 and 72 h post-transfection and was passed through 45-µm filters (Invitrogen, F2502-3) to remove any remaining cell debris. 50% of PEG8000 (Sigma Aldrich, P2139) was used to concentrate virus mix at a final concentration of 10%, and the mixture was incubated at 4°C for 72 h. The concentrated viruses were centrifuged at 2500 rpm for 20 mins, and they were resuspended in PBS as 100X stocks and stored at -80°C.

To transduce target cells, 8×10^4 cells were seeded into a 6-well plate. The following day, transduction was performed by adding 5 µL of virus particles to each well, along with protamine sulphate (Merck, P3369). After 48 h, the cells were selected using puromycin (Merck, P7130) and seeded into 96-well plates at a density of one cell per well for monoclonal expansion. The growing colonies were analyzed for knockout efficiency using WB as described in Chapter 2.13.

Table 2.3. Oligonucleotide sequences were used for this study.

Guide	Oligonucleotide Sequence
gRNA-PRMT5 #1	*Fwd Primer*: CAC CGT CTT CCA TCC GCG TTT CAA G *Rev Primer*: AAA CCT TGA AAC GCG GAT GGA AGA C
gRNA-PRMT5 #2	*Fwd Primer*: CAC CGA TGA ACT CCC TCT TGA AAC G *Rev Primer*: AAA CCG TTT CAA GAG GGA GTT CAT C
gRNA-NT	*Fwd Primer*: CAC CGT ATT ACT GAT ATT GGT GGG *Rev Primer*: AAA CCC CAC CAA TAT CAG TAA TAC

2.9. RNA Isolation

RNA isolation was performed with manufacturer's instructions (Zymo, R1055). Cells were harvested by centrifugation at 300 g for 5 min. Pellets were resuspended in a lysis buffer and centrifuged at 11.000 x g for 1 min. After supernatant was mixed with 96% ethanol (Merck, 1.00983), it was loaded onto the column, and centrifuged at 11.000 x g for 1 min. Columns were incubated by DNaseI for 15 min at room temperature. After washing twice with RNA wash buffer and centrifugation (11.000 x g for 1 min), the RNAs were eluted with 50 µL of nuclease-free water. Concentration and purity of samples were determined using the NanoDrop instrument.

In preparation of RNA-seq samples, to identify differentially expressed genes (DEGs) between siControl and siPRMT5 treated Du145-DtxR cells, RNA samples were collected as described as three biological replicates.

2.10. cDNA Synthesis

M-MLV Reverse Transcriptase (Thermo Fisher Scientific, 28025013) was used for cDNA synthesis (Thermo Fisher Scientific, 28025013). A mixture of 10 mM dNTPs, 1 µM Oligo dT primer, and 500 ng of RNA was incubated at 65°C for 5 min and RNA solution was incubated with 4 µL of reaction buffer including 1 µL of 0.1 M DTT, and 1 µL of RNase inhibitor at 37°C for 2 min. Subsequently, 1 µL of M-MLV RT was added, and allowed to be incubated at 37°C for 1 h. In the final step, the RT enzyme was inactivated at 75°C for 15 min.

2.11. Quantitative Real Time PCR (qRT-PCR)

Gene expression levels were assessed using the LightCycler 480 SYBR Green I Master mix (Roche Diagnostics, 50-720-3180). qRT-PCR was performed in a total volume of 20 µL (SYBR Green I Master Mix, 10 µL; forward and reverse primer mix, 150 nM final concentration; cDNA template, 10ng; NFW, up to 20 µL) on a LightCycler 480 System II (Roche Diagnostics) machine. The reaction was set as follows; initial denaturation, 95°C, 5 min; [40 cycles of] denaturation, 95°C, 15 sec; annealing, 55°C, 10 sec; elongation, 72°C for 30 sec. The fold change levels of gene expression were determined using the $2^{(-\Delta\Delta CT)}$ method and normalized to the expression of a housekeeping gene (ACTB or GAPDH).

Table 2.1. qRT-PCR primers specific to PRMT5 and housekeeping genes GAPDH and ACTB.

Name	Sequence (5' - 3')
ACTB	*Fwd Primer:* TCA CCA TGG ATG ATG AT CGC *Rev Primer:* ATA GGA ATC CTT CTG ACC CAT GC
GAPDH	*Fwd Primer:* AGC CAC ATC GCT CAG ACA C *Rev Primer:* GCC CAA TAC GAC CAA ATC C
PRMT5	*Fwd Primer:* TAA GCC AGA ACC GTC CTC CA *Rev Primer:* AGA TGG CCT GCT GGT ACT GA

RNA Seq samples were prepared as described in Chapter 2.9 and qRT-PCR validation was carried out as described above. The forward and reverse primers (designed for hit genes) that were used are listed in Table 2.4.

Table 2.4 DEGs from RNA-seq hit and specific primer sequences

Hit genes	Sequence (5'-3')
MYC	*Fwd Primer:* TTC CCC TAC CCT CTC CGA *Rev Primer*: CAG AGA ATC CGA GGA CGG AG
HSPA8	*Fwd Primer:* TGG CAC CAC CTA CTT TGT G *Rev Primer*: TTG GAG TGG TTC GGT TTC CC
GINS4	*Fwd Primer:* TTG AAT GAC GGC TCT ACG TCC *Rev Primer*: AGA GGA TGT AAA GTG CTC CGT G
DDX39A	*Fwd Primer:* CGG CGG AAA ACC GAA GTT G *Rev Primer*: AGC TGT GGA TGG AAA CGT AGG
EGR1	*Fwd Primer:* GCA TGT GTC AGA GTG TTG TTC C *Rev Primer*: ATC AGC AAG GCG CAT CAC A
FOSL1	*Fwd Primer:* CTC TGG AGC CCT AAC CCC TT *Rev Primer*: GTT GGG TGG ATC ACA GGA AGA
ODC1	*Fwd Primer:* GGC ACA CGC AGA GGG ATT T *Rev Primer*: GTC CAG AAT GTC CTT GGC AGT A
RAN	*Fwd Primer:* ACG ACT TAG AGG TTG CTC AGA C

	Rev Primer: TAG ACT TCT GAC GCT GGG CT
SRM	*Fwd Primer:* GTC TGT CTC TCT GGC GTT CC *Rev Primer*: GTG AGT GAG GGG CAA CAG AA
PRMT5	*Fwd Primer:* TAA GCC AGA ACC GTC CTC CA *Rev Primer*: AGA TGG CCT GCT GGT ACT GA
GAPDH	*Fwd Primer:* AGC CAC ATC GCT CAG ACA C *Rev Primer*: GCC CAA TAC GAC CAA ATC C

2.12. Protein Isolation and Quantification of Protein Concentration (BCA Assay)

Protein isolation was performed by lysing the cell pellet with RIPA Lysis Buffer (Sigma Aldrich, R0278) containing Protease Inhibitor Cocktail (Cell Signaling Technology, 5871) and 1mM PMSF (Sigma Aldrich, 10837091001). Cell pellets were incubated on ice for 30 min and centrifuged at 17.000 g for 20 min at 4°C. The protein-containing supernatant was collected and subjected to further processing to determine the protein concentration.

Protein concentrations were quantified using the Pierce^{TM} BCA Protein Assay Kit (Thermo Fisher Scientific, 23225). Reagent A and Reagent B were mixed to make a BCA working solution with a ratio of 50:1. BSA standards (0.4, 0.8, 1.2, 1.6, and 2 mg/ml) and samples were added to 96-well plates, and they were mixed with BCA working solution. After incubation at 37°C for 30 min, color intensity was measured at 562 nm (Synergy H1 Hybrid reader, BioTek). All measurements were normalized to blank values, and a standard curve was generated to determine protein concentrations.

2.13. Histon Extraction

Histon extraction was performed by lysing the cell pellet with Triton Extraction Buffer (TEB) containing 2 mM PMSF (Merck, 10837091001) on ice for 10 min at a final concentration of (1×10^6) cells/ml. The lysate was centrifuged at 6.500 x g for 10 min at 4°C. After that, the supernatant was discarded, and the pellet (the nuclei) was washed with TEB Buffer, centrifugated again at 6.500 x g for 10 min at 4°C. After discarding the supernatant, the pellet (nuclei) was resuspended with 0.2N HCl (Sigma Aldrich, 320331)

at 4°C overnight to extract the histones with the aid of an acid environment. Next day, samples were centrifugated at 6.500 x g for 10 min at 4°C and the supernatant was neutralized with 2M NaOH (Sigma Aldrich, 221465) at 1:10 of the volume of the supernatant.

2.14. Nuclear/Cytosolic Isolation

The BioVision Nuclear/Cytosol Fractionation Kit (BioVision, K266) reagents were prepared as per the manufacturer's instructions. Ice-cold Cell Lysis Buffer from the kit was added to the and the cells were incubated on ice for 10-15 minutes, with gentle swirling to ensure complete cell lysis. The lysate was centrifuged at 500 x g for 5 minutes at 4°C to separate the nuclei from the cytoplasmic fraction. The supernatant, containing cytosolic proteins, was transferred to a fresh microcentrifuge tube, and stored on ice. The supernatant was carefully removed, ensuring the nuclear pellet was undisturbed. The nuclear pellet was resuspended in the Nuclear Extraction Buffer. The suspension was incubated on ice for 30 minutes with intermittent vortexing. After incubation, the nuclear suspension was centrifuged at 10,000 x g for 10 minutes at 4°C to pellet any insoluble material. The supernatant, containing nuclear proteins, was transferred to a new pre-chilled microcentrifuge tube. Protein samples were stored at -80°C for long-term preservation.

2.15. Western Blotting

Proteins were mixed with a Laemmli sample buffer (Bio-Rad Laboratories, 1610747) and β-mercaptoethanol (2-BME) (Bio-Rad Laboratories, 1610710), subsequently boiled at 95°C for 10 minutes for denaturation. A 4-15% SDS-PAGE gel (Mini-PROTEAN® TGXTM Precast Gels, BIORAD, 161-0317) was loaded with 30 µg of protein. SDS-PAGE was conducted at 100 V for 60 to 90 min and a wet transfer system was utilized to transfer the proteins onto a PVDF membrane (Bio-Rad, 1620177) that had been pre-activated with methanol (Merck, 1.06009). The transfer was performed at 200 mA for 120 min at 4°C. After washing the membrane with TBST buffer, it was blocked with 5% NFDM (Bio-Rad Laboratories, 1706404) at RT for 1 h. The membrane was incubated overnight at 4°C with primary antibodies (Abcam, ab9485; Cell Signaling Technology, 79998; Cell Signaling Technology, 13222; Abcam, ab18521). In the

upcoming day, membrane was incubated with HRP-conjugated secondary antibodies, specifically Goat anti-Rabbit (Abcam, ab205718) and Goat anti-Mouse IgG (Abcam, ab97023) for 1 h at RT after washing with TBST five times at 10-mins intervals.

For visualization, Immobilon Forte Western HRP substrate (Millipore, WBKLS0500) was used, and membranes were imaged using the LI-COR Odyssey FC Imaging system (LI-COR Biosciences). Intensities of the bands were quantified by ImageJ software (Schneider, Rasband, and Eliceiri 2012).

2.16. Cellular Thermal Shift Assay (CETSA)

A total of 8×10^6 Du145-DtxR cells were harvested and incubated with PRMT5 inhibitors (5 μM) and DMSO (Sigma Aldrich, S-002-D) as a vehicle in 15 ml Falcon tubes for 1 h at 37°C. Then, cells were collected by centrifugation at 500 g for 5 min and resuspended in 700 μL of PBS (Biowest, L0615) containing Protease Inhibitor Cocktail Pi (Cell Signaling Technology, 5871) and 1 mM PMSF (Sigma Aldrich, 10837091001). The cell suspension was then divided equally into 200 μL tubes and heated for 3 min on a Thermal Cycler (BIORAD T100) at temperatures ranging from 55°C to 70°C. The cells were lysed by freeze-thaw cycles, where they were snap-frozen with liquid nitrogen and then thawed at 25°C in the thermal cycler. This freeze-thaw process was repeated twice. Subsequently, the cell lysates centrifuged at 4°C and 17.000 g for 15 min. The supernatant containing the proteins was collected and subjected to WB as described in Chapter 2.13.

2.17. Calcein-AM Assay

Du145 parental (4×10^3) and resistant (7.5×10^4) cells were seeded in 96-well plates. Cells were treated with PRMT5 inhibitors (5 μM) for 24 h and then incubated with 125 nM Calcein-AM (Invitrogen, C1430) for 30 min at 37°C. Images were acquired by an inverted fluorescence microscope (Leica DMI8).

2.18. RNA sequencing and Analysis

The Poly-A capture, library preparation, and next-generation sequencing processes were outsourced to BGI Group. BGI-seq was performed for the sequencing, producing 150 bp double-ended reads with 20 million reads per sample. For this study,

RNA sequencing was chosen as a reproducible method, and biological repeats (n=3) were preferred rather than technical repeats. The obtained sequencing data was analyzed to a standard RNA-seq scheme. Initially, the quality of the reads was assessed using FastQC software, ensuring rigorous quality control of the sequencing results (http://www.bioinformatics.babraham.ac.uk/projects/fastqc/). Subsequently, the high-quality sequencing data was aligned to the latest reference genome (NCBI GRCh38) using the TopHat alignment software (https://ccb.jhu.edu/software/tophat). Mitochondrial and mis-spliced genes were removed in this computational step, which was executed on the Koç University high-performance computer cluster. Following the alignment of sequencing reads, the relative abundance of each transcript was determined using Cufflinks (http://cufflinks.cbcb.umd.edu/). Subsequently, CuffDiff (http://cole-trapnell-lab.github.io/cufflinks/cuffdiff/) was employed to identify differentially expressed genes (DEGs) by comparing the samples. The biological functions of the identified genes were then analyzed using Gene Set Enrichment Analysis (http://software.broadinstitute.org/gsea). The RNA-Sequencing and subsequent bioinformatics analysis were kindly conducted by Dr. Hamzah Syed from the School of Medicine at Koç University.

2.19. Annexin-V Staining Flow Cytometry Assay

Parental and resistant cells were seeded in 6-well plates and treated with PRMT5 inhibitors (5 µM), taxanes (at their respective IC_{50} values), and a combination of both for 72 h. After the treatment, the cells were harvested at 300 g for 5 min. The drug treated and untreated cells were then suspended in PBS containing 1% FBS to a concentration of 100-500 cells per µL for further analysis.

75 µL of cell suspension was mixed with 75 µL of Muse® Annexin-V dye, which also included the vital dye 7-AAD (7-aminoactinomycin D) to assess membrane integrity. The mixture was then incubated in the dark at RT for 20 min. Following the incubation, the cells were quantified using Muse® Cell Analyzer (Millipore).

2.20. Caspase 3/7 Activation Flow Cytometry Assay

Parental and resistant cells were seeded in 6-well plates and treated with PRMT5 inhibitors (5 µM), taxanes (at their respective IC_{50} values), and a combination of both for

72 h. After the treatment, the cells were harvested at 300 g for 5 min. The drug treated and untreated cells were then suspended in PBS containing 1% FBS to a concentration of 100-500 cells per µL for further analysis.

50 µL of cell suspension and 5 µL of caspase 3/7 reagent (prepared in PBS at a ratio of 1:8) (MCH4700-1505) was incubated for 30 min at 37 °C. Then, 150 µL of 7-AAD dye solution which was diluted with 1X Assay Buffer (MCH4700-1360) at a ratio of 1:75 (MCH4700-1505) was added to the cell suspension and incubated for an additional 5 min at RT. Cells were quantified using Muse® Cell Analyzer (Millipore).

2.21. Cell Cycle Analysis

Parental and resistant cells were seeded in 6-well plates and treated with PRMT5 inhibitors (5 µM), taxanes (at their respective IC_{50} values), and a combination of both for 24 h. After the treatment, the cells were harvested at 300 g for 5 min. The drug treated and untreated cells were then suspended in PBS containing 1% FBS to a concentration of 100-500 cells per µL for further analysis.

Cell cycle analysis was conducted using the Muse® Cell Cycle Assay kit (MCH100106). Following drug treatment, cells were centrifuged at 300 g for 5 min, washed with cold PBS, and fixed with 70% ethanol for 3 h at -20°C. Subsequently, the cells were washed with PBS and incubated in the dark with 200 µl of Cell Cycle Reagent for 30 min. The distribution of cells in different cell cycle phases was determined using the Muse® Cell Analyzer (Millipore).

2.22. Immunofluorescence (IF) Staining

Immunofluorescence (IF) Staining was performed in U2OS, Du145-P, MIA-Paca-2, MDA-MB-231, HEK-293T and RPE1 cell lines. The cells were seeded (2×10^5) with coverslips in 6-well plates. The next day, the cells were rinsed with PBS and were fixed using methanol (Merck, 1.06009) for 15 min at -20°C then were blocked with 5% BSA (Sigma, A8022) for an hour. They were incubated overnight at 4°C for primary antibodies (Cell Signaling Technology, 79998; Sigma, T5192) (Only a maximum of 2 antibodies can be used concurrently on a single glass coverslip.). Following this, they were incubated

with secondary antibodies (Thermo Scientific, A11029 and A11032) for an hour in dark at RT, and then were affixed to slides using a cover solution including DAPI, a DNA dye (Vectashield, H1200). Observations were observed using a Zeiss Axio Imager M1 fluorescence microscope.

2.23. Cell Cycle Arrest

U2OS cells were synchronized using standard synchronizing agents, including double thymidine block (Sigma, T1895) and S-trityl-L-cysteine/Colcemid (Sigma, 164739; Sigma, 10295892001). For the double thymidine block method, 2×10^5 cells were placed in 6-well plates. After 6 hours, 2.5 mM of thymidine was introduced to the medium. The thymidine-containing medium was discarded 18 hours later, and the cells were rinsed twice with PBS before fresh medium was added. Another thymidine dose (2.5 mM) was administered 8 hours later. 18 hours post this addition, cells were found halted at the end of G1 phase and beginning of the S phase. S-trityl-L-cysteine acts as a microtubule inhibitor, causing cell arrest in the S/G2 phase (Apraiz et al., 2017). By applying 10 µM for 16-18 hours, cell synchronization in the G2/M phase was achieved. Also, another compound was used for cell cycle arret, Colcemid. It binds to microtubules and arrests the cells in metaphase. By applying 0.5 µg/mL for 16-18 hours, cell synchronization in the metaphase was achieved. Three distinct experimental setups were executed: solely double thymidine block, a combination of double thymidine and STLC, and just colcemid. The results of the cell cycle synchronization were evaluated using the Muse analyzer (Millipore) according to the procedures outlined in Chapter 2.21.

2.24. Statistical Analysis

GraphPad Prism 8 was used to analyze all statistical tests as described in figure legends. The *p <0.05 was evaluated and noted as significant.

Chapter 3:

RESULTS

3.1. Generation of Taxane Resistant CRPCa Cell Models

To establish an *in vitro* model for taxane resistance in CRPCa, two distinct cell lines, DtxR (Docetaxel-resistant) and CbzR (Cabazitaxel-resistant), were successfully generated by Buse Cevatemre, Ph.D, and İpek Bulut, MSc, using the cell lines Du145 and 22Rv1. This process took approximately 8 to 12 months. The taxane sensitive cells (Du145-P and 22Rv1-P) were seeded overnight and then incubated for 72h in the presence of Dtx/Cbz for drug hits. After those hit cells had recovered, the hit and recovery cycle was repeated (Figure 3.1A). The level of acquired resistance to Dtx/Cbz, was visualized and quantified via SRB cell viability and colony formation assays (Figure 3.1B, C).

A.

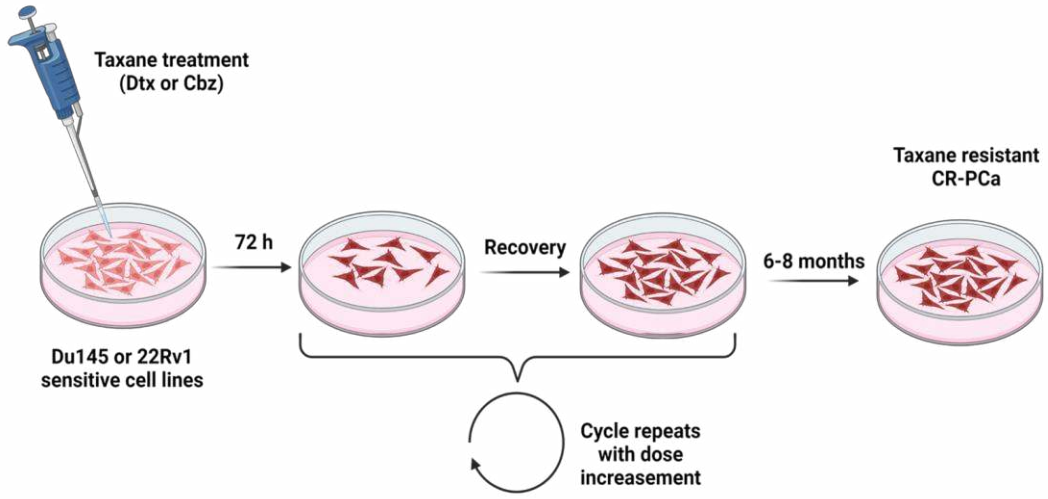

B.

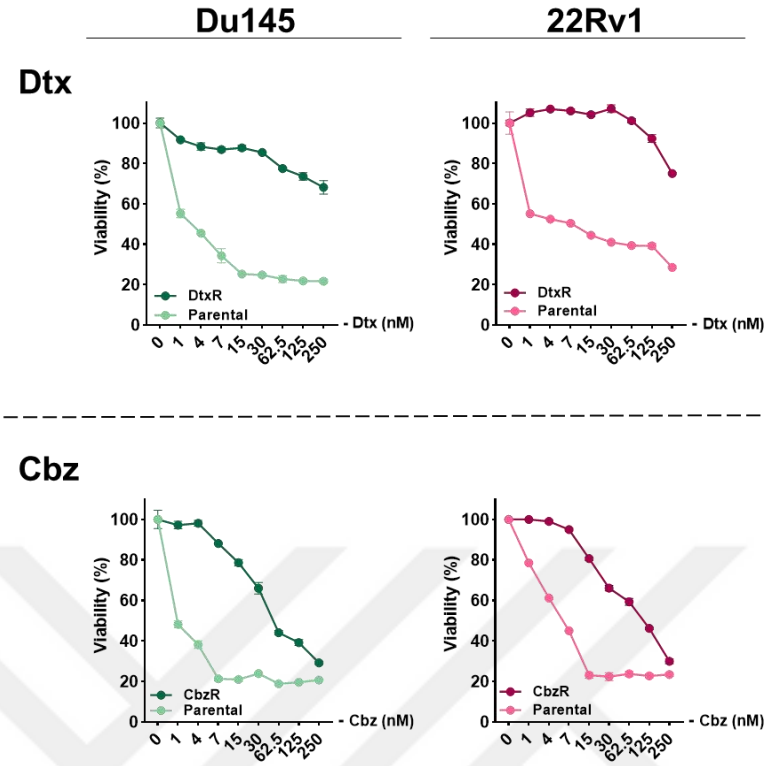

C.

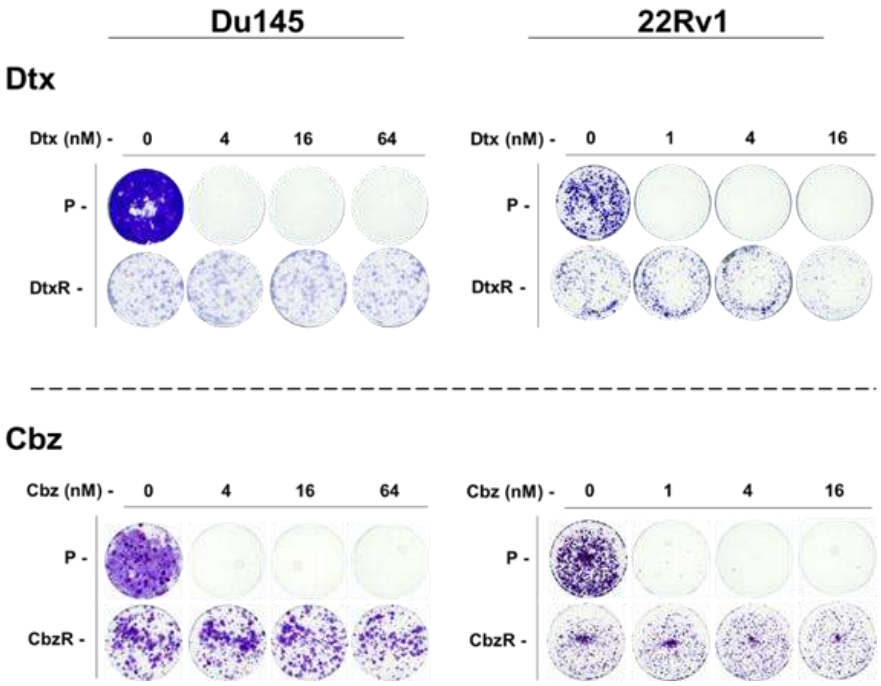

İpek Bulut, MSc.
Buse Cevatemre, Ph.D

Figure 3.1. Establishment and characterization of taxane resistant cells. (A) The framework for generation of taxane resistant cell models. The figure was adapted from Cevatemre et al. (2023) and illustrated using BioRender. **(B)** The dose-response curve after Dtx or Cbz treatment (72h) on both parental and resistant cell lines via SRB cell viability assay. **(C)** The clonogenic capacity of parental and resistant cells were shown after the taxane treatment. The relative colony forming ability of cells was evaluated at 10 to 15 days post-drug exposure. Error bars represent the SEM of three biological replicates.

Table 3.1 signifies the relative resistance (RR) to Dtx/Cbz observed in the resistant cells compared to their parental ones. It is also important to note that IC_{50} values of taxanes in resistant cells exceeded the maximum treatment dose, let alone being more than ten-fold higher than the parental compartments.

Table 3.1. Comparison of the IC_{50} values and relative resistance of Dtx/Cbz resistant cells.

Cell Lines	IC_{50} Values (Dtx - nM)	RR Index
Du145 – P	3.02	1.00
Du145 – DtxR	>250	>82.69
22Rv1 – P	8.38	1.00
22Rv1 – DtxR	>250	>29.82
Cell Lines	IC_{50} Values (Cbz - nM)	RR Index
Du145 – P	1.92	1.00
Du145 – CbzR	54.09	28.05
22Rv1 – P	6.58	1.00
22Rv1 – CbzR	106.9	16.22

Buse Cevatemre, Ph.D

3.2. The Effect of Taxane Resistance on Cell Proliferation

Doubling time was evaluated to determine the proliferation rates of both parental and taxane-resistant cells. The results of this assay provided significant insights into the growth dynamics of two cell populations: Du145-P and Du145-DtxR. Doubling time

assay result graphically represents the progressive increase in cell numbers over time, highlighting the overall expansion of the parental cells when compared to their resistant counterparts (Figure 3.2). This observed growth pattern suggests active cell division and continual augmentation of cell numbers in the parental cells throughout the experimental duration. The findings from this study demonstrate the active cell division and progressive growth of the Du145 cells as evident by the increase in cell divisions over time and the continuous rise in cell numbers in doubling time across different passages. The assay results significantly broadened our knowledge about growth behavior and dynamics of resistant and sensitive cells, thus providing invaluable information for further investigations. This experiment was kindly done by Beyza Dedeoğlu Aydın, MSc.

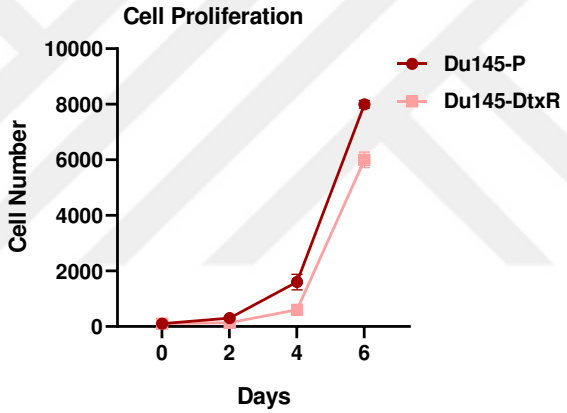

Beyza Dedeoğlu Aydın, MSc.

Figure 3.2. Difference in proliferation capacities of Du145-P and Du145-DtxR cells. Cell proliferation rates were depicted, with the number of cells increasing over observed time-points. Error bars represent standard deviation (StDev) of two biological replicates.

3.3. The Reversion of Taxane Resistance via PRMT5 Inhibition in CRPCa

3.3.1. Epigenetic drug library screening identifies PRMT5 as a re-sensitizer to taxanes

Buse Cevatemre, PhD, and İpek Bulut, MSc, conducted an epigenetic drug library screening to elucidate potential targets upon the epigenetic mechanisms that lead to taxane resistance in CR-PCa (Figure 3.3A). The epigenetic drug library contains 145 compounds. The top 5 classes of epigenetic targets that induced the resensitization of resistant compartments were identified, CBP/p300, BRPF, Menin-MLL, PRMT5, and

SIRT1 (Figure 3.3B). Subsequently, the significance of PRMT5 inhibitors (Figure 3.3C) was underscored, primarily due to the dearth of existing literature concerning drug resistance in prostate cancer. Consequently, the advent of PRMT5 presented a promising opportunity to explore novel avenues for therapeutic interventions.

A.

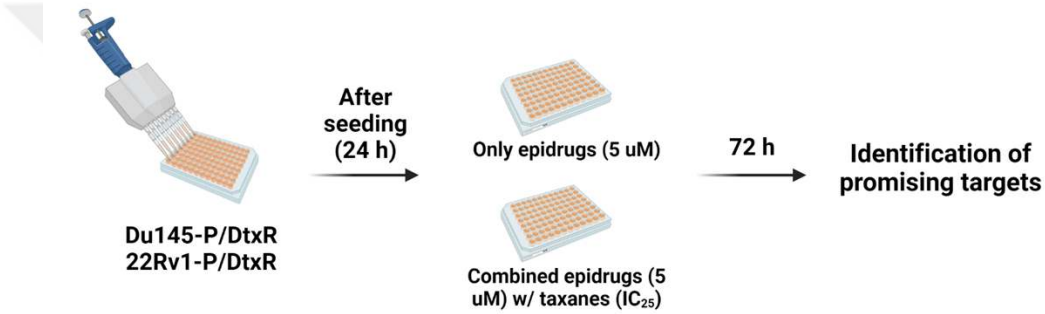

B.

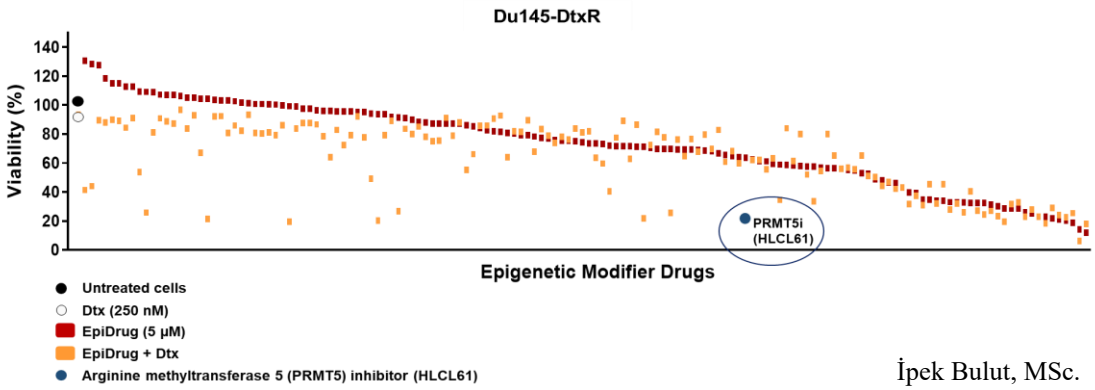

İpek Bulut, MSc.
Buse Cevatemre, Ph.D

C.

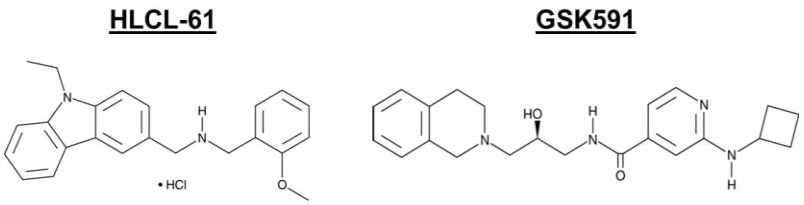

Figure 3.3. Epigenetic drug library screening on Du145-DtxR cells. **(A)** A schematic representation of epigenetic drug library screening. The figure was adopted from Cevatemre et al. (2023) and illustrated using BioRender. **(B)** The SRB cell viability assay was performed to identify the epigenetic modulators capable of overcoming taxane resistance by screening 145 targeted epidrugs. The results were obtained in Du145-DtxR cells. The cellular viability observed upon the individual application of each epidrug was represented using red dots, while the synergistic cytotoxic impact arising from their combinatorial treatment with Dtx was illustrated using the orange dots. One of the re-sensitizers of the drug library, HLCL-61 (PRMT5 inhibitor), is indicated as a blue dot. **(C)** Chemical structure of PRMT5 inhibitors.

The family of PRMT enzymes function as epigenetic "writers" responsible for catalyzation of three methylation marks in the context of post-translational modifications (PTMs) (H. Kim and Ronai 2020). Arginine methylation, a widespread pattern of PTM, plays a crucial role in major cellular biological processes. PRMT5 is primarily responsible for catalyzing symmetric dimethylation (me2s) of arginine residues (Jing, Xie, et al. 2018) in H3 and H4 histones. These methylation marks are commonly associated with the transcriptional repression (F. Liu et al. 2020). PRMT5 is involved in the modification of factors that govern the cell cycle, thereby facilitating activation at cell cycle checkpoint and DNA repair facilitated by homologous recombination. Moreover, PRMT5 is also involved in the complexity in oncogenesis, since it is known to control the expression of genes which promote and suppress the tumorigenesis (H. Kim and Ronai 2020).

We validated this hit by initially subjecting PRMT5 inhibitors to a broader dose range screening. It was observed that, as the doses of these inhibitors increased, resistant cells exhibited increased sensitivity to taxanes (Figure 3.4A) while no sensitization was

observed on parental cells (Figure 3.4B). These findings were supported by colony formation assays (Figure 3.5).

A.

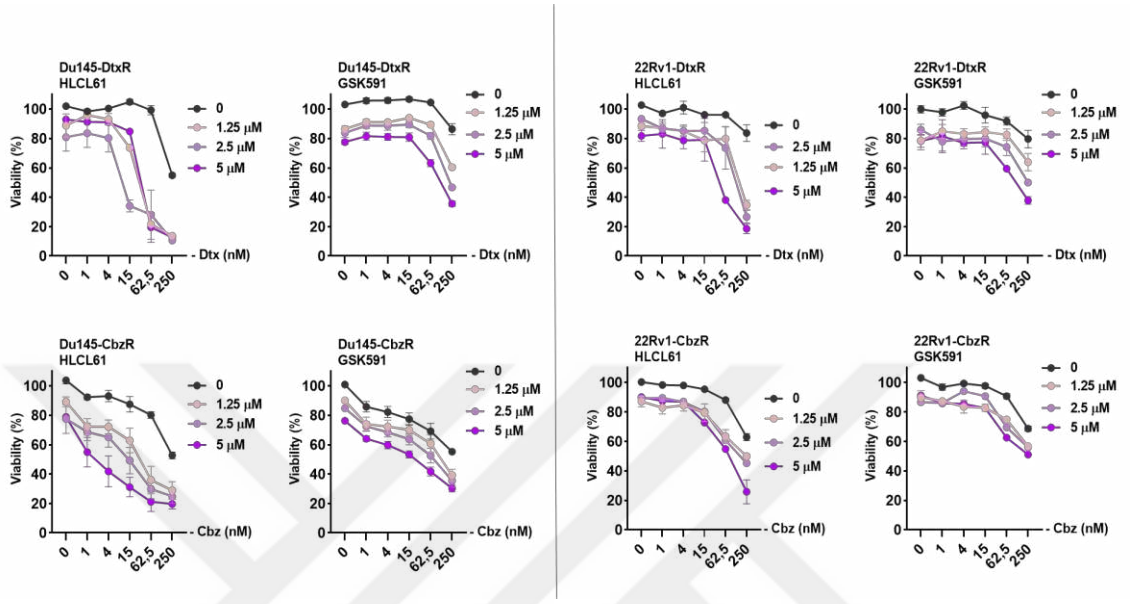

B.

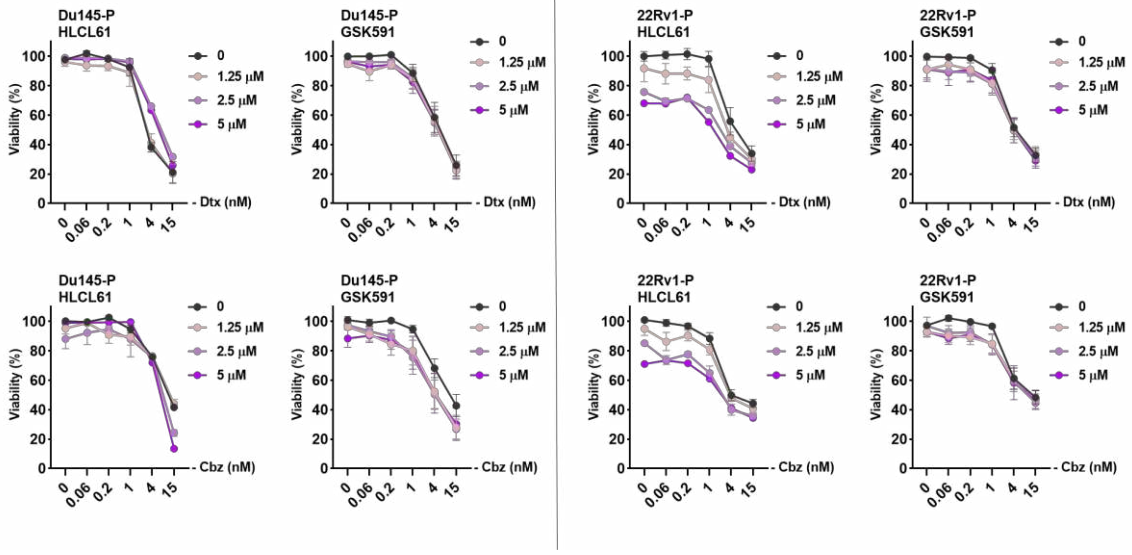

Figure 3.4. Inhibition of PRMT5 exerts an effect of overcomed taxane resistance. The dose-response curves of taxane treatment in combination with PRMT5 inhibitors (HLCL-61 and GSK591) for 72 h were validated on both Du145 and 22Rv1 resistant cells **(A)** and Du145 and 22Rv1 parental cells **(B)**. Error bars represent the Standard Error of the Mean (SEM) from three biological replicates.

A.

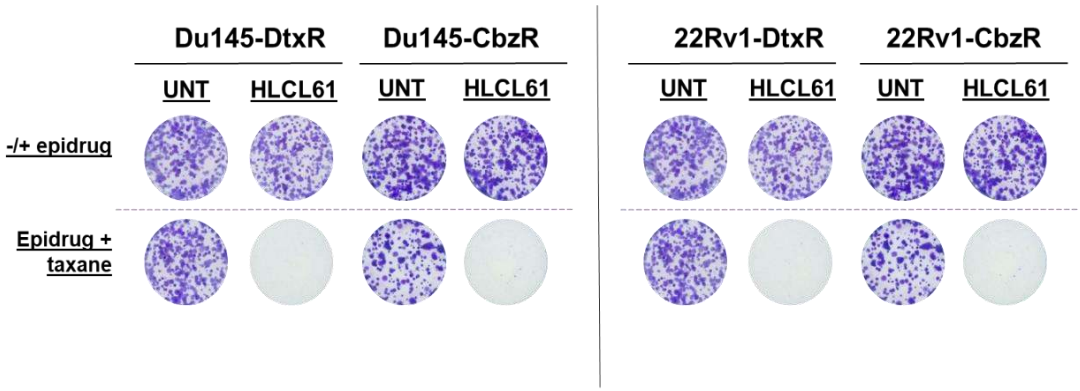
Du145-DtxR
Du145-CbzR
22Rv1-DtxR
22Rv1-CbzR
UNT
HLCL61
-/+ epidrug
Epidrug + taxane

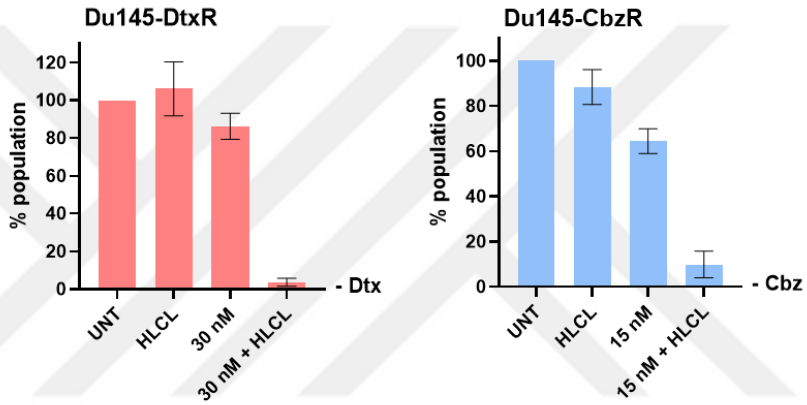
Du145-DtxR
% population
- Dtx
UNT
HLCL
30 nM
30 nM + HLCL
Du145-CbzR
- Cbz
15 nM
15 nM + HLCL

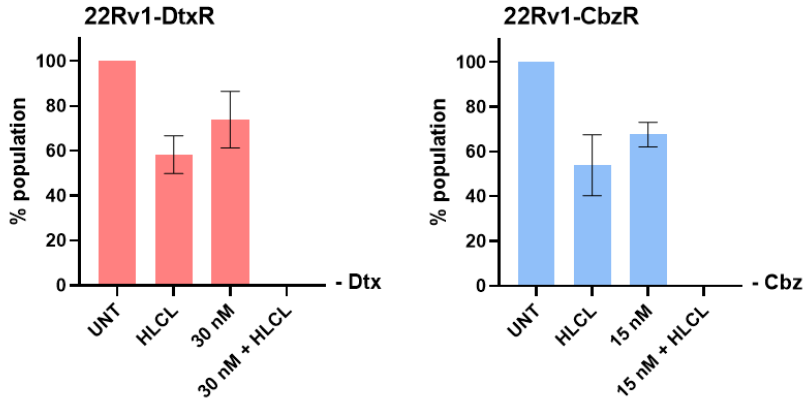
22Rv1-DtxR
% population
- Dtx
UNT
HLCL
30 nM
30 nM + HLCL
22Rv1-CbzR
- Cbz
15 nM
15 nM + HLCL

B.

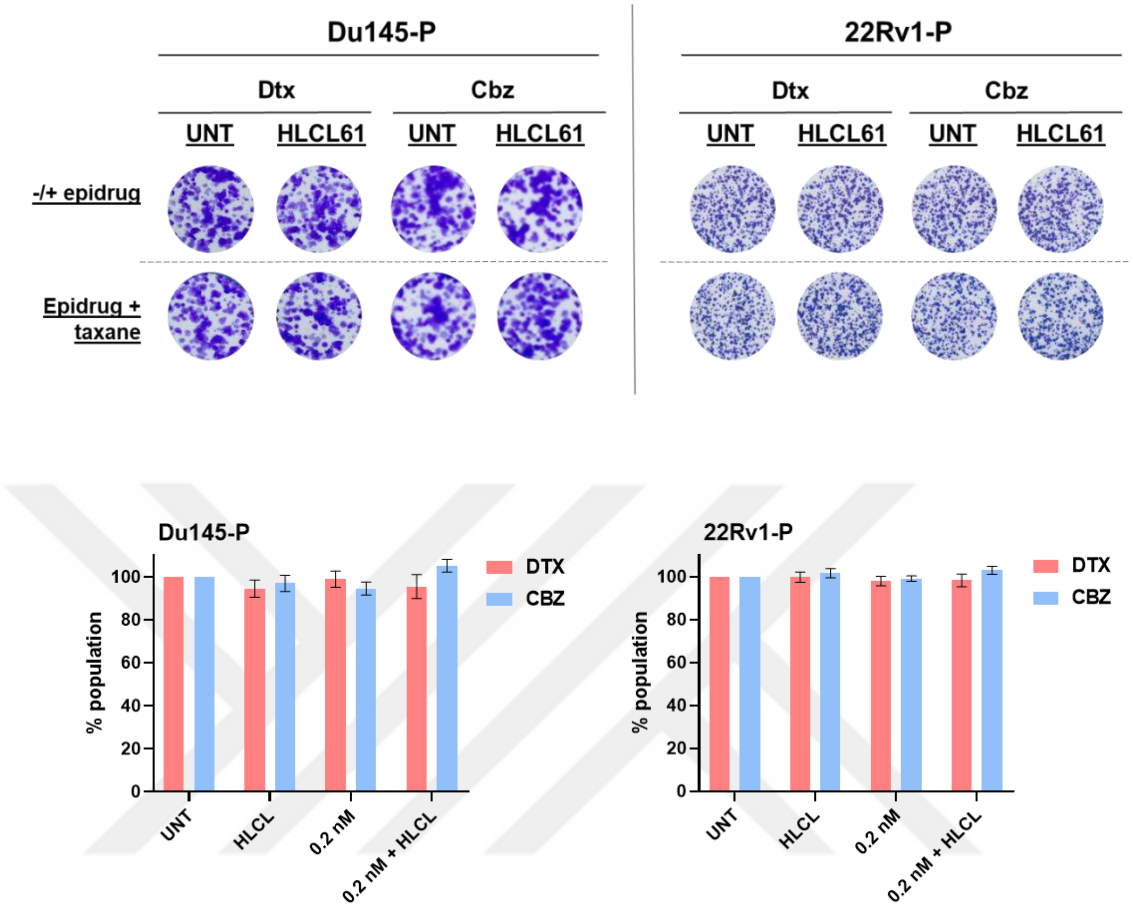

Figure 3.5. Pharmacological inhibition of PRMT5 affects the clonogenic capacity of taxane-resistant cells. Clonogenic capacity of resistant **(A)** and parental **(B)** cells were analyzed by treating cells with the specified drugs for 72 h, allowing the colony formation for 10-15 days post-treatment (The concentrations used are as follows; untreated (UNT), Dtx/Cbz; 0.2 nM for parental cells; Dtx/Cbz 30/15 nM for resistant cells, and PRMT5 inhibitor; 5 µM). The quantification of colony area was performed using ImageJ software and graphs shown below. Error bars represent the SEM of means of two biological replicates.

3.3.2. The effect of PRMT5 knock-down on clonogenic capacity of cells

This study investigated whether both siRNA mediated knockdown and CRISPR guided knockout (Figure 3.8) would yield similar effects to epi-drug treatments. Upon evaluating the colony formation assay, it was observed that PRMT5 silenced (Figure 3.7) cells exhibited reduced growth in all cell lines (Figure 3.6). Moreover, PRMT5 inhibition

exhibited greater growth suppression in resistant cells compared to parental ones. The identical phenomenon was observed in PRMT5 knock-out cells as well (Figure 3.8). These findings highlight the significance of PRMT5 in taxane resistance.

A.

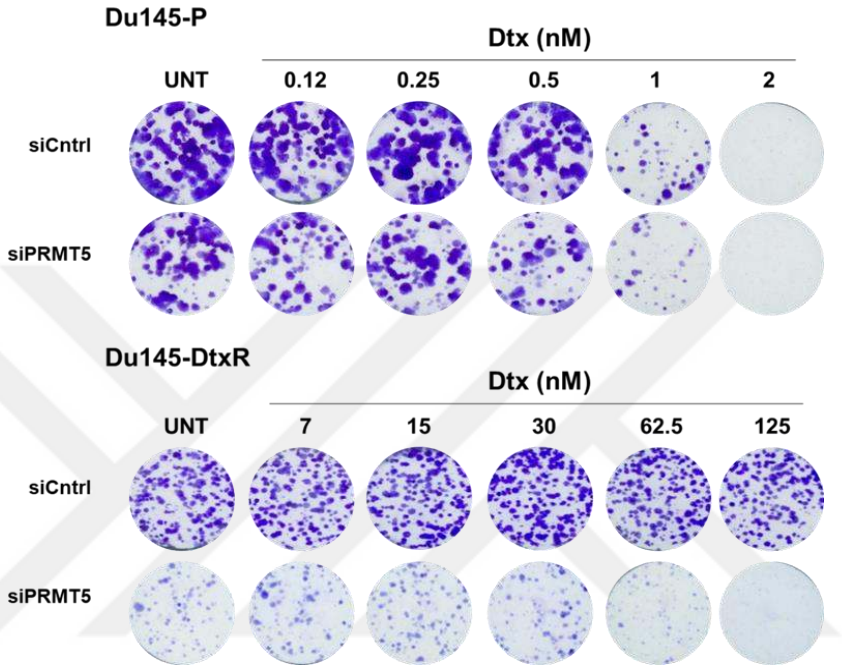

B.

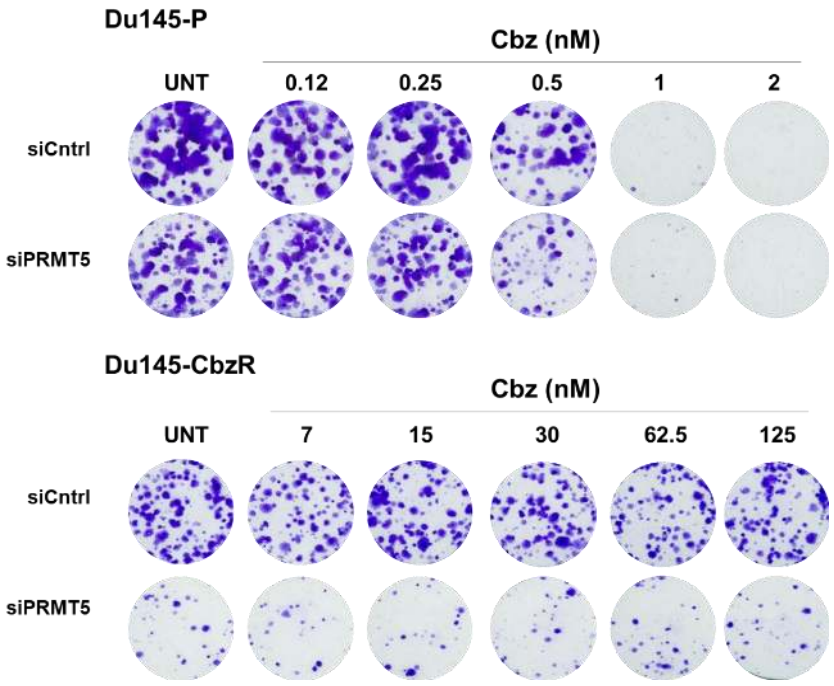

C.

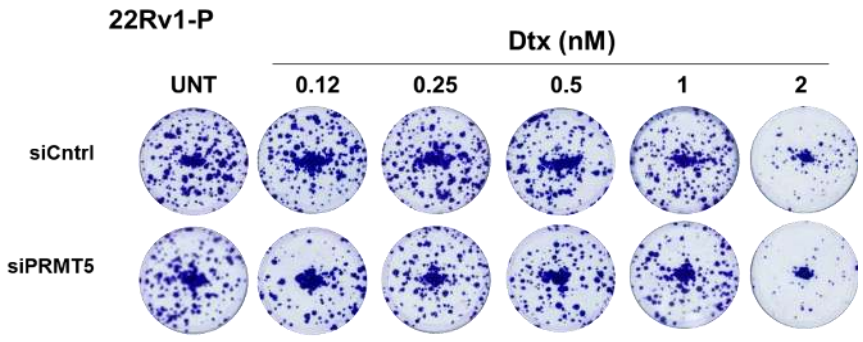

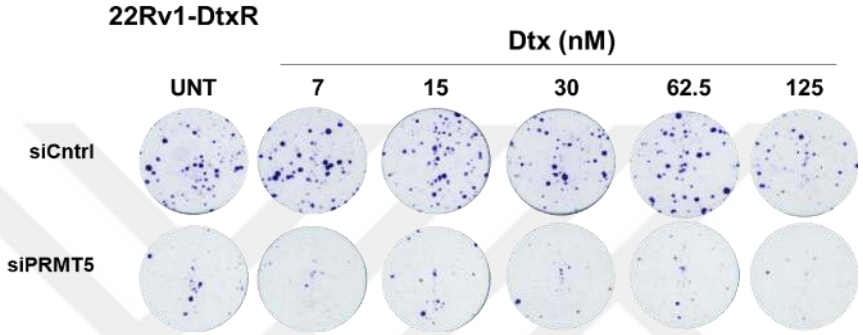

D.

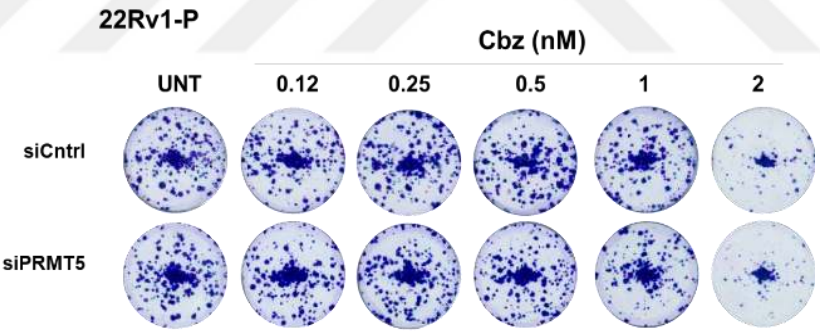

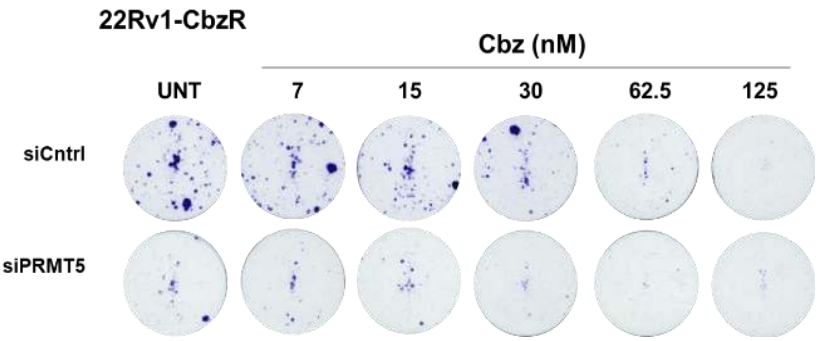

Figure 3.6. Colony formation capacity of Du145 cells after PRMT5 knock-down. Clonogenic capacity of Du145 **(A)** Dtx resistant and parental cells, Du145 **(B)** Cbz resistant and parental cell, 22Rv1 **(C)** Dtx resistant and parental cells, and 22Rv1 **(D)** Cbz

resistant and parental cells were analyzed by treating cells with the siRNA (**siCntrl**: control siRNA; **siPRMT5**: siRNA for PRMT5) for 72 h, allowing the colony formation for 10-15 days post-treatment (72 h). (The concentrations used are as follows; Dtx/Cbz; 0 (**untreated**: UNT), 0.12, 0.25, 0.5, 1 and 2 nM for parental cells; Dtx/Cbz 0 (**untreated**: UNT), 7, 15, 30, 62.5 and 125 nM for resistant cells).

A.

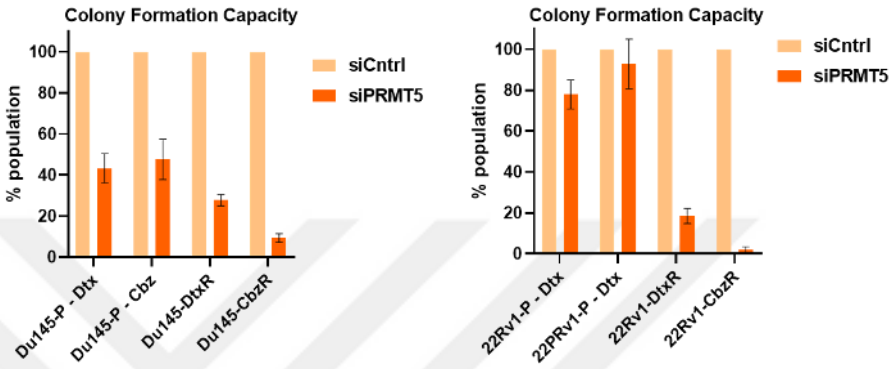

B.

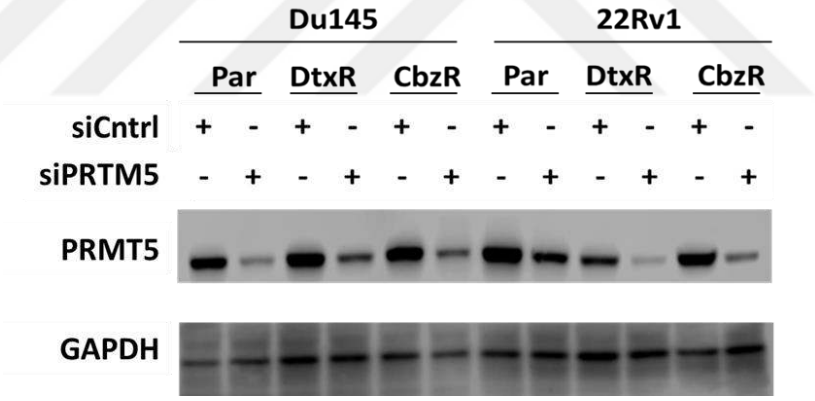

Figure 3.7. Quantification clonogenic capacity of cells after PRMT5 knock-down. **(A)** The quantification of colony area was performed using ImageJ software. The data is presented as mean ± SEM of two biological repeats. **(B)** Western blot results of PRMT5 knock-down after siPRMT5 silencing in parental and taxane resistant cells.

Efforts to generate PRMT5 knockout monoclonal cells were not successful, as the introduction of PRMT5-targeted gRNAs led to the inability of resistant cells to survive. This observation indicated the critical role of PRMT5 for the resistance phenotype.

A.

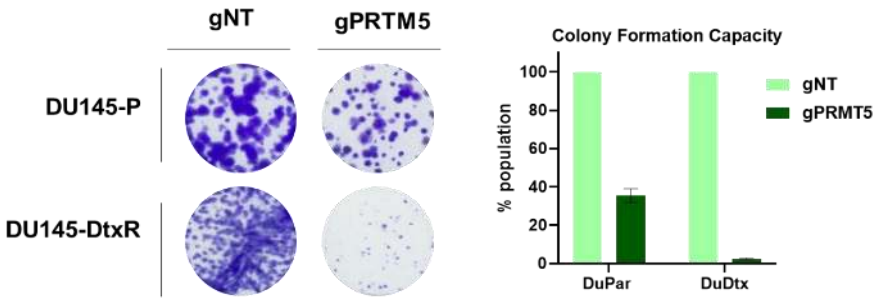

B.

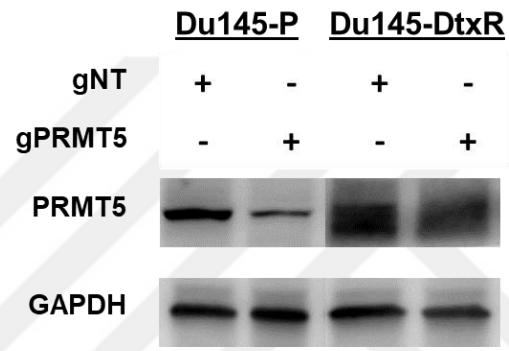

Figure 3.8. Clonogenic capacity of cells after CRISPR-Cas9-mediated knock-out of PRMT5. (A) Clonogenic images were obtained after generation of PRMT5 knock-out parental and resistant cells, and they were allowed for colony formation for 10-15 days. The quantification of colony area was performed utilizing ImageJ software (right), and the results are represented as a percentage relative of "mean ± SEM" to the cell population (**gNT**: non-targeting guide RNA; **gPRMT5**: PRMT5 specific guide RNA). **(B)** Reduction in PRMT5 expression in cells after targeting with gRNA is shown in western blot analysis.

3.3.3. The effect of PRMT5 Silencing on the Proliferation of Taxane-Sensitive and Resistant Cells

To gain a comprehensive understanding of the growth kinetics and proliferation rates of taxane-sensitive and resistant cell populations upon PRMT5 inhibition. A doubling time assay was conducted by using siRNA-treated cells. A decrease in proliferation in siPRMT5-treated cells in both the resistant and sensitive compartments of Du145 cell line (Figure 3.9) were observed. In conclusion, the results demonstrate that

siPRMT5 treatment resulted in reduced cell division and growth in both the Du145 parental and resistant cells. Furthermore, PRMT5 inhibition significantly decelerated the growth of resistant cells in comparison to parental cells.

A.

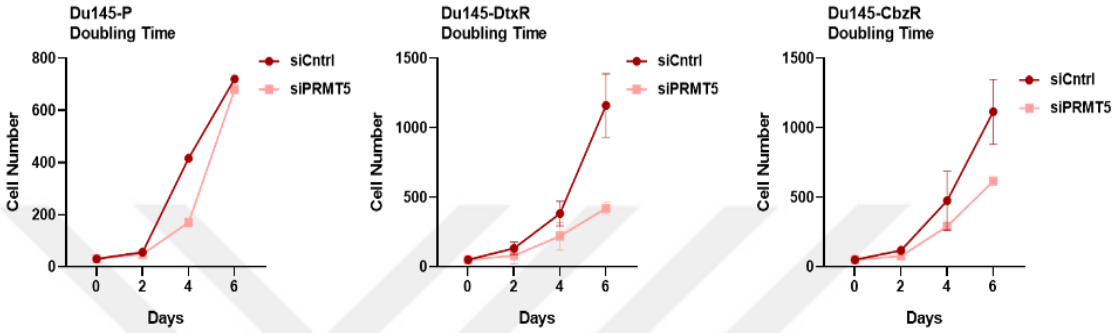

B.

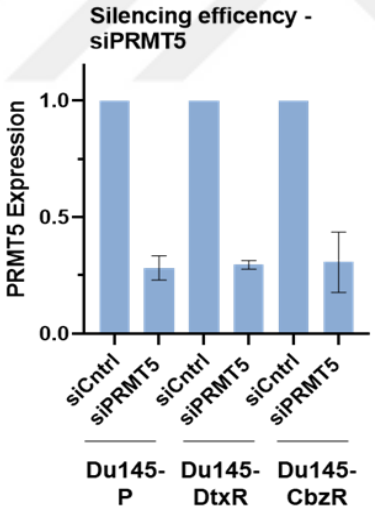

Figure 3.9. The effect of PRMT5 knock-down on cell proliferation in taxane sensitive and resistant cells. **(A)** Cell proliferation rates were depicted after siPRMT5 treatment for 72 h, with the number of cells increasing over observed time-points (days). Error bars represent StDev of two biological replicates. **(B)** PRMT5 siRNA knock-down efficiencies were checked via RT-qPCR 72 h post-treatment of siPRMT5. The data is presented as mean ± SEM of two biological replicates.

3.4 Characterization of PRMT5 Inhibitors

3.4.1. The effect of PRMT5 inhibitors on sDMA

PRMT5 functions as a type II PRMT, responsible for catalyzing the sDMA on a broad spectrum of targets which could be histones, TFs, splicing factors, and epigenetic regulators (Stopa, Krebs, and Shechter 2015; Mueller et al. 2021).

To assess the intracellular selectivity of the inhibitors, we intend to determine the protein level of symmetric dimethylarginine (sDMA) addition. Results confirmed a slight reduction in sDMA levels after HLCL-61 treatment in Du145-DtxR cells, whereas GSK591 treatment resulted in a more significant decrease in sDMA protein levels across all cell lines (Figure 3.10A). It is important to signify the reduction phenotype of sDMA modification on target proteins after GSK591 treatment when compared to HLCL-61 treatment.

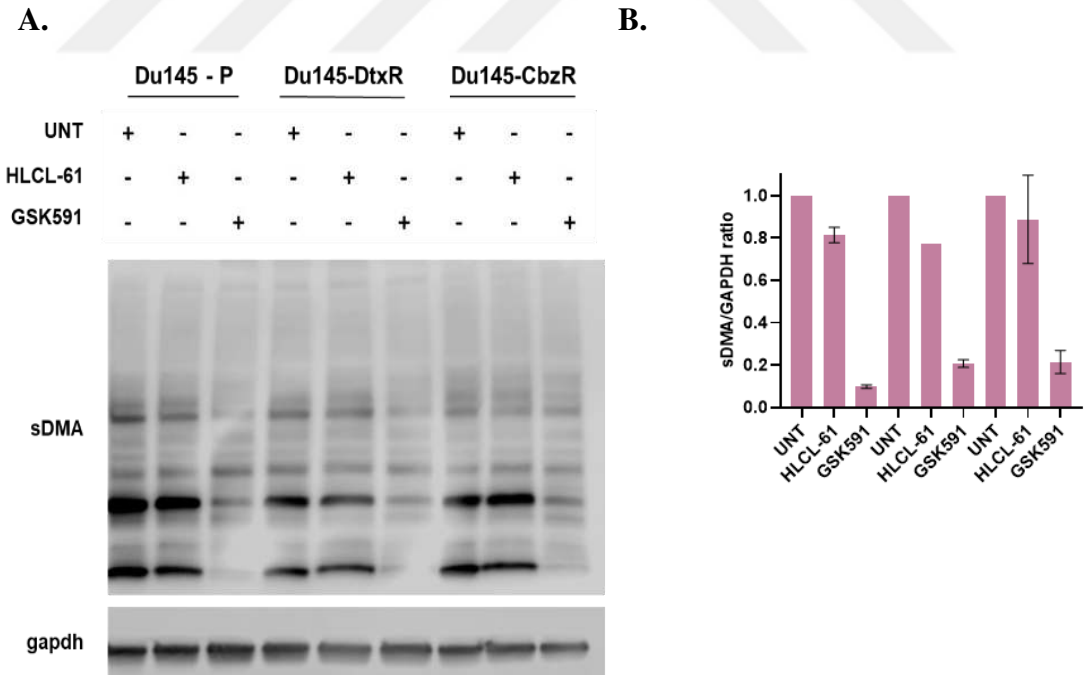

Figure 3.10. The sDMA modified target protein levels upon treatment with the PRMT5 inhibitors in Du145 parental and taxane resistant cells. (A) Western blot analysis shows the effect of PRMT5 inhibitors (**UNT**: untreated), HLCL-61 and GSK591; 72 h of treatment) on sDMA (Symmetric Dimethyl Arginine) modification levels. **(B)**

The quantification of bands was performed by using ImageJ software and represented as sDMA/GAPDH ratio. Error bars represent SEM of two biological replicates.

In addition to changes in sDMA modification on target proteins post-treatment with PRMT5 inhibitors, we also tested the change in sDMA modification on histones on Du145 parental and resistant cells. The results of the Western Blot analysis of histone extraction indicate that both HLCL-61 and GSK591 inhibitors reduced sDMA modification on histones in Du145-P cells. On the other hand, treatment with GSK591 on Du145-DtxR cells resulted in a more observable decrease in symmetrically demethylated arginine on histones as compared to treatment with HLCL-61. Conversely, in Du145-CbzR cells, neither of the PRMT5 inhibitors exhibited any alteration in sDMA modification levels on histones (refer to Figure 3.11). These findings collectively corroborate the inhibition of PRMT5 activity by using its inhibitors, as evidenced by changes in sDMA modification on both target proteins and histones.

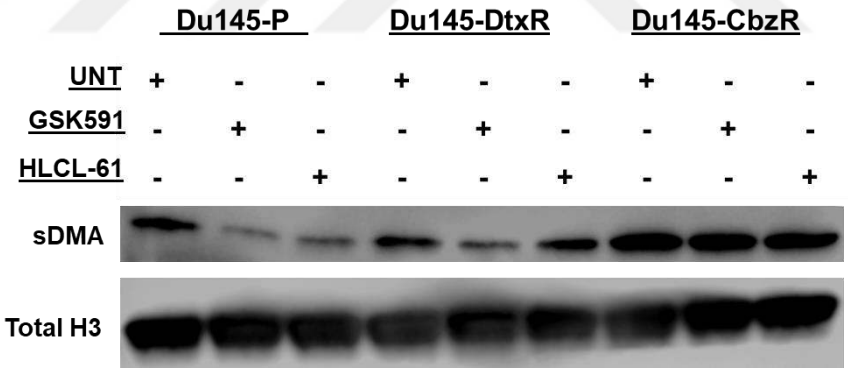

Figure 3.11. The sDMA modified histone levels upon treatment with the PRMT5 inhibitors in Du145 parental and taxane resistant cells. Western blot analysis shows the effect of PRMT5 inhibitors (UNT: untreated, HLCL-61 and GSK591; 72 h of treatment) on sDMA (Symmetric Dimethyl Arginine) modification levels on histones on Du145-P, Du145-DtxR, and Du145-CbzR cells.

We also evaluated the change in sDMA modified target protein levels after siRNA-mediated PRTM5 knock-down. 72 h post-transfection of siRNA on Du145-P and Du145-DtxR cells, sDMA modification and PRMT5 levels were checked via Western Blotting experiment. Compared to control siRNA, siPRMT5 samples have slightly

decreased levels of total sDMA modified proteins on both parental and docetaxel resistant Du145 cells (Figure 3.12). Overall, inhibitor- and siRNA-mediated inhibition of PRMT5 results in decreased levels of sDMA modifications on target proteins.

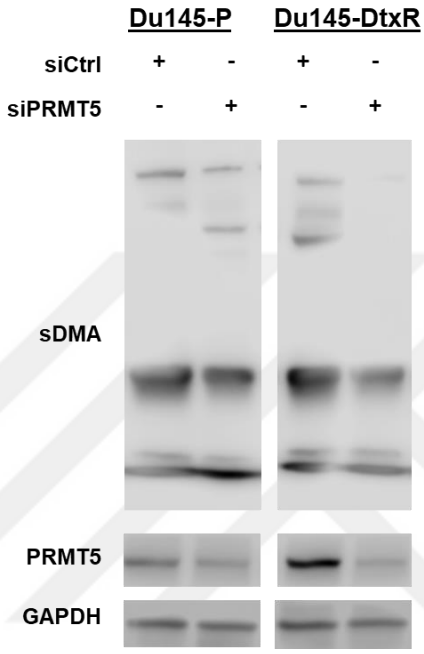

Figure 3.12. The sDMA modified target protein expression levels upon siRNA-mediated PRMT5 knock-down on Du145-P and Du145-DtxR cells. Western blot analysis shows the effect of siPRMT5 (72h) knock-down on sDMA modified total protein level on Du145 parental and docetaxel resistant cancer cells.

3.4.2. Evaluation of Target Engagement of PRMT5 Inhibitors by CETSA

To evaluate the target engagement (TE) of the inhibitors, the Cellular Thermal Shift Assay (CETSA) was employed. Cellular thermal shift assay (CETSA) serves as a valuable method for assessing drug/inhibitor-protein interactions, also referred to as target engagement (Jafari et al. 2014) (Figure 3.11B). This assay enables the observation of how a ligand binds to a protein by monitoring its stabilization through increasing temperature. The fundamental principle underlying CETSA lies in evaluating the strength of the interaction between the target protein and the tested inhibitor. To conduct the CETSA assay, cells were treated with the compound of interest and a DMSO control,

subsequently were subjected to varying temperatures through a thermal cycler, inducing a heat shock. As the temperature increases, the target protein gradually unfolds and aggregates. The temperature at which this aggregation occurs is indicative of the inherent thermal stability of the specific protein within the cell.

When the drug engages with the target protein, it confers greater stability upon the protein, requiring higher temperatures for unfolding due to additional bonding between the protein and the small molecule of interest. Therefore, by comparing the aggregation temperatures observed in the presence and absence of the drug, the thermodynamic shifts indicate the engagement trend. This methodology (Jafari et al. 2014) provides a valuable approach for assessing drug/inhibitor-protein interactions within cellular environments, yielding insights into target engagement and inhibitor efficacy. The CETSA results showed that GSK591 demonstrated PRMT5 engagement in all cells compared to the vehicle control. (Figure 3.11A).

Furthermore, this study focused on assessing the inhibitory effect of GSK591 on PRMT5 expression. Results showed that there was no significant change in the PRMT5 expression in parental cells, whereas GSK291 treatment made a significant reduction in the protein level of PRMT5 in taxane resistant cells (Figure 3.11C).

A.

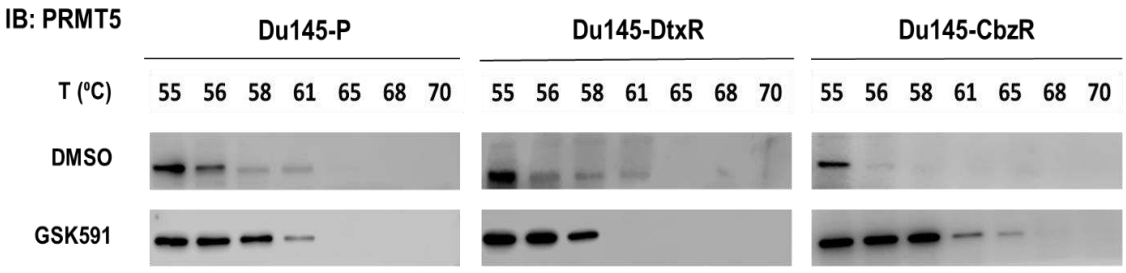
IB: PRMT5
Du145-P
Du145-DtxR
Du145-CbzR
T (°C)
55 56 58 61 65 68 70
DMSO
GSK591

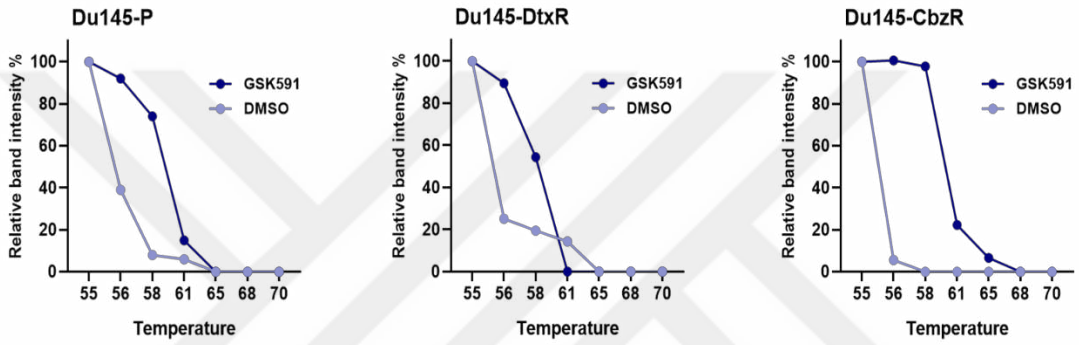
Du145-P
Du145-DtxR
Du145-CbzR
Relative band intensity %
100
80
60
40
20
0
GSK591
DMSO
55 56 58 61 65 68 70
Temperature

B.

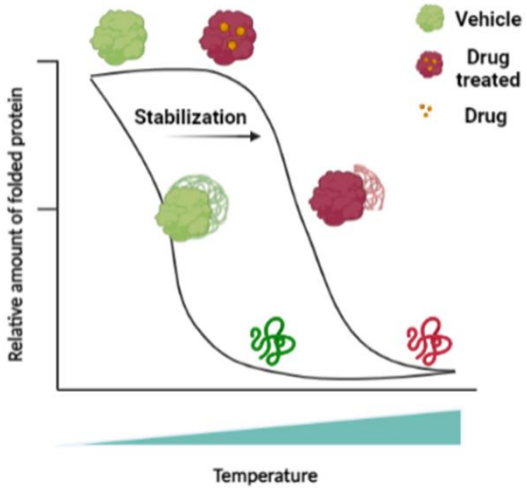
Vehicle
Drug treated
Drug
Stabilization
Relative amount of folded protein
Temperature

C.

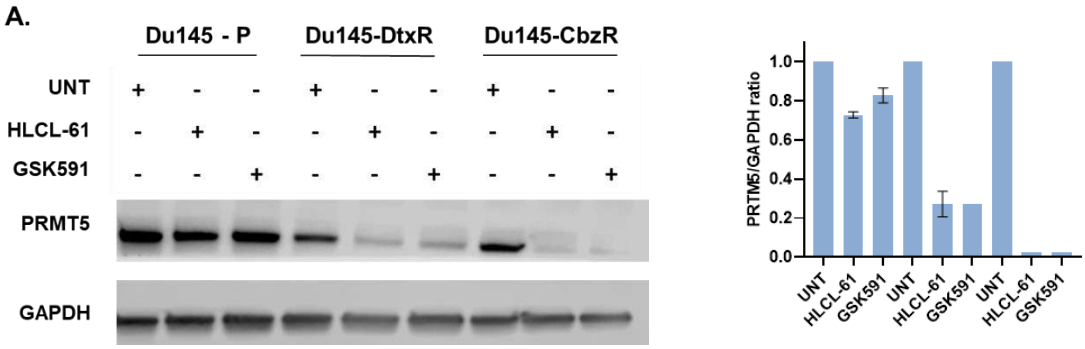

Figure 3.13. The effect of PRMT5 inhibitor GSK591 on target engagement and PRMT5 expression in Du145 cells. (A) Target engagement of PRMT5 inhibitor GSK591 was evaluated through CETSA in all Du145 parental and taxane resistant cell lines (5 µM, 1 h). The quantification of bands was performed by using ImageJ software, shown below. **(B)** A schematic illustration of CETSA (the figure was generated by BioRender). **(C)** Western blot analysis showing the reduction levels of PRMT5 expression after GSK591 treatment (5 µM, 72 h) (left). The quantification of bands was performed using ImageJ software (right).

3.5. The Underlying Cause of Resistance: ABCB1

ABCB1 is a transmembrane efflux protein playing a pivotal role in expelling diverse substrates from cells. Notably, this protein is associated with the resistant phenotype developed against various chemotherapeutic agents including docetaxel, doxorubicin, and paclitaxel (Lombard et al. 2017). ATP-binding cassette (ABC) transporters play an important role in conferring multidrug resistance in cancer, particularly with ABCB1 serving as a mediator of resistance to various chemotherapeutic agents (Hodges et al. 2011). ABCB1 functions as an efflux pump located on the cellular membrane, facilitating drug efflux, and consequently lowering intracellular drug concentration, leading to a reduction in drug activity (Figure 3.12A).

In a previous analysis performed by Buse Cevatemre, Ph.D, and İpek Bulut, MSc, gene expression analysis of Du145-DtxR and Du145-CbzR cells compared to Du145-P cells was conducted using the RNA sequencing method. A notable finding was the increased ABCB1 gene expression in taxane-resistant cells (Figure 3.12B). To confirm

this observed overexpression, WB analysis was performed and revealed significantly elevated levels of ABCB1 expression in DtxR and CbzR cells (Figure 3.12C).

A.

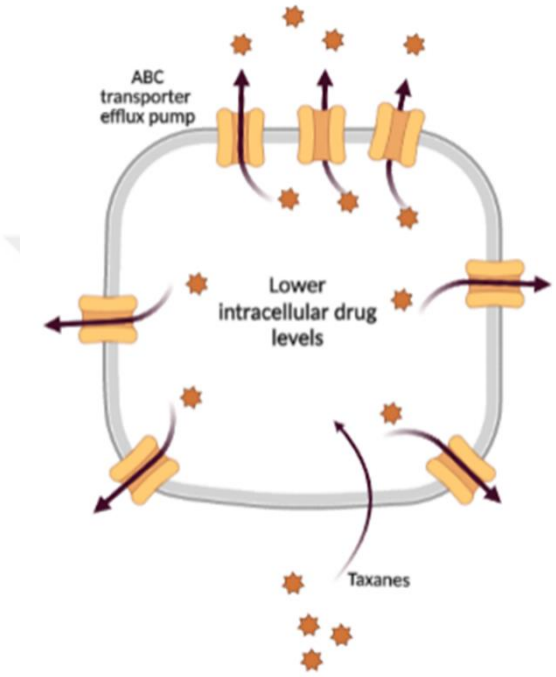

B.

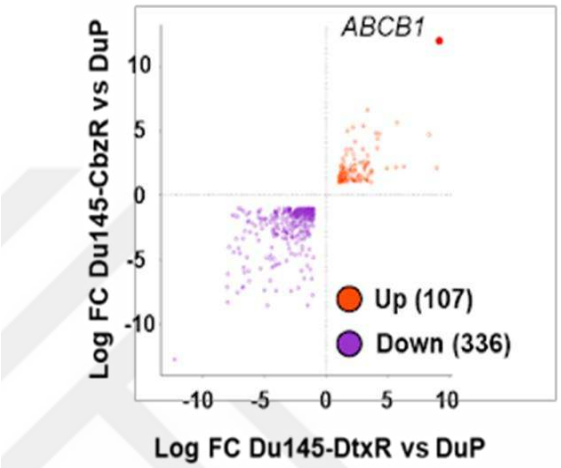

Buse Cevatemre, Ph.D

C.

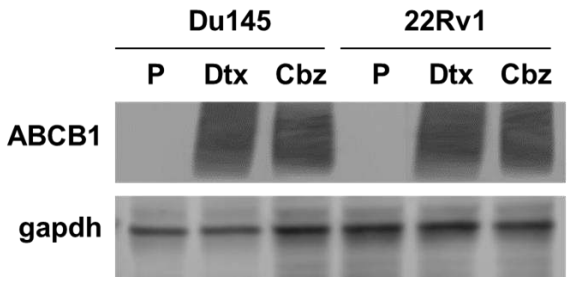

Figure 3.14. ABCB1 overexpression in taxane resistant cells. **(A)** A schematic representation of ABC transporter efflux pump (the figure was generated by BioRender). **(B)** Genes exhibiting differential expression (FDR < 0.05, and Log2FC ≥ 1 or ≤ -1) between cells resistant to Dtx and Cbz were categorized according to the direction of their expression changes (either **upregulated** or **downregulated**). One of the notable genes among these hits is **ABCB1**. **(C)** Western blot analysis was performed to see change in ABCB1 expression in all Du145 and 22Rv1 cell lines.

As stated before, in prior investigations, it was noted that there was an increase in ABCB1 expression as parental cells become taxane resistant, shown in both Du145 znd 22Rv1 cells (both Dtx and Cbz resistant cells). Interestingly, it was observed (by Buse Cevatemre, PhD and İpek Bulut, MSc) that the inhibition of ABCB1 substantially reversed the resistance, leading to the parental phenotype. This phenotypic observation was enough to note that an increase in ABCB1 expression alone is sufficient to transform parental cells into resistant states (data not shown).

A calcein uptake assay was carried out to assess if PRMT5 inhibitors influence ABCB1 function. In this assay, Calcein-AM serves as a substrate for ABCB1, whereby it is internalized by cells and subsequently enzymatically cleaved by cytoplasmic esterases, resulting in the production of green, fluorescent calcein (Figure 3.13A). Consequently, resistant cells due to elevated ABCB1 levels effectively efflux the calcein-AM from the plasma membrane, leading to reduced fluorescence within the cytosol. Conversely, parental cells, with minimal ABCB1 expression, show intracellular hydrolysis of calcein-am, thus exhibiting the higher fluorescence (Figure 3.13A). Upon the treatment of PRMT5 inhibitors to parental and resistant cells, a significant increase in green fluorescence was observed in taxane-resistant cells, while the parental compartment remained unaffected (Figure 3.13B).

A.

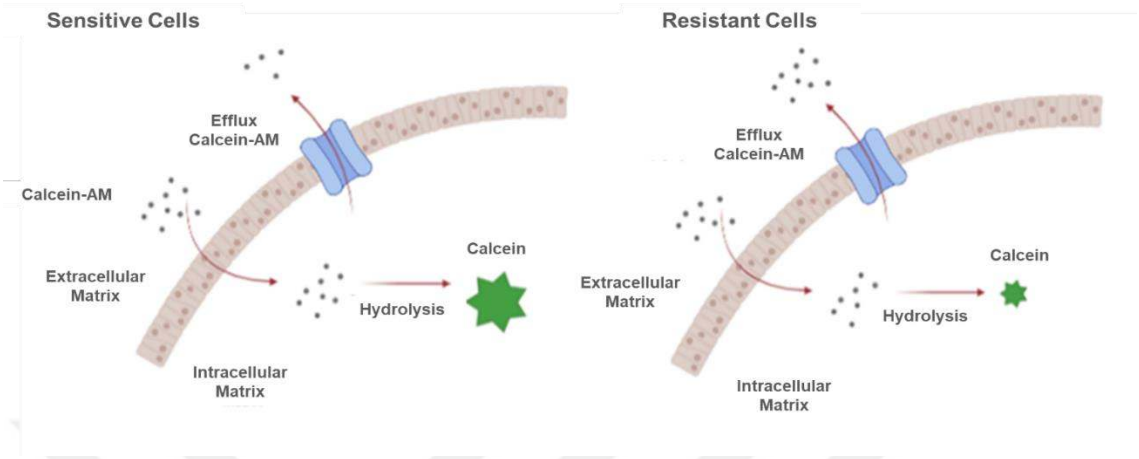

B.

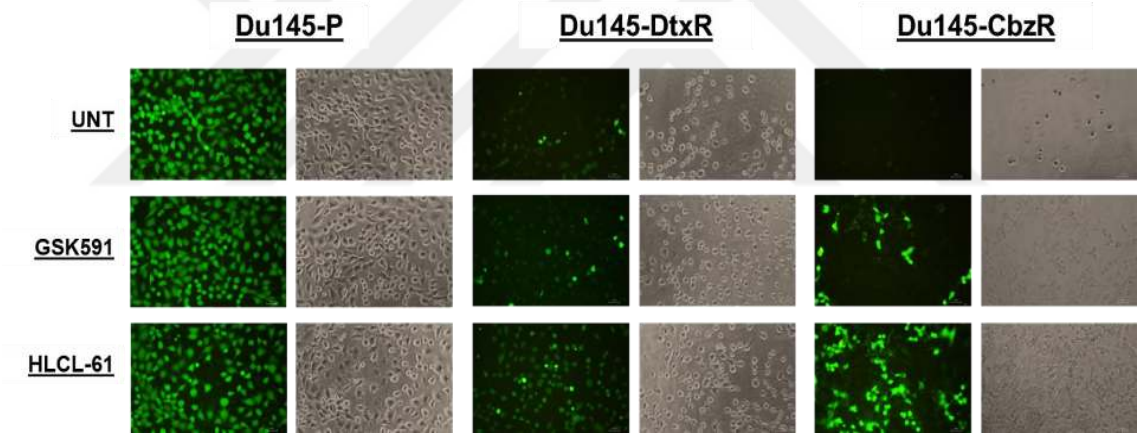

Figure 3.15. Calcein uptake assay in parental and resistant cells upon PRMT5i treatment. (A) A schematic illustration of Calcein-AM retention assay (the figure was generated by BioRender). **(B)** PRMT5 inhibitors were applied (HLCL-61 and GSK591; 5 μM, 24 h) and cells were further incubated with Calcein-AM to assess the fluorescent signal and visualized using a fluorescence microscope.

Based on our findings, we hypothesized that there might be a potential relationship between ABCB1 expression and PRMT5 activity. However, there was no significant alteration in mRNA expression detected after PRMT5 knock-down (Figure 3.14).

Consequently, this has prompted the consideration that the resistance mechanism associated with PRMT5 might manifest through alternative pathways.

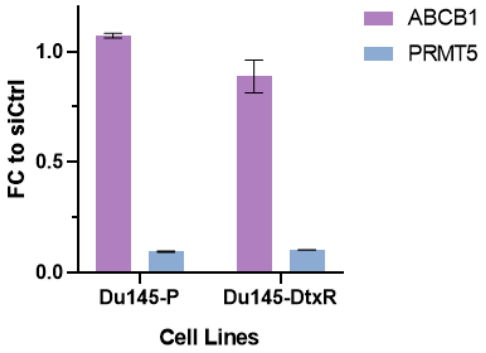

Figure 3.16. The change in ABCB1 expression after PRMT5 silencing. The mRNA levels of ABCB1 and PRMT5 were investigated after siRNA knockdown in Du145-P and Du145-DtxR cells. The error bars represent the SEM of two biological replicates.

3.6. Transcriptomic Changes upon PRMT5 Inhibition

3.6.1. RNA Sequencing after PRMT5 Knock-Down

To reveal the potential mechanisms underlying the reversal of taxane resistance in CRPCa cells upon PRMT5 inhibition, we conducted RNA sequencing analysis to identify differentially expressed genes following siRNA treatment. We deliberately opted for RNA silencing as our primary method rather than direct drug inhibition, to mitigate the potential risk of off-target effects (Figure 3.15A).

RNA sequencing preparation was performed by Buse Cevatemre, Ph.D, with the objective of discerning distinct genes, gene sets, and pathways that demonstrate varied regulation in resistant cells compared to their parental cells. Moreover, this study aimed to identify shared genes and pathways affected by PRMT5-silencing, which could potentially reverse the resistance phenotype to the parental state. During the investigation, the focus was on identifying and scrutinizing Differentially Expressed Genes (DEGs)

between the resistant cells and parental cells, thereby facilitating an in-depth comprehension of the specific epigenetic modifications associated with the acquisition of resistance. Furthermore, the Gene Set Enrichment Analysis (GSEA) showed that the positively enriched gene sets are as follows: Myc pathways, G2/M checkpoint, E2F targets, and TNF-α (Figure 3.15B).

A.

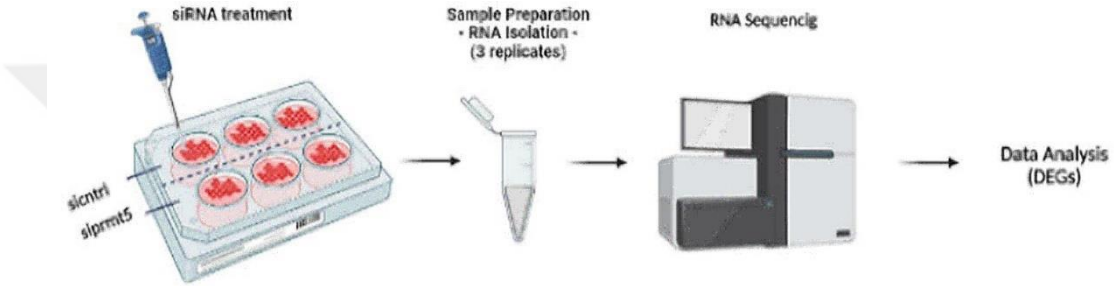

B.

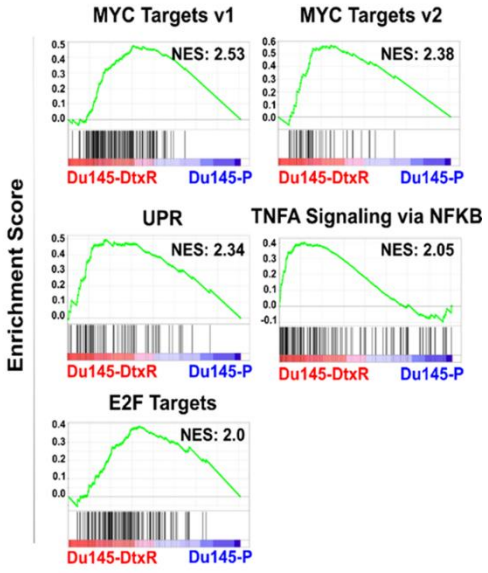

Buse Cevatemre, Ph.D

Figure 3.17. RNA sequencing analysis revealed the top enriched GSEA pathways. **(A)** A schematic workflow of RNA Sequencing (the figure was generated by BioRender). **(B)** Detailed enrichment plots with normalized enrichment scores (right) obtained from Hallmark Gene Sets.

The primary objective of our study was to identify specific genes that demonstrate varying levels of expression in Du145-DtxR cells after the inhibition of PRMT5. This investigation holds significance in gaining a comprehensive understanding of crucial genes implicated in drug resistance. To comprehend the mechanism by which PRMT5 inhibition effectively reverses taxane resistance, an in-depth analysis of genes that are upregulated in resistant cells but downregulated in cells treated with siPRMT5 was undertaken. To assess the efficacy of siPRMT5 in reducing gene expression, qPCR was performed (see Figure 3.16A). Subsequently, we employed RNA sequencing to elucidate changes in the cellular transcriptome resulting from the downregulation of PRMT5 gene expression in Du145-DtxR cells using siRNA treatment.

A Principal Component Analysis (PCA) plot (Figure 3.16B), presents the gene expression profiles of the siRNA treatment groups in a multidimensional space. Each data point represents an RNA sequencing sample, and the positioning reflects its respective gene expression pattern. This PCA plot allows for a comprehensive assessment of the similarity or dissimilarity between samples based on their gene expression profiles. Notably, the PCA plot demonstrates that replicates from each group of siCntrl (control siRNA) and siPRMT5 treated cells cluster together within their respective groups and are distinctly separated from one another based on global transcriptome profiles. Furthermore, volcano plots (Figure 3.16C) were utilized to visually represent the differential gene expression between the siRNA treatment groups. These plots graphically represent the $\log_2$-fold change (logFC) in gene expression against the statistical significance (represented as $-\text{Log}_{10}$FDR). All the visualizations were executed by Dr. Hamzah Syed.

The comprehensive investigation of gene expression changes resulting from the inhibition of PRMT5 through RNA sequencing, coupled with the subsequent utilization of PCA and volcano plots for data analysis, has yielded substantial insights into the potential genes involved in the reversal of taxane resistance. This thereby enhances our understanding of the underlying mechanisms contributing to drug resistance in Du145-DtxR cells.

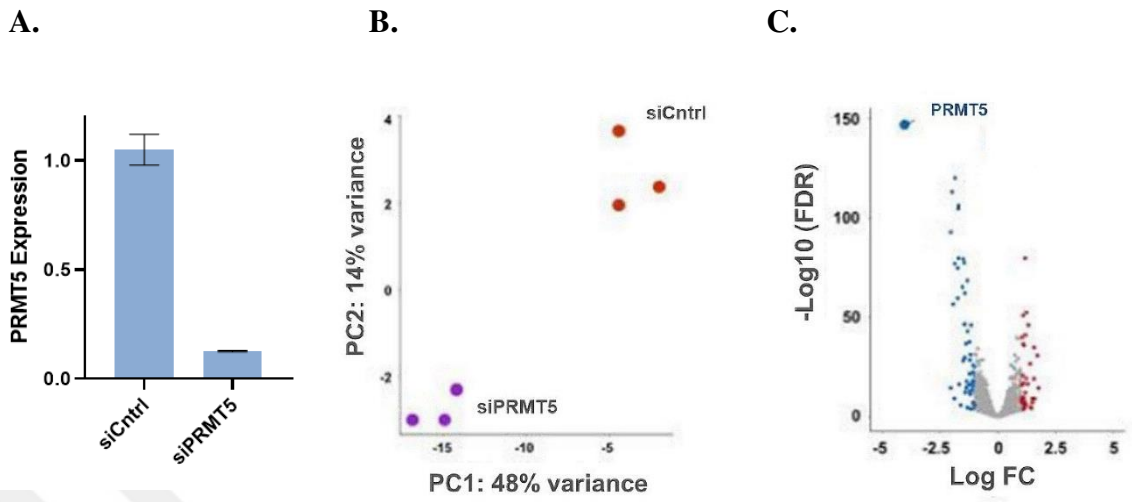

Figure 3.18. RNA sequencing analysis confirms the knock-down of PRMT5. (A) qPCR validation of siPRMT5 samples from RNA sequencing. **(B)** PCA plot of siCtrl and siPRTM5 in Du145-DtxR cells. The red and purple dots represent **siCntrl** and **siPRTM5**, respectively. **(C)** The DEGs from Volcano Plot (FDR < 0.05, and Log2FC ≥ 1 or ≤ -1) of siCntrl and siPRMT5 treated cells. The red and blue dots represent **upregulated** and **downregulated** genes, respectively.

Our focus centered on genes exhibiting reversed expression patterns following siPRMT5 treatment, specifically those that were upregulated in Dtx-resistant Du145 cells in comparison to parental cells but downregulated after siPRMT5 treatment (Figure 3.17A). A total of 494 genes demonstrated differential expression between samples treated with siPRMT5 and siCntrl. Furthermore, GSEA showed that the positively enriched gene sets are as follows: Myc pathways, G2/M checkpoint, E2F targets, Unfolded Protein Response (UPR) and TNF-α (Figure 3.167 and C).

A.

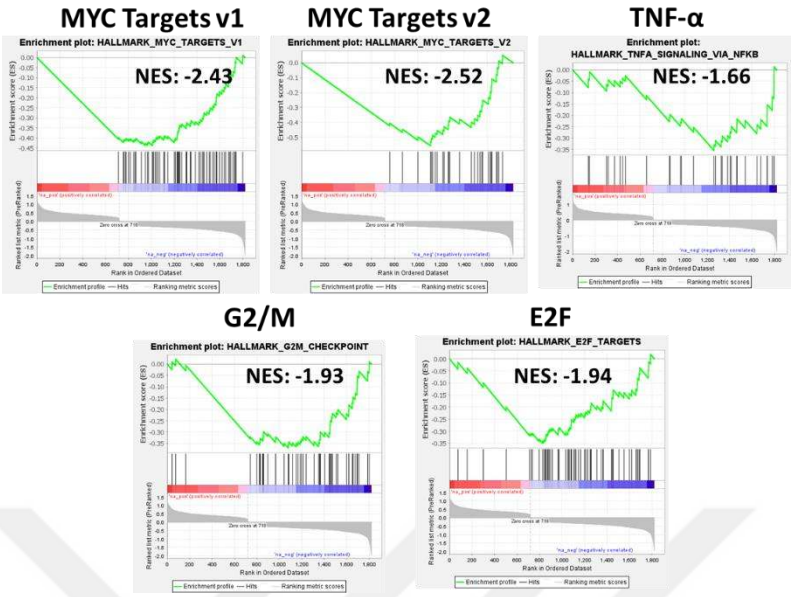

B.

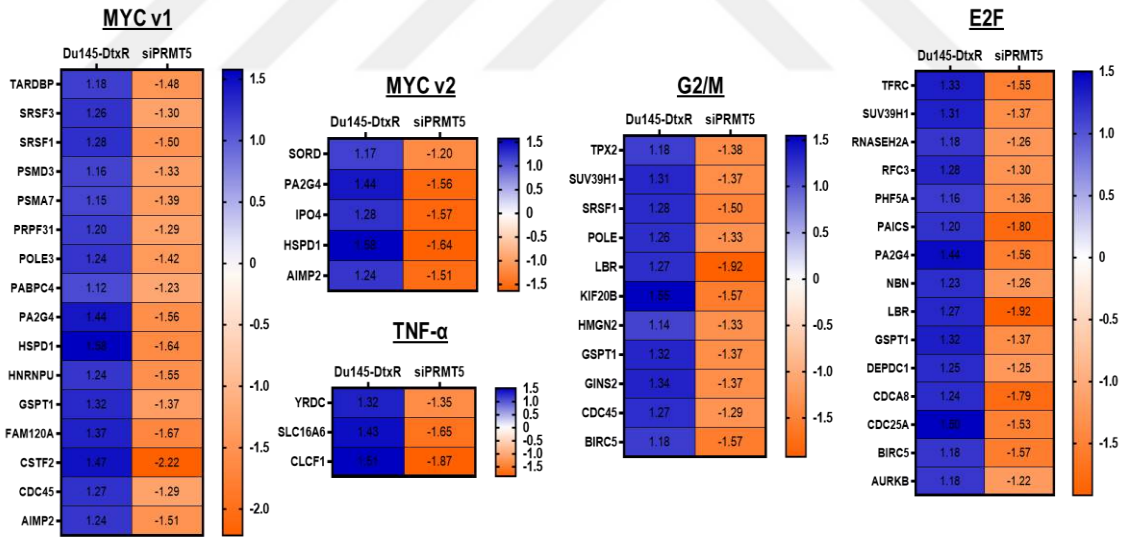

Figure 3.19. Analysis of shared genes between Du145-DtxR/Du145-P and siPRMT5/siCtrl on Du145 DtxR cells. **(A)** Enrichment Scores obtained from Hallmark Gene Sets. **(B)** The heatmap showing logFC of upregulated genes in Du145-DtxR/Du145-P group and downregulated genes in siPRMT5/siCtrl group in pathways that are significantly enriched in GSEA analysis.

Overall, these findings underline great insights about the specific biological processes and molecular functions elicited by PRMT5 inhibition, thus contributing to a deeper comprehension of the potential underlying mechanism of the taxane resistance reversal. Further exploration of these pathways and their associated genes holds promise for the improvement of targeted therapeutic modalities aimed at increasing taxane efficacy in cancer treatment.

3.6.2. Validation of RNA Sequencing

After identifying genes that exhibited differential expression, those potentially linked to drug resistance were chosen for further verification. Genes with a logFC value below -1 (indicating downregulation) and at least a 2-fold change, the functions of these identified genes, which displayed significant alterations, were thoroughly examined in existing literature to assess their potential involvement in overcoming drug resistance (Table 3.2). This investigation involved a detailed search for the association of these genes with resistance in various types of cancers and their connection to microtubules, which are the target of taxanes.

Table 3.2. The identification of DEGs from RNA Sequencing.

Gene Name	Correlation with drug resistance	Correlated Pathway from RNA Sequencing	Reference
HSPA8	HSPA8 interacted with other proteins associated with drug resistance, such as ATP-binding cassette (ABC) transporters.	G2/M	(Zheng et al. 2010)
HNRNPU	Overcoming cisplatin resistance in bladder cancer through the targeting of HNRNPU	G2/M	(Shi et al. 2022)

RBM14	RBM14 was found to be a new target oncogene and interact with proteins involved in the PI3K/AKT/mTOR signaling pathway, which is known to play a role in cancer drug resistance.	G2/M	(Shi et al. 2022; Y. Hu, Mu, and Deng 2023)
GSPT1	The role of GSPT1 in combination with MRP1 in melanoma drug resistance.	G2/M	(Depeille et al. 2005)
DKC1	DKC1 plays a role in drug resistance and EMT mechanism.	G2/M	(J.-H. Kim et al. 2022)
NCL	NCL induced cisplatin resistance in cervical cancer.	G2/M	(Ke et al. 2021)
GINS4	Potential biomarker for drug resistance in certain cancer types.	E2F	(B. Liu et al. 2021)
DDX39A	Overexpressed in doxorubicin resistant breast cancer.	E2F	(X. Wang et al. 2020)
EGR1	Induced autophagy to increase the drug resistance	TNF-α	(Peng et al. 2016)
FOSL1	Enhanced the drug resistance in breast cancer by mediating efflux pump.	TNF-α	(L. Li et al. 2022)
ODC1	A prospective approach to address drug resistance in the context of bladder cancer.	Myc	(Zhu et al. 2022)
RAN	Induced oxidative stress led to play a role in drug resistance	Myc	(Yuen et al. 2012)
SRM	Correlated with some upstream regulators that might be involved in drug resistance in bladder cancer	Myc	(Zhu et al. 2022)

WDR43	Induce chemoresistance in colorectal cancer by inhibiting p53	Myc	(Di et al. 2023)
PSMD1	PSMD1 showed resistance to bortezomib in myeloma cancer.	Myc	(Rubio et al. 2021)
NOLC1	Promotes sensitivity to MDR in lung cancer.	Myc	(H. Huang et al. 2018)

The provided information (Table 3.2) represents a concise overview of the literature related to gene resistance to drugs, derived from RNA sequencing data (including references and enriched pathways from RNA Sequencing). Notably, all genes exhibited a downregulation in expression following the siPRTM5 treatment in Du145-DtxR cells. The hits obtained from RNA Sequencing, that are found to be associated with resistance in literature search, were validated through qRT-PCR. (Figure 3.18).

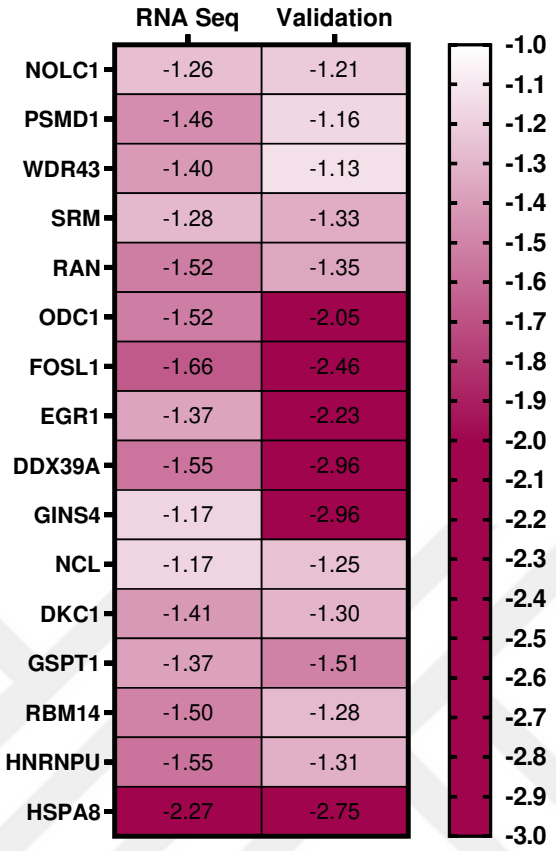

Figure 3.20. Heatmap of validation of down-regulated genes in siPRMT5/siCntrl on Du145-DtxR cells. The mRNA level of picked down-regulated genes in Du145-DtxR cells after PRMT5 silencing.

The expression of MYC was examined following siPRMT5 treatment. Although only a marginal difference was observed (Figure 3.19), further investigation of its effect on the phenotype was conducted through a colony formation assay using siMYC. It was anticipated that such a prominent pathway in the resistance mechanism would exert a substantial influence on the phenotype. However, the results of the assay revealed its impact on cell proliferation, rather than its effect on the resistance mechanism. A decrease in cell proliferation was observed irrespective of the taxane concentration in resistant cell lines even though the knockdown efficiency was %50 (Figure 3.20).

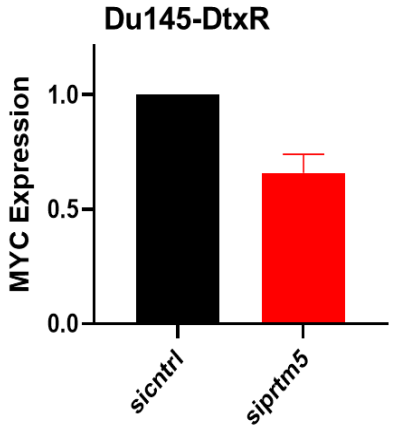

Figure 3.21. Change in MYC expressions after siPRMT5 in Du145-DtxR. Fold change of MYC and PRMT5 expressions after siPRMT5 silencing (72 h) was shown via qRT-PCR.

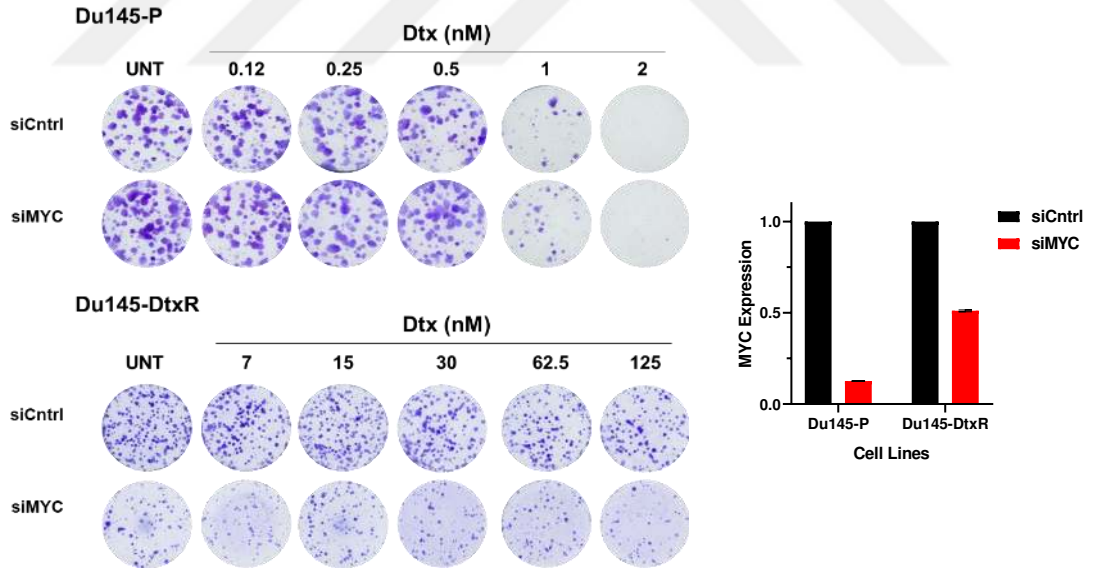

Figure 3.22. The effect of MYC silencing on clonogenic capacity of Du145-P and Du145-DtxR cells. Clonogenic images were obtained after treating cells with the siMYC for 72 hours, and the cells were allowed for colony formation for 10-15 days post-taxane exposure (72 h) (up). MYC knock-down efficiency was checked via qRT-PCR 72 h post-treatment of siMYC. The data is presented as the mean ± SEM of two biological replicates (down).

3.7. Cell Cycle Arrest Caused by The Pharmacological Inhibition of PRMT5

PRMT5 depletion leads to anomalous splicing events, such as exon skipping or retention of introns, affecting a group of genes responsible for cell cycle arrest and/or apoptosis (Koh et al. 2015). The DNA damage response (DDR) carries important roles in safeguarding genomic stability by instigating DNA repair and cell cycle checkpoint mechanisms against anti-cancer treatments like ionizing radiation and chemotoxicity (Koh et al. 2015). Notably, in prostate cancer, PRMT5 is found to be essential for DNA damage induced G2 cycle arrest, attributed to the epigenetic activation of WEE1 (Owens et al. 2020). In other types of cancer cells, PRMT5 governs G2 arrest through the methylation of RAD9 (He et al. 2011) and the accumulation of KLF4 (D. Hu et al. 2015).

Outcomes obtained from RNA Sequencing, starting from the decreased gene expressions involved in cell division and cell cycle (G2/M arrest), the effects on the cell cycle and cell division processes were investigated. The combination with HLCL-61 in Du145-DtxR cells led to the arrest of 67% of the cell population at the G2/M stage which corresponds approximately twice relative to the control and only inhibitor/taxane group. However, no significant alterations were observed in either the group treated solely with taxane or the group treated solely with the inhibitor. Similar effect was observed in Du145-CbzR cells; 71% of the cell population was arrested at the G2/M stage. GSK591 showed a similar distribution in Du145-DtxR and Du145-Cbz cells, while only the taxane group also caused G2/M arrest (Figure 3.21).

A.

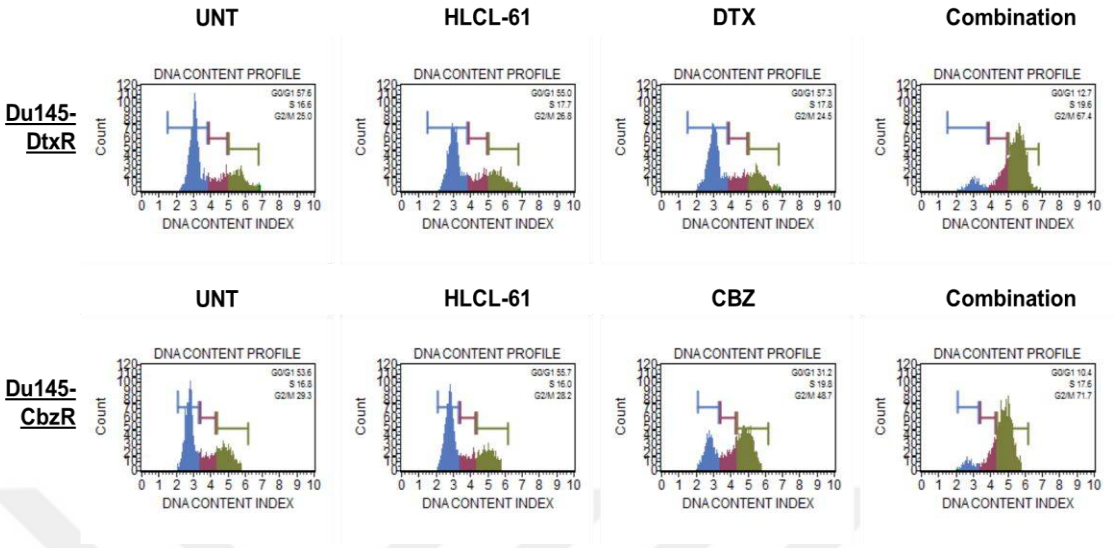
UNT
HLCL-61
DTX
Combination
Du145-DtxR
UNT
HLCL-61
CBZ
Combination
Du145-CbzR
DNA CONTENT PROFILE
Count
DNA CONTENT INDEX

B.

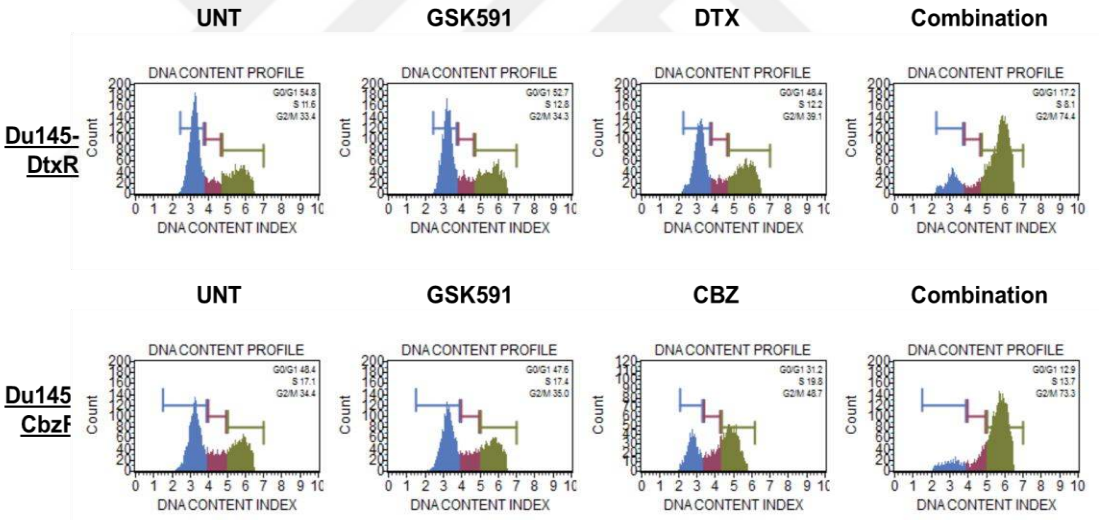
UNT
GSK591
DTX
Combination
Du145-DtxR
UNT
GSK591
CBZ
Combination
Du145 CbzR
DNA CONTENT PROFILE
Count
DNA CONTENT INDEX

C.

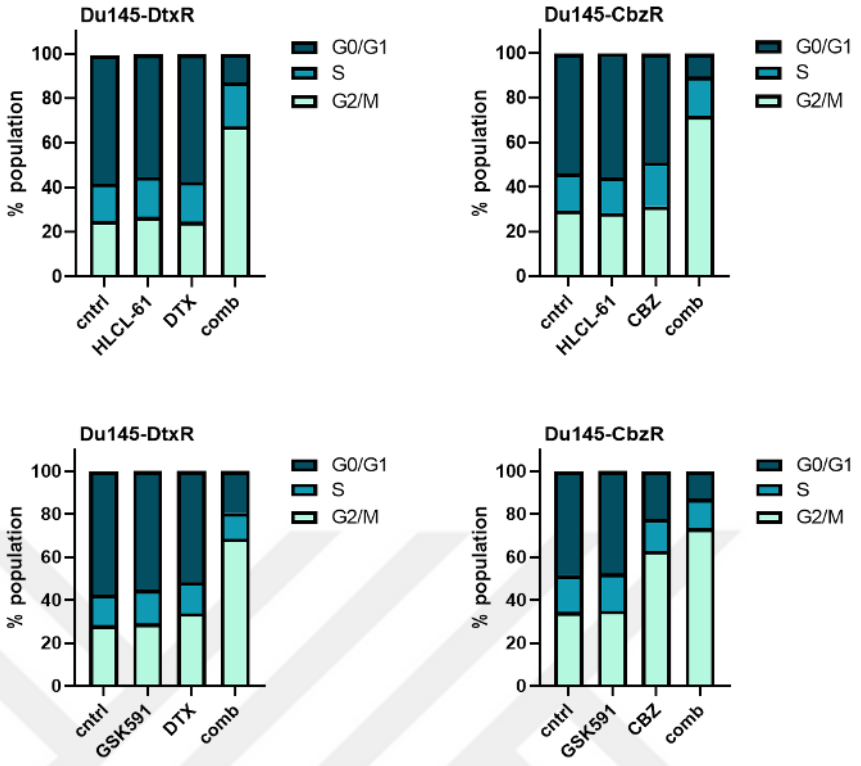

Figure 3.23. The distribution of cell cycle phases upon PRMT5 inhibition by flow cytometry. The cell cycle distribution of Du145 resistant cells upon **(A)** HLCL-61 and **(B)** GSK591 treatments. **(C)** Increase in G2/M arrest on Du145 DtxR and CbzR resistant cells resulting from treatments with PRMT5 inhibitors were shown in bar graphs. The concentrations used are as follows: Dtx; 125 nM, Cbz; 62,5 nM and PRMT5 inhibitors; 5 μM for 72 h.

The combination with HLCL-61 in Du145-DtxR cells led to the arrest of 67% of the cell population at the G2/M stage which corresponds approximately twice relative to the control and only inhibitor/taxane group. However, no significant alterations were observed in either the group treated solely with taxane, or the group treated solely with the inhibitor. Similar effect was observed in Du145-CbzR cells; 71% of the cell population was arrested at the G2/M stage. On the other hand, GSK591 showed a similar distribution in Du145-DtxR cells, while only the taxane group also led to G2/M arrest in Du145-Cbz cells.

3.8. Induction of apoptosis as a result of PRMT5 inhibition in Du145 taxane resistant cells

Apoptosis, a cell's way of leading itself to a programmed cell death, is a highly regulated and essential process in multicellular organisms. It plays a crucial role in the development of tissue homeostasis and eliminating damaged or infected cells. in addition, an impactful way to eliminate a cancer cell's propagation is making it undergo apoptosis through activation of apoptotic pathways.

In chemotherapeutics perspective, their toxicity and intracellular pressure leads to activation of apoptosis and subsequently leading to apoptosis-related cell death. Through numerous experimental results that we have obtained so far, we know that PRMT5 inhibition reverts the taxane resistance - making cells less susceptible to taxane toxicity. In order to reveal the mode of cell death, if it is through apoptosis, we performed apoptosis monitoring assays; Annexin V staining and Caspase3/7 activation.

3.8.1 Annexin V Staining

Phosphatidyl Serines (PS) are situated on the cellular membrane, facing the cell cytoplasm. During early apoptosis, the membrane's asymmetry is being disrupted, leading to the phosphatidylserine translocation to the outer side of cell membrane (Jing, Xie, et al. 2018; Lakshmanan and Batra 2013). Annexin V is an intracellular protein with a calcium-dependent affinity for binding to phosphatidylserine. The use of fluorochrome-labeled Annexin V dye allows the detection of early apoptotic cells by its interaction with PS. On the other hand, 7-AAD is a fluorescent DNA intercalator that cannot penetrate through an intact cell membrane. Consequently, it can only enter dead or damaged cells while being excluded from live cells (Toba et al. 1996). By co-staining Annexin V and 7-AAD, it becomes possible to distinguish live, apoptotic, and dead cell subpopulations. To address the enhanced apoptosis, the increased subpopulation of Annexin V and 7-AAD positive Du145 resistant cells were identified following combination treatment of HLCL61/GSK591 and Dtx/Cbz using flow cytometry (Muse® Cell Analyzer) (Figure 3.22).

A.

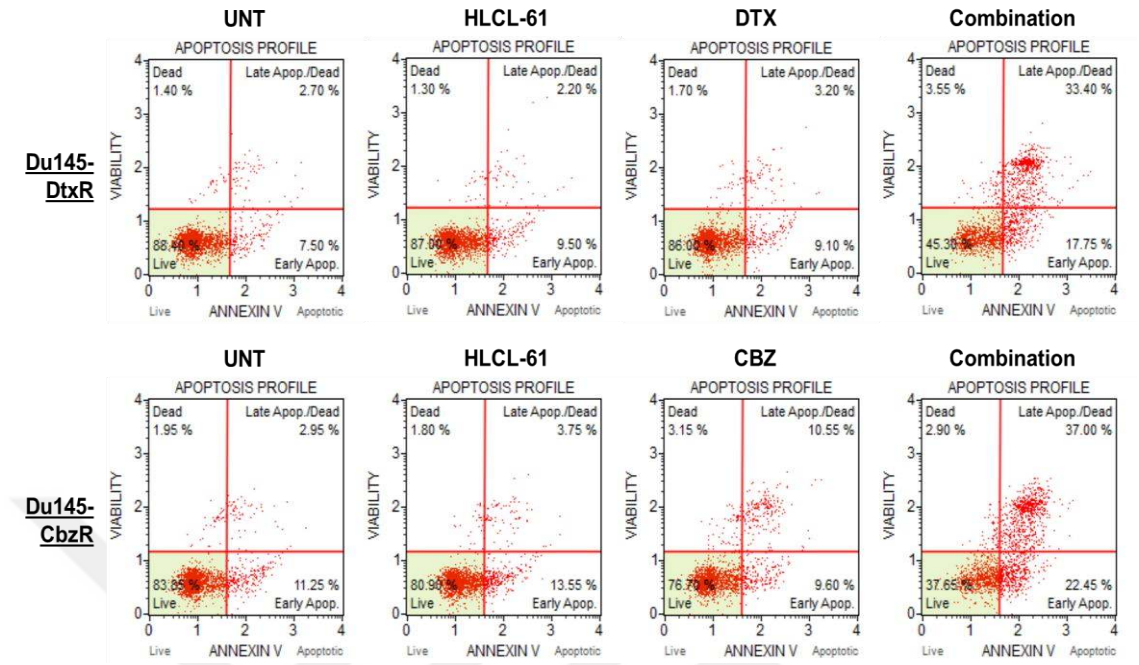
UNT
HLCL-61
DTX
Combination
Du145-DtxR
APOPTOSIS PROFILE
Dead 1.40 %
Late Apop./Dead 2.70 %
88.40 %
Live
7.50 %
Early Apop.
VIABILITY
ANNEXIN V
Live
Apoptotic
Dead 1.30 %
Late Apop./Dead 2.20 %
87.00 %
9.50 %
Dead 1.70 %
Late Apop./Dead 3.20 %
86.02 %
9.10 %
Dead 3.55 %
Late Apop./Dead 33.40 %
45.30 %
17.75 %
UNT
HLCL-61
CBZ
Combination
Du145-CbzR
Dead 1.95 %
Late Apop./Dead 2.95 %
83.85 %
11.25 %
Dead 1.80 %
Late Apop./Dead 3.75 %
80.90 %
13.55 %
Dead 3.15 %
Late Apop./Dead 10.55 %
76.70 %
9.60 %
Dead 2.90 %
Late Apop./Dead 37.00 %
37.65 %
22.45 %

B.

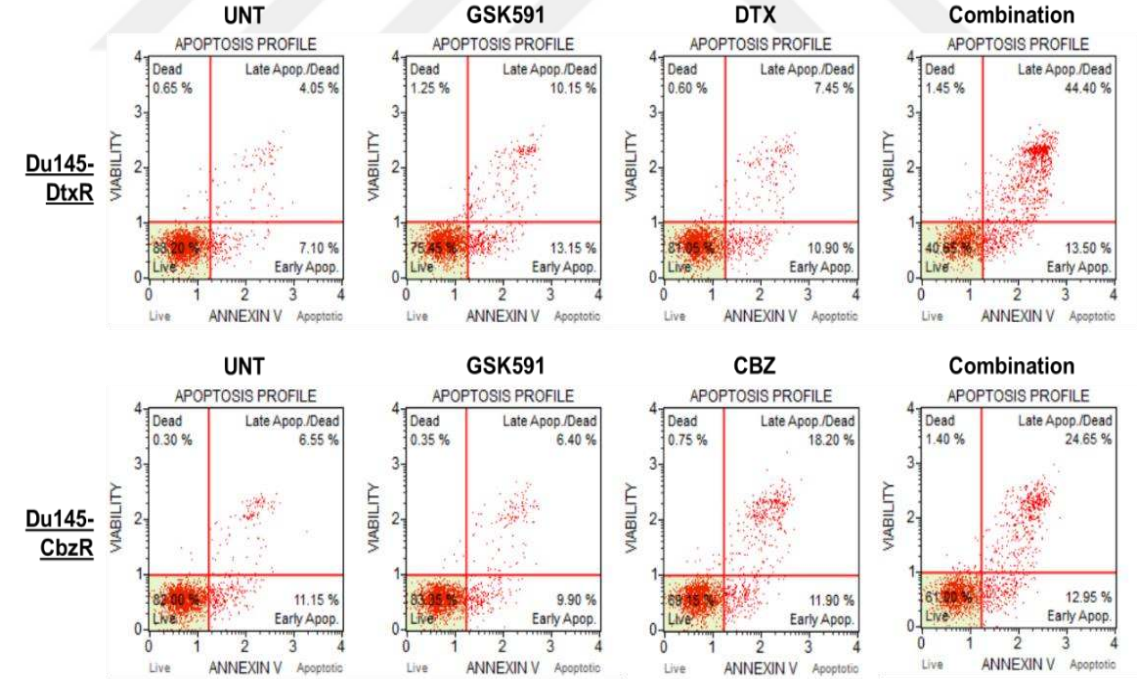
UNT
GSK591
DTX
Combination
Du145-DtxR
APOPTOSIS PROFILE
Dead 0.65 %
Late Apop./Dead 4.05 %
88.20 %
Live
7.10 %
Early Apop.
VIABILITY
ANNEXIN V
Live
Apoptotic
Dead 1.25 %
Late Apop./Dead 10.15 %
75.45 %
13.15 %
Dead 0.60 %
Late Apop./Dead 7.45 %
81.05 %
10.90 %
Dead 1.45 %
Late Apop./Dead 44.40 %
40.65 %
13.50 %
UNT
GSK591
CBZ
Combination
Du145-CbzR
Dead 0.30 %
Late Apop./Dead 6.55 %
82.00 %
11.15 %
Dead 0.35 %
Late Apop./Dead 6.40 %
83.35 %
9.90 %
Dead 0.75 %
Late Apop./Dead 18.20 %
69.15 %
11.90 %
Dead 1.40 %
Late Apop./Dead 24.65 %
61.00 %
12.95 %

C.

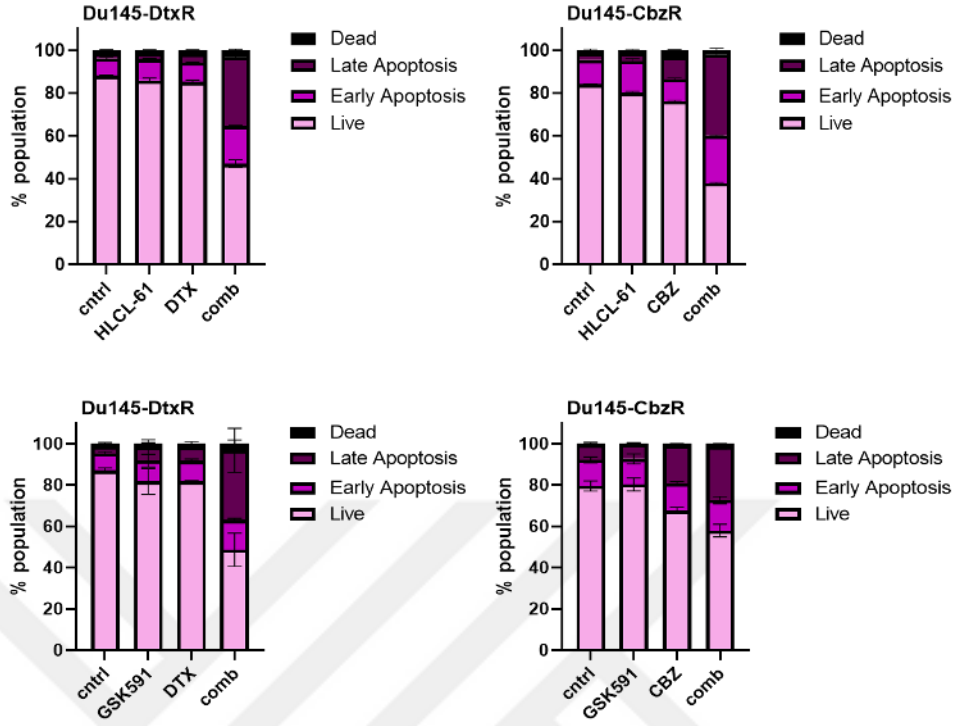

Figure 3.24. Annexin V staining flow cytometry on Du145 resistant cells shows an increased apoptosis after combinatorial treatment. The distribution of live/dead cells upon **(A)** HLCL-61 and **(B)** GSK591 treatments. **(C)** Increase in apoptosis on Du145-DtxR and Du145-CbzR cells resulting from combination treatments of Dtx/Cbz with PRMT5 inhibitors were shown as bar graphs. Concentrations used are as follows: Dtx; 125 nM, Cbz; 62,5 nM and PRMT5 inhibitors; 5 µM for 72 h. Data represented as the average of ± SEM from 2 biological replicates. Annexin V(-)/7-AAD(-) indicates live cells; Annexin V(+)/7-AAD(-) indicates early apoptotic cells; Annexin V(+)/7-AAD(+) indicates late apoptotic/dead cells; Annexin V(-)/7-AAD(+): indicates dead cells.

The combination with HLCL-61 in Du145-DtxR cells led to the apoptosis pathways of 33% of the cell population distributed at the late apoptosis which corresponds approximately twice relative to control and only inhibitor/taxane group. However, no significant change was observed in either the taxane only or the inhibitor only group. Similar effects were observed in Du145-CbzR cells, 37% of the cell population was distributed at late apoptosis. On the other hand, GSK591 showed a similar distribution in Du145-DtxR cells, while only taxane group also led to apoptosis in Du145-Cbz cells. As a result, such an increase in apoptosis in combination may be observed from increased

taxane activity on microtubule depolymerization when they are combined with PRMT5 inhibitors.

3.8.2 Caspase 3/7 Staining

The modality of cellular demise following the combined therapeutic approach was subjected to further investigation, with a particular focus on assessing the activation of executioner caspases 3 and 7 as a solid indicator of apoptosis (Jänicke et al. 1998), alongside the utilization of 7-AAD staining. Caspases, being critical proteases involved in the regulation of apoptosis, are categorized based on their established roles in apoptosis. Caspases 3 and 7, belonging to the class of executioner caspases, are responsible for the degradation of numerous cellular components, thereby instigating the morphological alterations required for controlled cell death (McIlwain, Berger, and Mak 2013). 7-AAD positively stained Du145 resistant cells were identified following combination treatment using flow cytometry (Muse® Cell Analyzer) (Figure 3.23).

A.

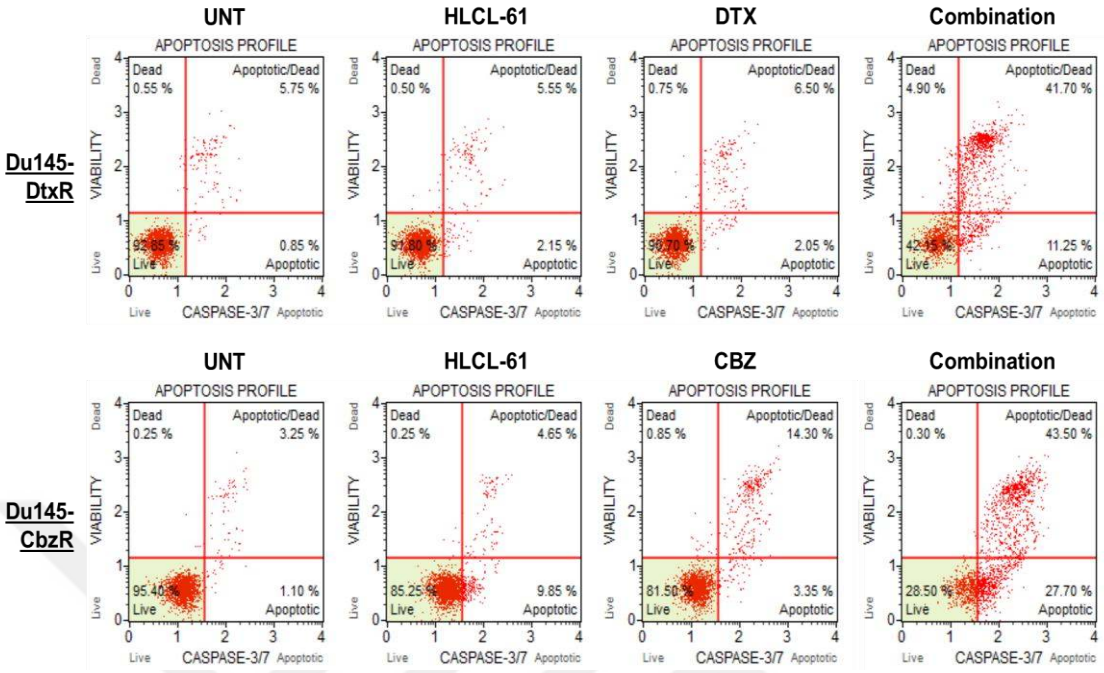
UNT
HLCL-61
DTX
Combination
APOPTOSIS PROFILE
Dead
Apoptotic/Dead
Live
Apoptotic
VIABILITY
CASPASE-3/7
0.55 %
5.75 %
92.85 %
0.85 %
0.50 %
5.55 %
91.80 %
2.15 %
0.75 %
6.50 %
90.70 %
2.05 %
4.90 %
41.70 %
42.15 %
11.25 %
Du145-DtxR
UNT
HLCL-61
CBZ
Combination
0.25 %
3.25 %
95.40 %
1.10 %
0.25 %
4.65 %
85.25 %
9.85 %
0.85 %
14.30 %
81.50 %
3.35 %
0.30 %
43.50 %
28.50 %
27.70 %
Du145-CbzR

B.

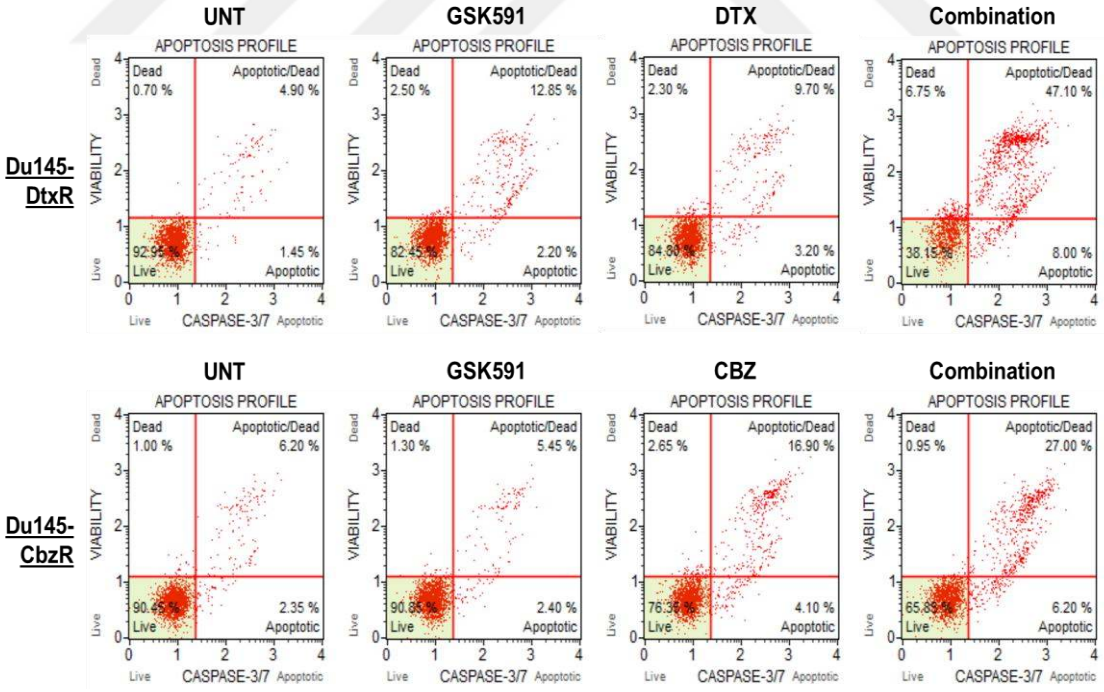
UNT
GSK591
DTX
Combination
APOPTOSIS PROFILE
Dead
Apoptotic/Dead
Live
Apoptotic
VIABILITY
CASPASE-3/7
0.70 %
4.90 %
92.95 %
1.45 %
2.50 %
12.85 %
82.45 %
2.20 %
2.30 %
9.70 %
84.80 %
3.20 %
6.75 %
47.10 %
38.15 %
8.00 %
Du145-DtxR
UNT
GSK591
CBZ
Combination
1.00 %
6.20 %
90.45 %
2.35 %
1.30 %
5.45 %
90.35 %
2.40 %
2.65 %
16.90 %
76.35 %
4.10 %
0.95 %
27.00 %
65.85 %
6.20 %
Du145-CbzR

C.

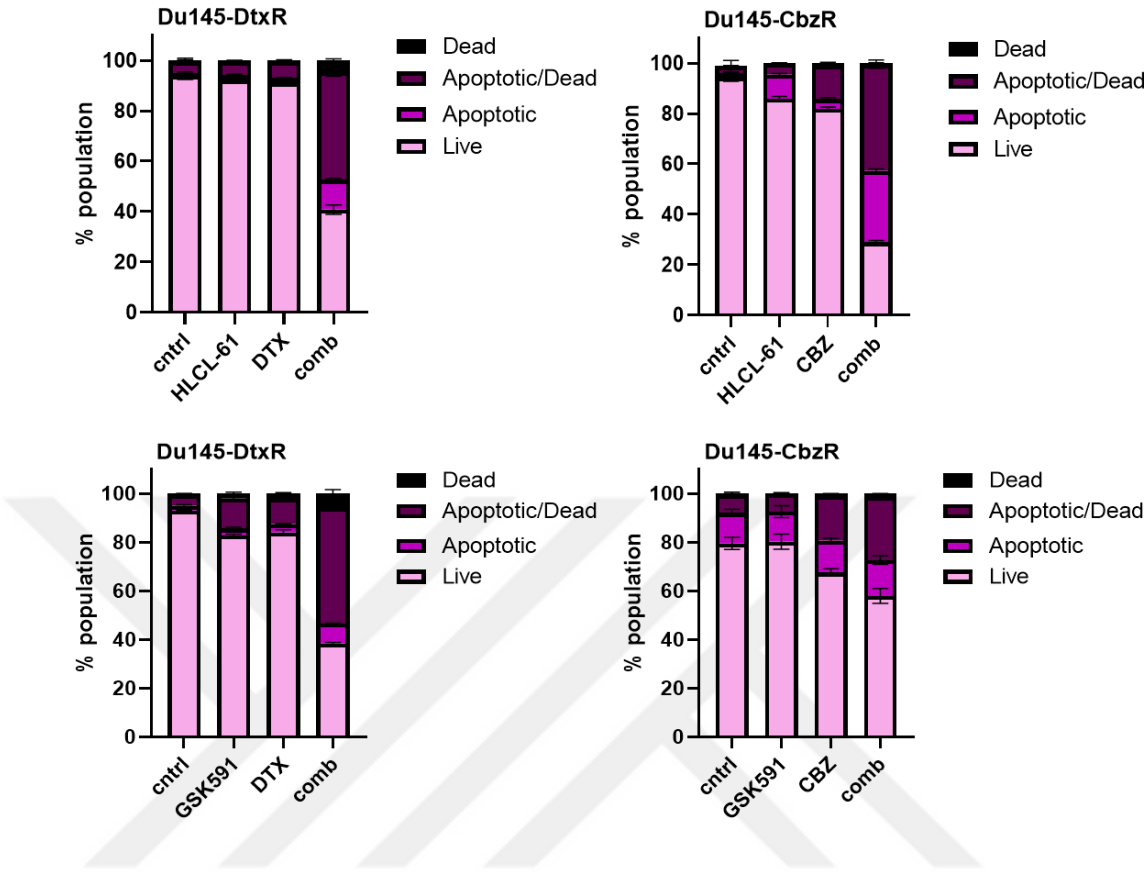

Figure 3.25. Annexin V staining flow cytometry on Du145 resistant cells shows an increased apoptosis after combinatorial treatment. The distribution of live/dead cells upon **(A)** HLCL-61 and **(B)** GSK591 treatments. **(C)** The histograms illustrate increased apoptosis of Du145-DtxR and Du145-CbzR cells after combinatorial treatment of taxanes with PRMT5 inhibitors. The concentrations used are as follows: Dtx; 125 nM, Cbz; 62,5 nM and PRMT5 inhibitors; 5 μM for 72 h. Data represented as the average of ± SEM from 2 biological replicates. Caspase-3/7(-)/7-AAD(-) indicates live cells; Caspase-3/7(+)/7-AAD(-) indicates apoptotic cells; Caspase-3/7(+)/7-AAD(+) indicates apoptotic/dead cells; Caspase-3/7(-)/7-AAD(+): indicates dead cells.

The combination with HLCL-61 in Du145-DtxR cells led to the apoptosis pathways of 41% of the cell population distributed at the late apoptosis which corresponds approximately twice relative to the DMSO control, inhibitor only, and taxane only groups. Additionally, there was no significant change observed in taxane only and inhibitor only treatment groups when compared to the DMA control group. Similar effects were observed in Du145-CbzR cells, 43% of the cell population was distributed at late

apoptosis. On the other hand, GSK591 showed a similar distribution in Du145-DtxR cells, while only the taxane group also led to apoptosis in Du145-Cbz cells. Consequently, when taxanes are combined with PRMT5 inhibitors, an increase of apoptosis was observed due to enhanced efficacy of taxanes. Both Annexin V and Caspase 3/7 staining flow cytometry experiments suggest apoptosis as the main mechanism for the observed cell death. Results of these two experiments clearly state that combinatorial treatments of taxanes and PRMT5 inhibitors increase the apoptosis. This enhancement is attributable to a synergistic mechanism of action, wherein the taxane-induced microtubule depolymerization amplifies the cytotoxic effects.

3.9. Cellular Localization of PRMT5 in Du145 Parental and Taxane Resistant Cells

PRMT5 is a type II arginine methyltransferase that has multiple protein targets, including cytosolic proteins, nuclear transcription factors, and histones. Studies show different subcellular localizations of PRMT5 in both nucleus and cytosol (Gu et al. 2012). In our study, we confirmed that PRMT5 inhibition through epigenetic modifier drugs called GSK591 and HLCL-61 cause significant reduction in PRMT5 expression (Figure 3.13) arginine demethylation on target proteins (Figure 3.10) and histones (Figure 3.11). These results cumulatively suggest the catalytic action of PRMT5 takes place in both nucleus and cytosol.

3.9.1. PRMT5 Selectively Localizes to Cytosol in Both Parental and Taxane Resistant Du145 Cells

After successfully representing the ability of PRMT5 to alter sDMA modification, we hypothesized that the subcellular localization of PRMT5 could vary as the mechanism of resistance evolves in Du145-DtxR cells. The nuclear/cytosol fractionation was performed, and WB results showed that in both Du145-P and Du145-DtxR cells, PRMT5 dominantly localizes to cytosol, indicating that despite its function as an epigenetic modifier, its role within the nucleus is limited (Figure 3.26). This outcome corroborates our results, wherein we showed a significant reduction in sDMA modification on the target protein levels, rather than on histone proteins. (Figure 3.10 and 3.11).

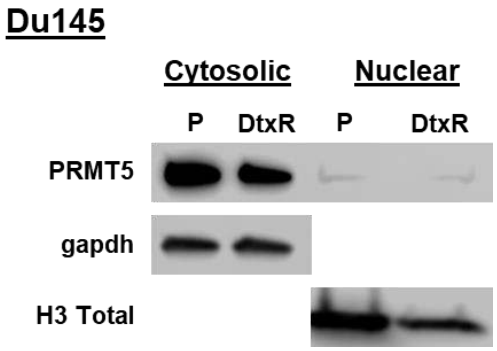

Figure 3.26. Nuclear and cytosolic localization of PRMT5 protein in Du145-P and Du145-DtxR cells. Nuclear and cytosolic proteins were fractionated on Du145 parental (P) and docetaxel resistant (DtxR) cells. PRMT5 expression was evaluated based on its localization at the cytosol and nucleus. GAPDH and total H3 expressions were used as expression control.

3.9.2. PRMT5 Co-Localizes to Centrosomes in a Cell Cycle-Dependent Manner

Regarding our data results showing PRMT5 expression being predominantly in the cytosol, IF staining was performed to visualize the protein expression according to specific localization. The predominantly cytosolic localization was expected to be observed by using PRMT5 antibody. Consistent with these expectations, florescence was mainly observed in cytosol of the cells and, IF staining experiments revealed that endogenous expression of PRMT5 locates two distinct locations within the cytosol during metaphase stage of the cell cycle. Since these two localizations in the cytosol could potentially represent spindle poles, we co-stained PRMT5 and γ-tubulin (centrosome marker) together on HEK293T cells. Our results showed that these two proteins could be co-localized, suggesting a cell cycle-specific localization of PRMT5 at centrosomes (Figure 3.27).

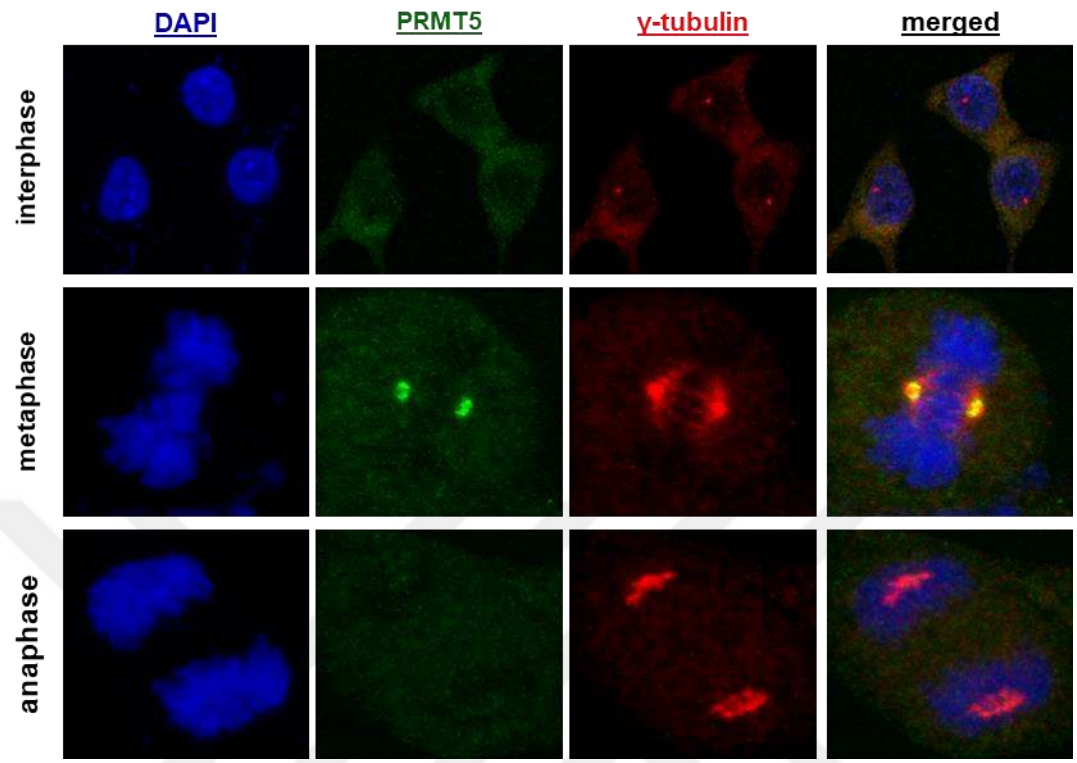

Figure 3.27. PRMT5 localizes centrosomes in cell cycle specific manner. Endogenous PRMT5 proteins were co-stained using anti-PRMT5 and anti-γ-tubulin antibodies in HEK293T cells. In an unsynchronized cell population, cells in interphase (top, 40X zoom), metaphase (middle, 40X and digital zoom), and anaphase (bottom, 40X and digital zoom) were closely visualized.

To determine whether the subcellular position of PRMT5 at the centrosomes is unique to HEK293T cells or is common across various cell types, Du145, U2OS, MDA-MB-231, and MIA-PaCa-2 cells were labelled with PRMT5 and γ-tubulin. In fact, every cell type showed colocalization at the centrosomes, indicating a possible function for PRMT5 in this location (Figure 3.28).

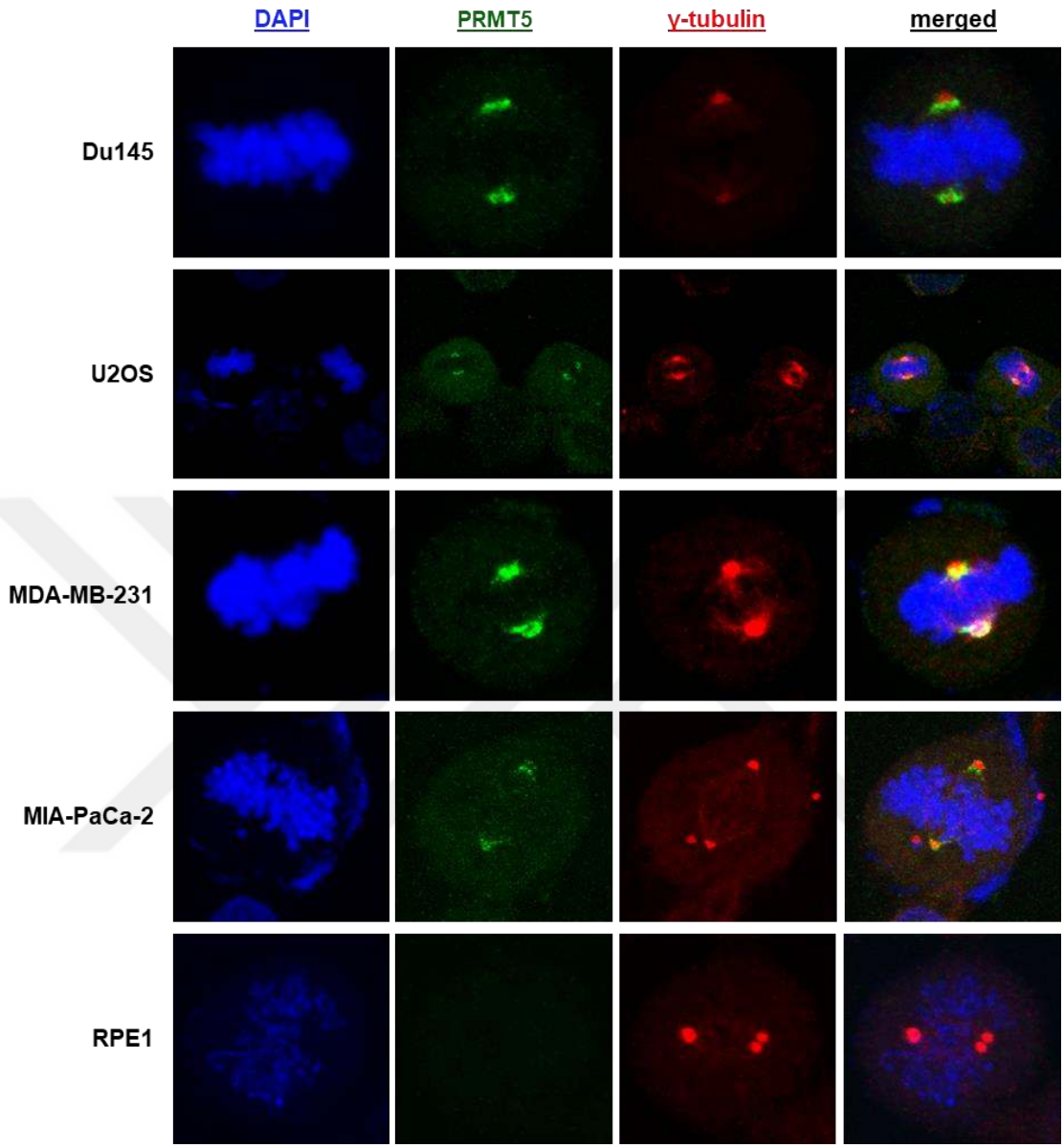

Figure 3.28. PRMT5 localizes centrosomes in metaphase in various cancer cells. Endogenous PRMT5 proteins were co-stained using anti-PRMT5 and anti-γ-tubulin antibodies on unsynchronized Du145, U2OS, MDA-MB-231, and MIA-PaCa-2 cancer cells. RPE-1 cells are used as a control normal cell. Digital zoom was applied to IF images of Du145, MDA-MB-231, MIA-PaCa-2 and RPE-1 cell lines.

Results shown in figures 3.27 and 3.28 signify the localization of PRMT5 at the centrosomes in unsynchronized cell population. In addition, we also performed cell cycle arrest at G2/M phase through various arrest treatments (double thymidine block (DTB), Colcemid, S-trityl-L-cysteine (STLC), and DTB + STLC). STLC causes cell cycle arrest

in the S/G2 phase, also acting like a microtubule inhibitor (Wu et al., 2018). Double Tymidine blocks the cells at end of G1 and beginning of the S phase. Colcemid acts as a microtubule inhibitor, causing cell arrest in metaphase (Chen and Deng, 2018). Figure 3.29A schematically represent the DTB+STLC treatments with time points. Figure 3.29B shows the cell cycle arrest at G2/M after indicated arrest treatments.

A.

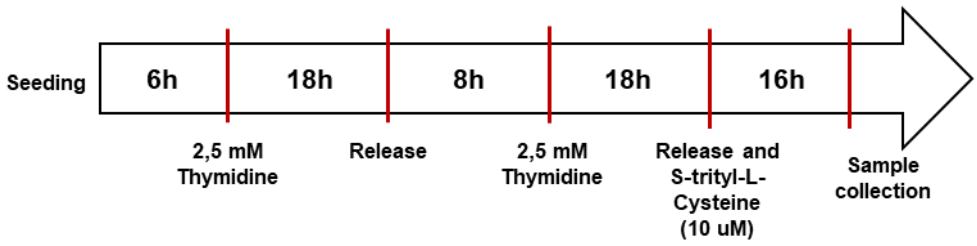

B.

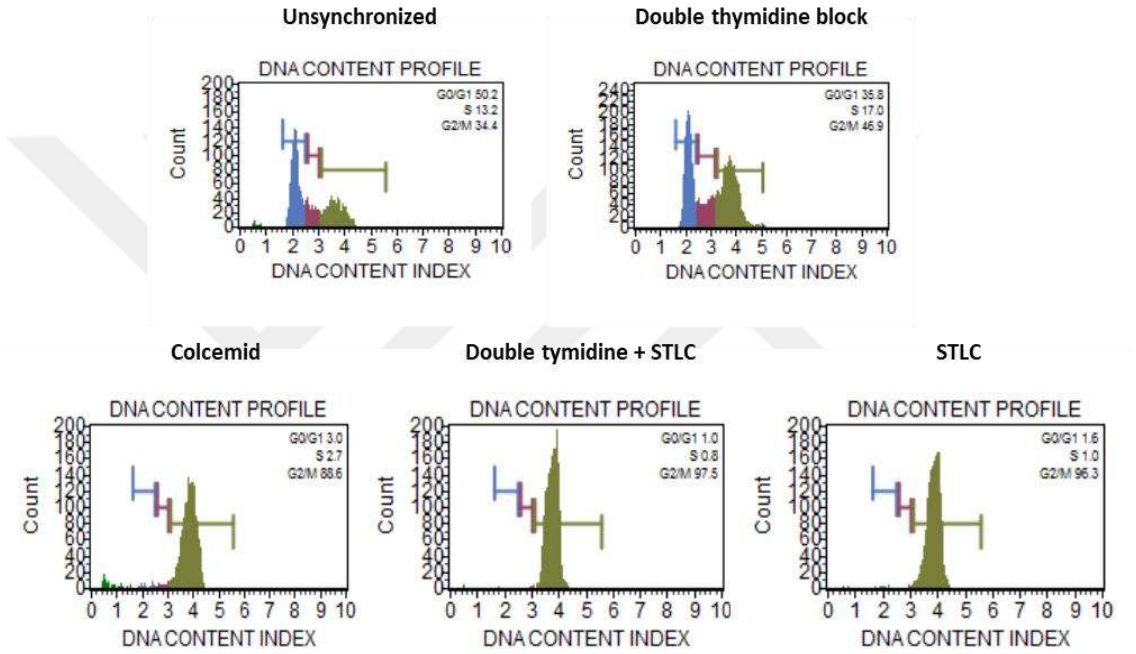

Figure 3.29. The confirmation of cell cycle arrest upon double thymidine block (DTB), STLC, and colcemid treatments on U2OS cells by flow cytometry. (A) Schematic representation of DTB and STLC treatment cell cycle arrest method. **(B)** Flow cytometry results showing that indicated treatments successfully arrested cells at G2/M stages of the cell cycle.

Immunofluorescence staining experiments after cell cycle arrest with different arrest treatments on U2OS cells also confirm that PRMT5 co-localizes with γ-tubulin at the centrosomes (Figure 3.30). All these immunofluorescence experiments confirm that PRMT5 localization at the centrosomes is cell cycle-dependent and this localization is taking place in different cancer cells.

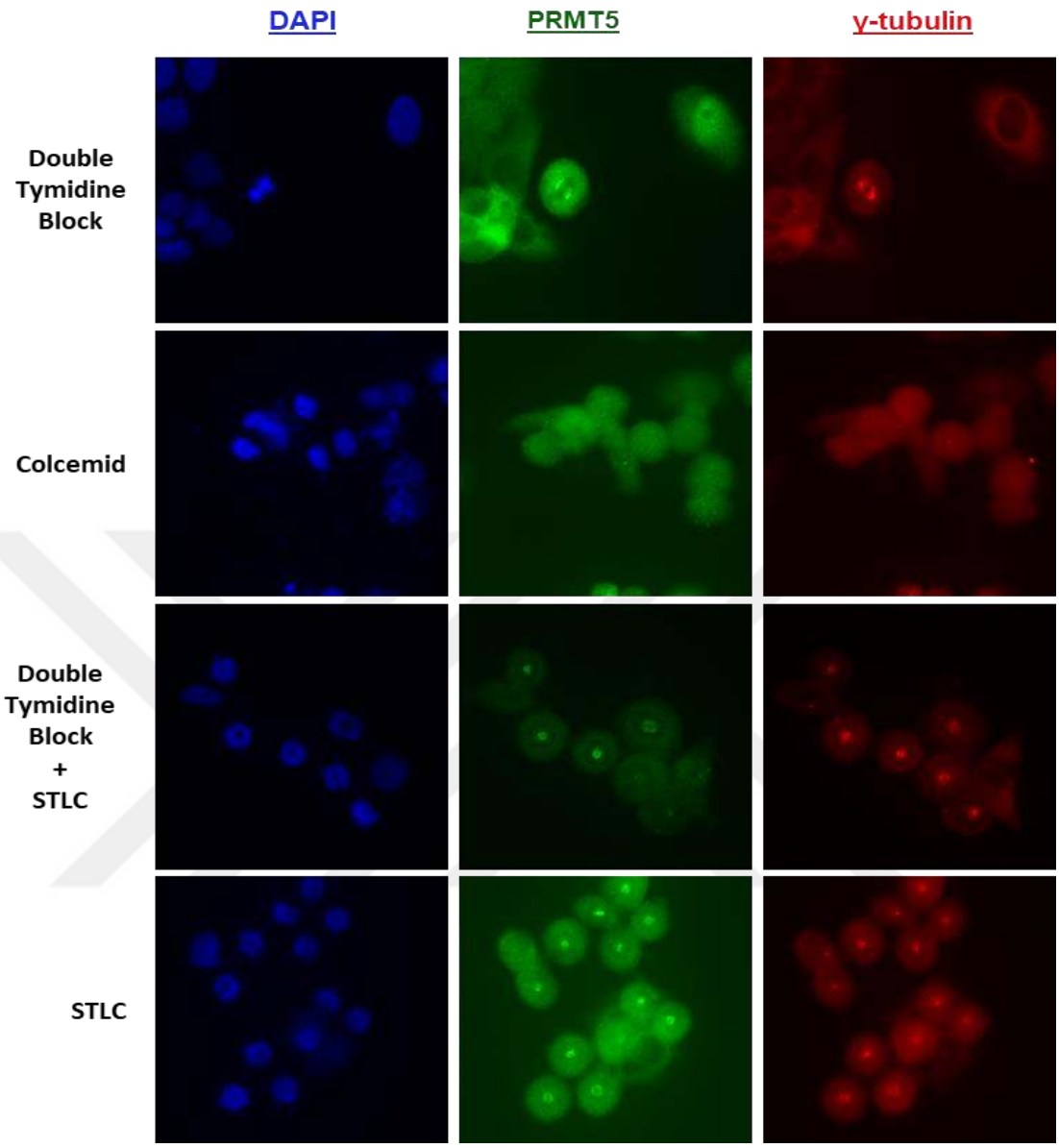

Figure 3.30. PRMT5 localizes centrosomes on cell cycle arrested U2OS cells. Endogenous PRMT5 proteins were co-stained using anti-PRMT5 and anti-γ-tubulin antibodies on U2OS cells after cells being arrested by double thymidine block (2.5mM, 18h, twice), colcemid (0.5 ug/ml, 16h), STLC (10uM, 16h), and double thymidine block and STLC treatments.

Next, we overexpressed PRMT5 and aimed to see the same localization at the centrosomes with ectopic PRMT5 expression. By doing overexpression studies, we would also be able to see if this localization at the centrosomes is variant specific. To this

end, we subcloned and used V5 tagged PRMT5 variant 1 lentiviral expression plasmid. After engineering U2OS PRMT5(var1)-V5 cells, we performed IF staining using anti-PRMT5 and anti-V5 antibodies. Fluorescence microscopy images of U2OS PRMT5(var1)-V5 cells showed protein aggregates in both IF images, possibly caused by excessive overexpression on U2OS cells that ended up misfolding and aggregate formation inside the cell (Figure 3.31).

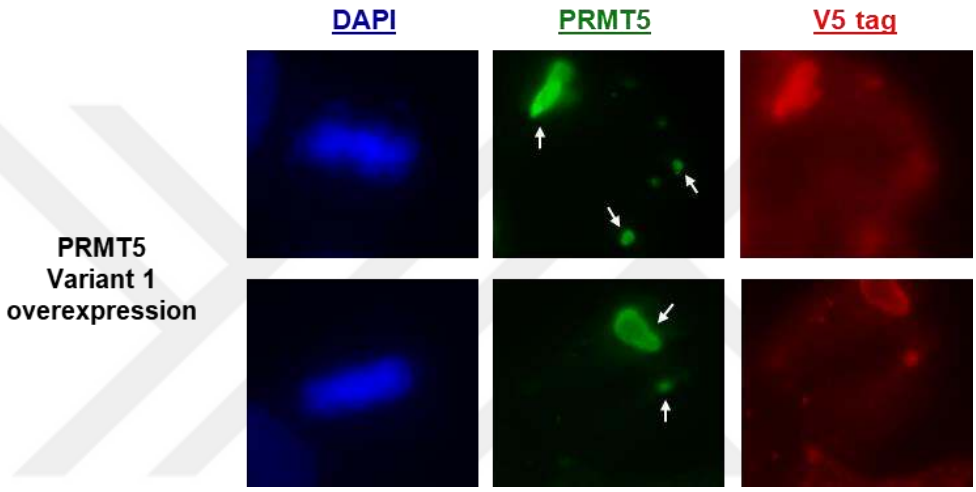

Figure 3.31. Localization of PRMT5 to centrosomes after PRMT5 overexpression on U2OS cancer cells. PRMT5 overexpressed U2OS cells were co-stained using anti-PRMT5 and anti-V5 tag antibodies. The formation of aggregates after PRMT5 overexpression were spotted with white arrows.

To investigate whether the localization at the centrosomes is diminished in the absence of PRMT5, IF was conducted following siPRMT5-mediated knockdown. Subsequent co-staining of PRMT5 with γ-tubulin after siPRMT5 transfection revealed that the co-localization within the cells at the metaphase stage remained unaltered. Intensity analysis in regions at the spindle poles during metaphase indicated no significant change in PRMT5 intensity (Figure 3.32B). This could be resulted from due to the half of reduction of PRMT5 expression, and still presence the residual of PRMT5 in siPRMT5-transfected cells.

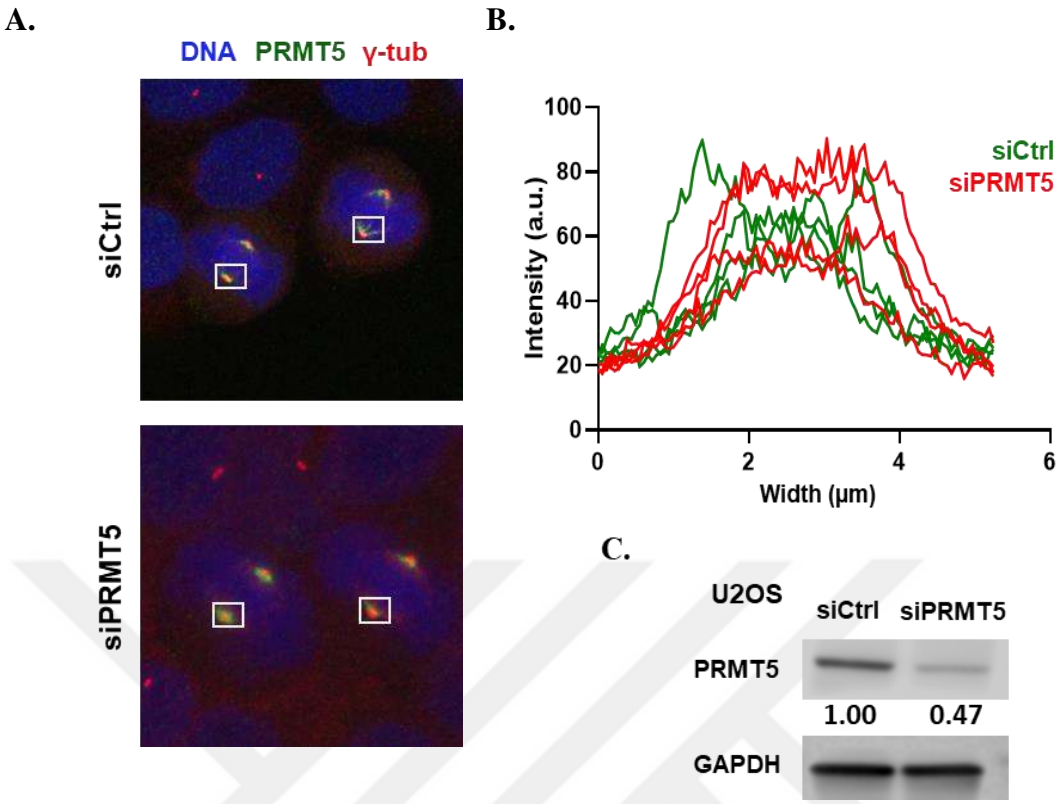

Figure 3.32. Co-staining of PRMT5 and y-tubulin and evaluation of PRMT5 localization after PRMT5 siRNA silencing. **(A)** After siRNA-mediated silencing, PRMT5 and y-tubulin co-staining confocal images were taken with the same exposure, merged, and selected white rectangular merged area were further investigated in intensity analysis. **(B)** Selected γ-tubulin and PRMT5 co-localized rectangular area were analyzed using ImageJ software intensity analysis tool and PRMT5 intensities were quantified. (C) siPRMT5 knock-down efficiency in U2OS cells were checked and PRMT5 knock-down was confirmed by Western Blot experiment.

Chapter 4:

DISCUSSION AND CONCLUSION

Prostate cancer (PCa) stands as the second most prevalent cancer type among men. The prevailing therapeutic interventions encompass active monitoring, surgical intervention, or radiation therapy. Hormone deprivation and cytotoxic medication regimens are conventionally preserved for advanced stages or instances of biochemical relapse, typified by CRPCa. However, their remedial potential remains limited due to the eventual acquired drug resistance by PCa cells. This phenomenon emanates from diverse cellular mechanisms that effectively bypass the intended mode of action of pharmaceutical agents. Given these circumstances, there arises a compelling imperative for pioneering therapeutic modalities. An alternative avenue for PCa treatment emerges through the repurposing of established pharmaceuticals initially designed for alternate medical modalities. By extrapolating the impacts of previously sanctioned medications onto the intracellular processes pertinent to PCa, the landscape of treatment possibilities stands to broaden substantially. Importantly, this approach proves to be fiscally prudent and operationally efficient, capitalizing on drugs already vouched for in terms of safety and efficacy (Bahmad et al. 2022).

The challenges in the field of prostate cancer research encompass the creation of novel and efficacious systemic therapeutic approaches, as well as the identification of mechanisms underlying the drug resistance. One of the instances of drug resistance involves tumor cells developing insensitivity to taxanes, which occurs through genetic and epigenetic modifications. These modifications trigger inherent resistance mechanisms within cancer cells. While the exact molecular and epigenetic pathways responsible for the development of taxane resistance remain to be precisely elucidated, it is widely acknowledged that this resistance is the outcome of a multifaceted process.

The scenario of taxane-resistant PCa presents as an intricate and heterogeneous ailment, posing challenges in pinpointing effective targets for innovative treatments. A comprehensive study about the mechanisms driving taxane resistance holds the potential to enhance the traditional treatments prefered on CRPCa. The imperative exists for

pioneering strategies aimed at overcoming taxane resistance in CRPCa. These initiatives encompass the exploration of fundamental resistance mechanisms, as well as the formulation of fresh pharmacological agents and synergistic therapeutic regimens (Maloney et al. 2020).

Epigenetic modifications have gained significant recognition as fundamental contributors to the development of resistance against anti-cancer pharmaceuticals. Consequently, targeting epigenetic regulators has become imperative in addressing drug-resistant malignancies (Biersack, Nitzsche, and Höpfner 2022). These epigenetic regulators, typically comprising enzymes or proteins that interact with chromatin, represent highly viable targets for therapeutic intervention using small inhibitory compounds. The reversible nature of epigenetic alterations enhances the appeal of epigenetic modifiers as valuable targets for therapeutic intervention. As such, the integration of chemotherapy with epigenetic inhibitors is emerging as a promising and prospective approach to counteract the phenomenon of drug resistance in cancer treatment (Clermont et al. 2016).

In this research, an analysis is conducted concerning epigenetic alterations in the context of taxane resistance, elucidating their growing acknowledgment as potential facilitators for surmounting taxane resistance in PCa. The emergence of drug resistance stands as a significant impediment in cancer therapy, notably in the case of taxane-derived regimens. Although the efficacy of taxane treatment is evident, its utility is impeded by the rise of resistance mechanisms. Hence, there is a compelling need to explore alternative strategies aimed at conquering this resistance phenomenon.

4.1. Summary of Principal Discoveries

In this study, the principal aim was to explore potential approaches for reversing the resistance mechanism to taxanes through the modulation of epigenetic regulators, thereby restoring cellular sensitivity to the taxanes. Additionally, we sought to elucidate the molecular pathways implicated in overcoming taxane resistance in CRPCa cells by investigating the role of PRMT5. This investigation led to the discovery of several noteworthy findings and insights. PRMT5 inhibitors successfully re-sensitized taxane-resistant CRPCa cells to taxanes, indicating that targeting PRMT5 proteins could

effectively overcome taxane resistance (Figure 3.4 and 3.5). Furthermore, we observed that efficient silencing of PRMT5 caused a mild reversal of taxane resistance in these cells. However, it also resulted in a notable decrease in proliferation in comparison with the parental cells (Figure 3.6). Nevertheless, our attempts to generate PRMT5 knock-out in Dtx-resistant cells were unsuccessful, implying the essentiality of PRMT5 especially on proliferation. Furthermore, in the experiment conducted to corroborate our observation of cell division, it was noted that the cells exhibit a significantly lower rate of division in comparison to the parental cells (Figure 3.9).

To assess the inhibitor's intracellular selective effectiveness, sDMA protein level was evaluated. The findings indicate that GSK591 demonstrated considerable potency, while HLCL-61 exhibited only a marginal effect on sDMA expression (Figure 3.10). In order to evaluate the impact on histone modifications, histone extraction was performed subsequent to sDMA in the total protein. Based on our understanding that PRMT5 symmetrically demethylates on H3R4, H3R8, H3R2, and H3AR3, we observed a similar impact on histones as observed in the total protein (Figure 3.11). In addition, sDMA modifications of certain PRMT5 target proteins were observed some alterations following siRNA knock-down, and this pattern was also seen with the drug treatments. A mild reduction was observed as expected upon PMRT5 having a role on sDMA modification to its target proteins (Figure 3.12). To assess the proper target engagement of inhibitors, GSK591 demonstrated significant engagement with PRTM5. In addition, inhibitors affect the expression of PRMT5 significantly in resistant cells, whereas they do not change the PRMT5 expression in parental cells.

A previous study showed that the upregulation of ABCB1 could play a potential role in CRPCa. An investigation employing the calcein uptake assay was conducted to evaluate the potential impact of PRMT5 inhibitors on the functionality of ABCB1. Upon administering PRMT5 inhibitors to both parental and resistant cells, a notable augmentation in green fluorescence was exclusively observed in taxane-resistant cells, with no discernible impact on the parental population. Based on our research discoveries, we hypnotized the possibility of a potential association between ABCB1 and PRMT5. Nevertheless, no significant change in mRNA expression was observed, irrespective of the administration of treatments aiming to suppress gene expression (Figure 3.14).

Consequently, these results have led us to contemplate the prospect that the resistance mechanism linked to PRMT5 could be manifested through alternative pathways.

Through RNA sequencing analysis, DEGs in both Dtx-resistant cells and PRMT5 silenced cells were identified. Inhibition of PRMT5 led to an altered expression profile of these genes, which showed an approach to the parental phenotype. Moreover, RNA sequencing analysis unveiled several mechanisms (such as MYC pathways, G2/M arrest, E2F, etc.) that potentially play an important role in PRMT5's ability to reverse taxane resistance. (Figure 3.17). For instance, the MYC pathway was shown to be downregulated, although MYC was not one of the genes that was identified as being significantly altered by the analysis. Therefore, we investigated the expression level of MYC. A mild reduction in MYC levels was observed, which could potentially explain why the genes in the myc pathway were downregulated.

It was anticipated that the inhibition of the PRTM5 enzyme in drug resistance would yield a comparable effect on the reversion mechanism through the MYC pathways. However, the outcomes were not as expected since the silencing of the MYC pathway did not exhibit a similar effect. Instead, a reduction in cell viability was observed in Dtx resistant cell line by MYC silencing. Moreover, data showed that the co-treatment of PRMT5i and taxanes induced cell death in taxane-resistant cells, further supporting our findings (Figure 3.20). In conclusion, our ongoing experiments based on RNA sequencing data strongly suggest that the use of PRMT5 inhibitors in combination with taxanes can effectively revert the resistance mechanism in taxane-resistant cells, offering promising prospects for addressing taxane resistance in CRPCa.

The findings derived from RNA sequencing analysis revealed a reduced expression of genes associated with cell division and cycle, leading to G2/M arrest. Subsequently, an in-depth investigation was conducted to explore the effects of this downregulation on the cellular division and cycle mechanisms (Figure 3.21). In addition, the relation between apoptosis and PMRT5 was evaluated, and the findings indicated that the concurrent administration of inhibitors and taxane demonstrated a favorable outcome in reversing taxane resistance (Figure 3.22 and 3.23). Additional inquiry and elucidation are imperative to attain a more profound comprehension of PRTM5 and its associated

pathways. Subsequent investigations are warranted to shed light on the prospective clinical implications arising from these discoveries.

Recent studies have demonstrated that PRMT5 located in the cytoplasm is essential for the proliferation of prostate cancer cells; however, when located in the nucleus, it inhibits their growth. (Gu et al. 2012). In accordance with the provided data, after nuclear/cytosol fractionation in our cells, PRMT5 predominantly localized within the cytosol. This has prompted inquiries regarding the specific subcellular compartment of PRMT5. To address this uncertainty utilizing immunofluorescence (IF) staining, a specific localization of PRMT5 was observed, particularly during the metaphase stage of the cells. This method enabled the detection of the endogenous PRMT5 protein. Since studies on centrosome biology are conducted in our laboratory, it has been ascertained that PRMT5 co-localizes with centrosomes. As a result, a co-staining with γ-tubulin (in HEK-293T cell line) was performed, a known centrosome marker, and a co-localization of PRMT5 with γ-tubulin was identified, predominantly during the metaphase stage, which diminishes in the interphase or anaphase stages (Figure 3.27). For further investigation, different cancer cell lines were also used for whether to observe the similar pattern (cancer cell lines; MDA-MB-231, MIA-Paca-2, Du145, U2OS as a control RPE1 cell line was used) (Figure 3.28). Despite the varying origins of cancers, our study showed that every type of cancer co-localized with γ-tubulin, predominantly during the metaphase phase.

To demonstrate that this localization is specific to metaphase and to expand the number of sample population, all cells were arrested in metaphase using different methods (Figures 3.29). IF staining indicated that nearly all cells in the population were arrested at the metaphase phase, and co-localization was noted (Figure 3.30).

PRMT5 has six types of variants, including these variants, variant 1, 2, 4 and 5 contain all domains (differences in the 5' coding region compared to variant 1) while variant 3 and 6 contain only the catalytic domain (Rasheed et al. 2023). In these variations, the lengthiest isoform is encoded by variant 1. To determine if this localization is specific to a variant, IF staining was conducted by overexpressing of PRMT5 variant 1. While we experienced protein aggregation following overexpression of PRMT5 variant

1 (Figure 3.31), our attempts to determine PMRT5 variant-specific localizations were not successful. Consequently, additional studies are required to identify which PRMT5 variant is localized at the centrosome.

Nevertheless, a validation experiment was performed utilizing U2OS cells, which demonstrated the absence of localization following siPRMT5 treatment. Yet, no significant difference was noted in comparison to the control group (Figure 3.32). The insufficiency of adequate knock-down or the non-specific binding of the antibody may account for this observation. Alternatively, another PRMT5 antibody can be used to prevent non-specific binding, or a more accurate result can be obtained by generating PRMT5 knock out cells.

4.2. Contrasting Findings with Prior Research

Our discoveries correspond with prior research that has illustrated the capacity of epigenetic control in counteracting taxane resistance. The effective modulation of PRMT5 proteins has exhibited efficacy in restoring sensitivity in taxane-resistant CRPCa cells.

A study showed that a direct interaction was discovered between the c-Myc protein and PRMT5, resulting in the transcriptional suppression of a set of genes. This gene cohort includes PTEN, CDKN2C, CDKN1A, CDKN1C, and p63, ultimately facilitating gastric cancer cell growth (M. Liu et al. 2020). It was indicated that PRMT5 is crucial for promoting cell proliferation of certain cancer types both in vitro and in vivo. Additionally, an enrichment of two factors, namely PRMT5-mediated H4R3me2s and c-Myc, was observed in the promoters of these genes. Notably, the recruitment of two factors (H4R3me2s and c-Myc) at the target gene promoters subsequently resulted in decrease in gene expression. Clinical relevance was gained by this molecular interaction, as elevated levels of both c-Myc and PRMT5 expression have been observed in primary human gastric cancer tissues. Of significant importance, an inverse correlation with clinical outcomes was exhibited by the levels of their expression (M. Liu et al. 2020).

Another study showed that cell cycle progression is facilitated by PRMT5 through the enhancement of cell cycle regulatory proteins including β-catenin, Cyclin D1,

CDK4/6, and CCND1/D2/E1 (M. Li et al. 2019). Inhibition of PRMT5 leads to a reduction in the proportions of the G1 and S phases, coupled with an elevation in the G2/M phase accumulation. This inhibition also promotes apoptosis in the sub-G1 phase. Suppression of PRMT5 (Fong et al. 2019), triggers an extension of the G1 phase in HCC cells, concomitant with a corresponding decline in the S and G2/M phases.

PRMT5 and Myc proteins exhibit distinct co-localization patterns, primarily within the cell nucleus. Disrupting the interaction of PRMT5 with c-Myc has been demonstrated to impede the proliferation of medulloblastoma cells and induce apoptosis in Myc-dependent tumors specifically (M. Li et al. 2019). The PRMT5 depletion significantly influences the binding of SRSF1 to both mRNAs and proteins. This alteration leads to the alternative splicing of numerous critical genes, ultimately resulting in the demise of human acute myeloid leukemia cells (Ichikawa et al. 2020). Furthermore, PRMT5's interaction with Zili and Vasa proteins is notable, wherein it directly catalyzes the symmetric dimethylation (sDMA) of Vasa and Zili proteins.

4.3. Contribution of Results for Drug Resistance in CRPCa

The regulation of cancer through epigenetic mechanisms significantly influences the development, advancement, and resistance to treatment of tumors. Epigenetic alterations have recently gained recognition for their pivotal role in the proliferation, progression, and drug refractoriness of PCa. Notably, epigenetic modulators, which encompass chromatin-affiliated proteins or enzymes, present themselves as promising targets for therapeutic intervention using small inhibitory compounds.

Collected data reveals that the pharmacologic suppression of PRTM5 effectively restores sensitivity to taxane treatment in CRPCa. Co-administration of taxanes alongside PRMT5 inhibition synergistically enhances the efficacy against taxane-resistant CRPCa cells. These findings not only elucidate the underlying mechanisms but also hold the potential for future therapeutic applications in managing taxane-resistant CRPCa.

The outcomes of this investigation carry significant implications for both the understanding and management of cancer, with relevance to taxane-resistant CRPCa. The

identification of PRTM5 proteins as key contributors to drug resistance offers valuable insights into conceivable targets for therapeutic intervention. The inhibition of PRMT5 emerges as a promising strategy to combat taxane resistance, thereby potentially ameliorating treatment outcomes for individuals afflicted with CRPCa.

First, RNA sequencing (conducted by Buse Cevatemre, Ph.D., and İpek Bulut, MSc.) was performed to reveal the fundamental differences between the two cell lines. This was done to distinguish the gene sets and pathways between the parental and resistant cell lines, as resistant cells exhibit a more aggressive phenotype. Moreover, our discoveries indicate that the process by which PRMT5 inhibition leads to reversion involves multiple pathways, including the MYC pathway and G2/M phase. In addition to these pathways, several pathways were identified in the GSEA analysis. These included the Unfolded Protein Response (UPR), mTOR, inflammatory response, and oxidative phosphorylation. However, within the scope of our research, we chose to focus on pathways related to cell division. This insight provides new opportunities for the creation of efficacious treatments targeting taxane-resistant CRPCa. There is potential for the utilization of PRMT5 inhibition in conjunction with taxane therapy for enhanced therapeutic outcomes.

4.4 Future Perspectives

Targeting epigenetic pathways represents a viable strategy for overcoming drug resistance, offering an alternative approach to combat this challenging issue. Epigenetic alterations encompass modifications in gene expression without any changes to the underlying DNA sequence. Epigenetic modifiers present themselves as valuable therapeutic targets due to their capability to reverse or counteract the epigenetic changes responsible for drug resistance. Furthermore, preliminary evidence suggests that epigenetic alterations might serve as predictive biomarkers. To effectively address drug-resistant cancers, it is imperative to direct our efforts towards targeting epigenetic regulators. Through the manipulation of these regulators' activity, we may be able to surmount drug resistance and improve treatment outcomes. One particularly promising strategy involves combining conventional chemotherapy with epigenetic modifiers,

aiming to harness the synergistic effects of chemotherapy drugs and epigenetic modulation for the treatment of resistant tumors. In summary, the integration of chemotherapy with epigenetic inhibitors holds significant promise for managing drug-resistant tumors.

Based on the insights derived from this study, we can propose several recommendations for future research studies. Further investigation into the specific functions of PRMT5 and its role in taxane resistance is required for a comprehensive understanding of its contributions. Additionally, we should conduct comprehensive studies to elucidate the precise mechanisms through which PRMT5 inhibition impacts the identified pathways and genes.

Taken together, the findings of this study lay the groundwork for future research on PRMT5 in taxane-resistant CRPCa. Future investigations should focus on unraveling the functional significance of PRMT5 and the inhibition of non-histone proteins, as well as exploring their interplay in tumorigenesis and chemotherapy resistance. Such research holds the potential to identify therapeutic targets that can significantly enhance treatment outcomes for CRPCa patients. In addition, the literature presents numerous findings concerning the functions of PRMT5 in the cytosol. However, there is a limited number of studies addressing its centrosome localization. Notably, only one doctoral thesis provides evidence that aligns with our research; PRMT5 was identified as a novel PLK4 substrate and was noticed that PRTM5 localized to the centrosomes where PLK4 is known to be found. It has shown PLK4 to be epigenetically regulated in the context of cancer development and progression (Sivakumar, 2014). Compared to our data, the observed localization could have occurred due to the interaction between PRTM5 and PLK4. But it is imperative to conduct additional research to ascertain whether PRMT5 is located at the centrosome.

Furthermore, it is essential for future research to concentrate on validating the efficacy and safety of PRMT5 inhibitors in both preclinical and clinical settings. The exploration of clinical applications of PRMT5 inhibition, both as a monotherapy and in combination with taxanes or other treatment modalities, presents a promising avenue for improving outcomes in taxane-resistant CRPCa patients.

4.5. Conclusion

In conclusion, epigenetic modifiers play a significant role in conferring drug resistance. Within this category, numerous epigenetic regulators and their inhibitors offer promising therapeutic avenues for addressing taxane-resistant CRPCa. The resulting combination studies imply that inhibiting PRTM5 enhances the sensitivity of CRPCa cells to commonly utilized taxanes like docetaxel and cabazitaxel in a synergistic manner.

In this work, we elucidate the capacity of PRTM5 to counter taxane resistance in CRPCa, shedding light on its reversal effect. Our acquired data underscores the involvement of several pathways in the regulation of PRTM5 (Figure 4.1). While epigenetic inhibitors are in their early stages of clinical development, our findings regarding the underlying mechanisms hold potential for shaping future strategies in prostate cancer therapy.

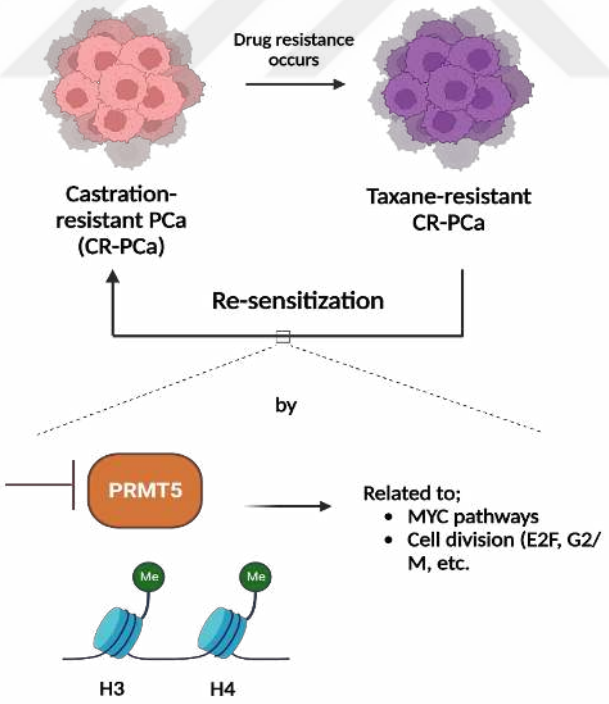

Figure 4.1. A schematic model of PRMT5 inhibition effect on taxane resistant CRPCa.

BIBLIOGRAPHY

Andreu-Pérez, Pedro, Rosaura Esteve-Puig, Carlos de Torre-Minguela, Marta López-Fauqued, Joan Josep Bech-Serra, Stephan Tenbaum, Elena R. García-Trevijano, et al. 2011. "Protein Arginine Methyltransferase 5 Regulates ERK1/2 Signal Transduction Amplitude and Cell Fate through CRAF." Science Signaling 4 (190): ra58.

Antonysamy, Stephen, Zahid Bonday, Robert M. Campbell, Brandon Doyle, Zhanna Druzina, Tarun Gheyi, Bomie Han, et al. 2012. "Crystal Structure of the Human PRMT5:MEP50 Complex." Proceedings of the National Academy of Sciences of the United States of America 109 (44): 17960–65.

Bahmad, Hisham F., Timothy Demus, Maya M. Moubarak, Darine Daher, Juan Carlos Alvarez Moreno, Francesca Polit, Olga Lopez, et al. 2022. "Overcoming Drug Resistance in Advanced Prostate Cancer by Drug Repurposing." Medical Sciences (Basel, Switzerland) 10 (1). https://doi.org/10.3390/medsci10010015.

Baldwin, R. Mitchell, Alan Morettin, and Jocelyn Côté. 2014. "Role of PRMTs in Cancer: Could Minor Isoforms Be Leaving a Mark?" World Journal of Biological Chemistry 5 (2): 115–29.

Bandyopadhyay, Smarajit, Daniel P. Harris, Gregory N. Adams, Gregory E. Lause, Anne McHugh, Emily G. Tillmaand, Angela Money, Belinda Willard, Paul L. Fox, and Paul E. Dicorleto. 2012. "HOXA9 Methylation by PRMT5 Is Essential for Endothelial Cell Expression of Leukocyte Adhesion Molecules." Molecular and Cellular Biology 32 (7): 1202–13.

Bedford, Mark T., and Steven G. Clarke. 2009. "Protein Arginine Methylation in Mammals: Who, What, and Why." Molecular Cell 33 (1): 1–13.

Bedford, Mark T., and Stéphane Richard. 2005. "Arginine Methylation an Emerging Regulator of Protein Function." Molecular Cell 18 (3): 263–72.

Beketova, Elena, Jake L. Owens, Andrew M. Asberry, and Chang-Deng Hu. 2022. "PRMT5: A Putative Oncogene and Therapeutic Target in Prostate Cancer." Cancer Gene Therapy 29 (3-4): 264–76.

Belkahla, Sana, Insha Nahvi, Supratim Biswas, Irum Nahvi, and Nidhal Ben Amor. 2022. "Advances and Development of Prostate Cancer, Treatment, and Strategies: A Systemic Review." Frontiers in Cell and Developmental Biology 10 (September):

991330.

Berry, W., S. Dakhil, M. A. Gregurich, and L. Asmar. 2001. “Phase II Trial of Single-Agent Weekly Docetaxel in Hormone-Refractory, Symptomatic, Metastatic Carcinoma of the Prostate.” Seminars in Oncology 28 (4 Suppl 15): 8–15.

Biersack, Bernhard, Bianca Nitzsche, and Michael Höpfner. 2022. “HDAC Inhibitors with Potential to Overcome Drug Resistance in Castration-Resistant Prostate Cancer.” Cancer Drug Resistance (Alhambra, Calif.) 5 (1): 64–79.

Blanc, Roméo S., and Stéphane Richard. 2017. “Arginine Methylation: The Coming of Age.” Molecular Cell 65 (1): 8–24.

Boisvert, François-Michel, Carol Anne Chénard, and Stéphane Richard. 2005. “Protein Interfaces in Signaling Regulated by Arginine Methylation.” Science’s STKE: Signal Transduction Knowledge Environment 2005 (271): re2.

Boisvert, François-Michel, Jocelyn Côté, Marie-Chloé Boulanger, and Stéphane Richard. 2003. “A Proteomic Analysis of Arginine-Methylated Protein Complexes.” Molecular & Cellular Proteomics: MCP 2 (12): 1319–30.

Bono, Johann Sebastian de, Stephane Oudard, Mustafa Ozguroglu, Steinbjørn Hansen, Jean-Pascal Machiels, Ivo Kocak, Gwenaëlle Gravis, et al. 2010. “Prednisone plus Cabazitaxel or Mitoxantrone for Metastatic Castration-Resistant Prostate Cancer Progressing after Docetaxel Treatment: A Randomised Open-Label Trial.” The Lancet 376 (9747): 1147–54.

Branscombe, T. L., A. Frankel, J. H. Lee, J. R. Cook, Z. Yang, S. Pestka, and S. Clarke. 2001. “PRMT5 (Janus Kinase-Binding Protein 1) Catalyzes the Formation of Symmetric Dimethylarginine Residues in Proteins.” The Journal of Biological Chemistry 276 (35): 32971–76.

Calle, Eugenia E., Carmen Rodriguez, Kimberly Walker-Thurmond, and Michael J. Thun. 2003. “Overweight, Obesity, and Mortality from Cancer in a Prospectively Studied Cohort of U.S. Adults.” The New England Journal of Medicine 348 (17): 1625–38.

Cha, Boksik, and Eek-Hoon Jho. 2012. “Protein Arginine Methyltransferases (PRMTs) as Therapeutic Targets.” Expert Opinion on Therapeutic Targets 16 (7): 651–64.

Chandrasekar, Thenappan, Joy C. Yang, Allen C. Gao, and Christopher P. Evans. 2015. “Mechanisms of Resistance in Castration-Resistant Prostate Cancer (CRPC).”

Translational Andrology and Urology 4 (3): 365–80.

Cheung, Ngai, Li Chong Chan, Alex Thompson, Michael L. Cleary, and Chi Wai Eric So. 2007. “Protein Arginine-Methyltransferase-Dependent Oncogenesis.” Nature Cell Biology 9 (10): 1208–15.

Cho, Er-Chieh, Shunsheng Zheng, Shonagh Munro, Geng Liu, Simon M. Carr, Jutta Moehlenbrink, Yi-Chien Lu, et al. 2012. “Arginine Methylation Controls Growth Regulation by E2F-1.” The EMBO Journal 31 (7): 1785–97.

Choi, Young Hee, and Ai-Ming Yu. 2014. “ABC Transporters in Multidrug Resistance and Pharmacokinetics, and Strategies for Drug Development.” Current Pharmaceutical Design 20 (5): 793–807.

Clermont, Pier-Luc, Francesco Crea, Yan Ting Chiang, Dong Lin, Amy Zhang, James Z. L. Wang, Abhijit Parolia, et al. 2016. “Identification of the Epigenetic Reader CBX2 as a Potential Drug Target in Advanced Prostate Cancer.” Clinical Epigenetics 8 (February): 16.

Davies, Alastair, Vincenza Conteduca, Amina Zoubeidi, and Himisha Beltran. 2019. “Biological Evolution of Castration-Resistant Prostate Cancer.” European Urology Focus 5 (2): 147–54.

Dawson, Mark A., and Tony Kouzarides. 2012. “Cancer Epigenetics: From Mechanism to Therapy.” Cell 150 (1): 12–27.

Depeille, P., P. Cuq, I. Passagne, A. Evrard, and L. Vian. 2005. “Combined Effects of GSTP1 and MRP1 in Melanoma Drug Resistance.” British Journal of Cancer 93 (2): 216–23.

Dewey, W. C., and H. H. Miller. 1969. “X-Ray Induction of Chromatid Exchanges in Mitotic and G1 Chinese Hamster Cells Pretreated with Colcemid.” Experimental Cell Research 57 (1): 63–70.

Di, Yuqin, Xiaoqian Jing, Kunhua Hu, Xiangqiong Wen, Lvlan Ye, Xiang Zhang, Jiale Qin, et al. 2023. “The c-MYC-WDR43 Signalling Axis Promotes Chemoresistance and Tumour Growth in Colorectal Cancer by Inhibiting p53 Activity.” Drug Resistance Updates: Reviews and Commentaries in Antimicrobial and Anticancer Chemotherapy 66 (January): 100909.

Domingo-Domenech, Josep, Cristina Oliva, Ana Rovira, Jordi Codony-Servat, Marta Bosch, Xavier Filella, Clara Montagut, et al. 2006. “Interleukin 6, a Nuclear Factor-kappaB Target, Predicts Resistance to Docetaxel in Hormone-Independent Prostate

Cancer and Nuclear Factor-kappaB Inhibition by PS-1145 Enhances Docetaxel Antitumor Activity." Clinical Cancer Research: An Official Journal of the American Association for Cancer Research 12 (18): 5578–86.

Durant, Stephen T., Er Chieh Cho, and Nicholas B. La Thangue. 2009. "p53 Methylation--the Arg-Ument Is Clear." Cell Cycle 8 (6): 801–2.

Duronio, Robert J., and Yue Xiong. 2013. "Signaling Pathways That Control Cell Proliferation." Cold Spring Harbor Perspectives in Biology 5 (3): a008904.

Eisenberger, M. A., R. Simon, P. J. O'Dwyer, R. E. Wittes, and M. A. Friedman. 1985. "A Reevaluation of Nonhormonal Cytotoxic Chemotherapy in the Treatment of Prostatic Carcinoma." Journal of Clinical Oncology: Official Journal of the American Society of Clinical Oncology 3 (6): 827–41.

Feng, You, Ranjan Maity, Julian P. Whitelegge, Andrea Hadjikyriacou, Ziwei Li, Cecilia Zurita-Lopez, Qais Al-Hadid, et al. 2013. "Mammalian Protein Arginine Methyltransferase 7 (PRMT7) Specifically Targets RXR Sites in Lysine- and Arginine-Rich Regions." The Journal of Biological Chemistry 288 (52): 37010–25.

Fojo, T., and M. Menefee. 2007. "Mechanisms of Multidrug Resistance: The Potential Role of Microtubule-Stabilizing Agents." Annals of Oncology: Official Journal of the European Society for Medical Oncology / ESMO 18 Suppl 5 (July): v3–8.

Fong, Jia Yi, Luca Pignata, Pierre-Alexis Goy, Kimihito Cojin Kawabata, Stanley Chun-Wei Lee, Cheryl M. Koh, Daniele Musiani, et al. 2019. "Therapeutic Targeting of RNA Splicing Catalysis through Inhibition of Protein Arginine Methylation." Cancer Cell 36 (2): 194–209.e9.

Gann, P. H., C. H. Hennekens, J. Ma, C. Longcope, and M. J. Stampfer. 1996. "Prospective Study of Sex Hormone Levels and Risk of Prostate Cancer." Journal of the National Cancer Institute 88 (16): 1118–26.

Guderian, Gernot, Christoph Peter, Julia Wiesner, Albert Sickmann, Klaus Schulze-Osthoff, Utz Fischer, and Matthias Grimmler. 2011. "RioK1, a New Interactor of Protein Arginine Methyltransferase 5 (PRMT5), Competes with pICln for Binding and Modulates PRMT5 Complex Composition and Substrate Specificity." The Journal of Biological Chemistry 286 (3): 1976–86.

Guo, Ailan, Hongbo Gu, Jing Zhou, Daniel Mulhern, Yi Wang, Kimberly A. Lee, Vicky Yang, et al. 2014. "Immunoaffinity Enrichment and Mass Spectrometry Analysis of Protein Methylation." Molecular & Cellular Proteomics: MCP 13 (1): 372–87.

Guo, Zhigang, Li Zheng, Hong Xu, Huifang Dai, Mian Zhou, Mary Rose Pascua, Qin M. Chen, and Binghui Shen. 2010. “Methylation of FEN1 Suppresses Nearby Phosphorylation and Facilitates PCNA Binding.” Nature Chemical Biology 6 (10): 766–73.

Gu, Zhongping, Shen Gao, Fahao Zhang, Zhiqiang Wang, Wencai Ma, Richard E. Davis, and Zhengxin Wang. 2012. “Protein Arginine Methyltransferase 5 Is Essential for Growth of Lung Cancer Cells.” Biochemical Journal 446 (2): 235–41.

Gu, Zhongping, Yirong Li, Peng Lee, Tao Liu, Chidan Wan, and Zhengxin Wang. 2012. “Protein Arginine Methyltransferase 5 Functions in Opposite Ways in the Cytoplasm and Nucleus of Prostate Cancer Cells.” PloS One 7 (8): e44033.

He, Wei, Xiaoyan Ma, Xiao Yang, Yun Zhao, Junkang Qiu, and Haiying Hang. 2011. “A Role for the Arginine Methylation of Rad9 in Checkpoint Control and Cellular Sensitivity to DNA Damage.” Nucleic Acids Research 39 (11): 4719–27.

Hodges, Laura M., Svetlana M. Markova, Leslie W. Chinn, Jason M. Gow, Deanna L. Kroetz, Teri E. Klein, and Russ B. Altman. 2011. “Very Important Pharmacogene Summary: ABCB1 (MDR1, P-Glycoprotein).” Pharmacogenetics and Genomics 21 (3): 152–61.

Ho, Meng-Chiao, Carola Wilczek, Jeffrey B. Bonanno, Li Xing, Janina Seznec, Tsutomu Matsui, Lester G. Carter, et al. 2013. “Structure of the Arginine Methyltransferase PRMT5-MEP50 Reveals a Mechanism for Substrate Specificity.” PloS One 8 (2): e57008.

Hong, Heng, Chinghai Kao, Meei-Huey Jeng, John N. Eble, Michael O. Koch, Thomas A. Gardner, Shaobo Zhang, et al. 2004. “Aberrant Expression of CARM1, a Transcriptional Coactivator of Androgen Receptor, in the Development of Prostate Carcinoma and Androgen-Independent Status.” Cancer 101 (1): 83–89.

Hou, Zhaoyuan, Hongzhuang Peng, Kasirajan Ayyanathan, Kai-Ping Yan, Ellen M. Langer, Gregory D. Longmore, and Frank J. Rauscher 3rd. 2008. “The LIM Protein AJUBA Recruits Protein Arginine Methyltransferase 5 to Mediate SNAIL-Dependent Transcriptional Repression.” Molecular and Cellular Biology 28 (10): 3198–3207.

Hsu, Jung-Mao, Chun-Te Chen, Chao-Kai Chou, Hsu-Ping Kuo, Long-Yuan Li, Chun-Yi Lin, Hong-Jen Lee, et al. 2011. “Crosstalk between Arg 1175 Methylation and Tyr 1173 Phosphorylation Negatively Modulates EGFR-Mediated ERK Activation.” Nature Cell Biology 13 (2): 174–81.

Huang, Huaping, Tangying Li, Mingjing Chen, Feng Liu, Haifeng Wu, Jie Wang, Jialiang Chen, and Xi Li. 2018. “Identification and Validation of NOLC1 as a Potential Target for Enhancing Sensitivity in Multidrug Resistant Non-Small Cell Lung Cancer Cells.” Cellular & Molecular Biology Letters 23 (November): 54.

Huang, Yiqiao, Xianhan Jiang, Xue Liang, and Ganggang Jiang. 2018. “Molecular and Cellular Mechanisms of Castration Resistant Prostate Cancer.” Oncology Letters 15 (5): 6063–76.

Hu, Dong, Mert Gur, Zhuan Zhou, Armin Gamper, Mien-Chie Hung, Naoya Fujita, Li Lan, Ivet Bahar, and Yong Wan. 2015. “Interplay between Arginine Methylation and Ubiquitylation Regulates KLF4-Mediated Genome Stability and Carcinogenesis.” Nature Communications 6 (September): 8419.

Hu, Yan, Hanshuo Mu, and Zhiping Deng. 2023. “RBM14 as a Novel Epigenetic-Activated Tumor Oncogene Is Implicated in the Reprogramming of Glycolysis in Lung Cancer.” World Journal of Surgical Oncology 21 (1): 132.

Ichikawa, Tomonaga, Obeid Shanab, Shingo Nakahata, Shunsuke Shimosaki, Nawin Manachai, Masaya Ono, Hidekatsu Iha, Kazuya Shimoda, and Kazuhiro Morishita. 2020. “Novel PRMT5-Mediated Arginine Methylations of HSP90A Are Essential for Maintenance of HSP90A Function in NDRG2 ATL and Various Cancer Cells.” Biochimica et Biophysica Acta, Molecular Cell Research 1867 (2): 118615.

Jafari, Rozbeh, Helena Almqvist, Hanna Axelsson, Marina Ignatushchenko, Thomas Lundbäck, Pär Nordlund, and Daniel Martinez Molina. 2014. “The Cellular Thermal Shift Assay for Evaluating Drug Target Interactions in Cells.” Nature Protocols 9 (9): 2100–2122.

Jänicke, R. U., M. L. Sprengart, M. R. Wati, and A. G. Porter. 1998. “Caspase-3 Is Required for DNA Fragmentation and Morphological Changes Associated with Apoptosis.” The Journal of Biological Chemistry 273 (16): 9357–60.

Jansson, Martin, Stephen T. Durant, Er-Chieh Cho, Sharon Sheahan, Mariola Edelmann, Benedikt Kessler, and Nicholas B. La Thangue. 2008. “Arginine Methylation Regulates the p53 Response.” Nature Cell Biology 10 (12): 1431–39.

Jing, Pengyu, Nianlin Xie, Ximing Zhu, Haizhou Dang, and Zhongping Gu. 2018. “The Methylation Induced by Protein Arginine Methyltransferase 5 Promotes Tumorigenesis and Progression of Lung Cancer.” Journal of Thoracic Disease 10 (12): 7014–19.

Jing, Pengyu, Nan Zhao, Mingxiang Ye, Yong Zhang, Zhipei Zhang, Jianyong Sun, Zhengxin Wang, Jian Zhang, and Zhongping Gu. 2018. “Protein Arginine Methyltransferase 5 Promotes Lung Cancer Metastasis via the Epigenetic Regulation of miR-99 family/FGFR3 Signaling.” Cancer Letters 427 (July): 38–48.

Karkhanis, Vrajesh, Yu-Jie Hu, Robert A. Baiocchi, Anthony N. Imbalzano, and Saïd Sif. 2011. “Versatility of PRMT5-Induced Methylation in Growth Control and Development.” Trends in Biochemical Sciences 36 (12): 633–41.

Ke, Jing, Chunming Gu, Heyan Zhang, Yang Liu, Wenhao Zhang, Huiling Rao, Shan Li, and Fuyun Wu. 2021. “Nucleolin Promotes Cisplatin Resistance in Cervical Cancer by the YB1-MDR1 Pathway.” Journal of Oncology 2021 (April): 9992218.

Khorasanizadeh, Sepideh. 2004. “The Nucleosome: From Genomic Organization to Genomic Regulation.” Cell 116 (2): 259–72.

Kim, Hyungsoo, and Ze’ev A. Ronai. 2020. “PRMT5 Function and Targeting in Cancer.” Cell Stress & Chaperones 4 (8): 199–215.

Kim, Jee-Heun, So-Yeon Park, So-El Jeon, Jang-Hyun Choi, Choong-Jae Lee, Tae-Young Jang, Hyeon-Ji Yun, et al. 2022. “DCLK1 Promotes Colorectal Cancer Stemness and Aggressiveness via the XRCC5/COX2 Axis.” Theranostics 12 (12): 5258–71.

Kim, Young-Rang, Byung Kook Lee, Ra-Young Park, Nguyen Thi Xuan Nguyen, Jeong A. Bae, Dong Deuk Kwon, and Chaeyong Jung. 2010. “Differential CARM1 Expression in Prostate and Colorectal Cancers.” BMC Cancer 10 (May): 197.

Koh, Cheryl M., Marco Bezzi, Diana H. P. Low, Wei Xia Ang, Shun Xie Teo, Florence P. H. Gay, Muthafar Al-Haddawi, et al. 2015. “MYC Regulates the Core Pre-mRNA Splicing Machinery as an Essential Step in Lymphomagenesis.” Nature 523 (7558): 96–100.

Krause, Christopher D., Zhi-Hong Yang, Young-Sun Kim, Jin-Hyung Lee, Jeffry R. Cook, and Sidney Pestka. 2007. “Protein Arginine Methyltransferases: Evolution and Assessment of Their Pharmacological and Therapeutic Potential.” Pharmacology & Therapeutics 113 (1): 50–87.

Krause, Werner. 2023. “Resistance to Prostate Cancer Treatments.” IUBMB Life 75 (5): 390–410.

Kroiss, Matthias, Katharina M. Brünger, Julia Wiesner, Matthias Grimmler, Albert Sickmann, and Utz Fischer. 2009. “Native Purification of Protein and RNA-

Protein Complexes Using a Novel Affinity Procedure." Fly 3 (3): 221–28.

Lakshmanan, Imayavaramban, and Surinder K. Batra. 2013. "Protocol for Apoptosis Assay by Flow Cytometry Using Annexin V Staining Method." Bio-Protocol 3 (6). https://doi.org/10.21769/bioprotoc.374.

Lian, Fei, Nitya V. Sharma, Josue D. Moran, and Carlos S. Moreno. 2015. "The Biology of Castration-Resistant Prostate Cancer." Current Problems in Cancer 39 (1): 17–28.

Li, Lin, Nan Wang, Youyi Xiong, Guangcheng Guo, Mingzhi Zhu, and Yuanting Gu. 2022. "Transcription Factor FOSL1 Enhances Drug Resistance of Breast Cancer through DUSP7-Mediated Dephosphorylation of PEA15." Molecular Cancer Research: MCR 20 (4): 515–26.

Li, Mingyue, Wentao An, Linyan Xu, Yidan Lin, Ling Su, and Xiangguo Liu. 2019. "The Arginine Methyltransferase PRMT5 and PRMT1 Distinctly Regulate the Degradation of Anti-Apoptotic Protein CFLAR in Human Lung Cancer Cells." Journal of Experimental & Clinical Cancer Research: CR 38 (1): 64.

Liu, Binfeng, Zhendong Liu, Yanbiao Wang, Xiaoyu Lian, Zhibin Han, Xingbo Cheng, Yongjie Zhu, Runze Liu, Yaoye Zhao, and Yanzheng Gao. 2021. "Overexpression of GINS4 Is Associated with Poor Prognosis and Survival in Glioma Patients." Molecular Medicine 27 (1): 117.

Liu, Fan, Ye Xu, Xiaoqing Lu, Pierre-Jacques Hamard, Daniel L. Karl, Na Man, Adnan K. Mookhtiar, et al. 2020. "PRMT5-Mediated Histone Arginine Methylation Antagonizes Transcriptional Repression by Polycomb Complex PRC2." Nucleic Acids Research 48 (6): 2956–68.

Liu, Ming, Bing Yao, Tao Gui, Chan Guo, Xiaobin Wu, Jiahuang Li, Lingling Ma, et al. 2020. "PRMT5-Dependent Transcriptional Repression of c-Myc Target Genes Promotes Gastric Cancer Progression." Theranostics 10 (10): 4437–52.

Liu, Ya-Ping, Can-Can Zheng, Yun-Na Huang, Ming-Liang He, Wen Wen Xu, and Bin Li. 2021. "Molecular Mechanisms of Chemo- and Radiotherapy Resistance and the Potential Implications for Cancer Treatment." MedComm 2 (3): 315–40.

Lombard, Alan P., Chengfei Liu, Cameron M. Armstrong, Vito Cucchiara, Xinwei Gu, Wei Lou, Christopher P. Evans, and Allen C. Gao. 2017. "ABCB1 Mediates Cabazitaxel-Docetaxel Cross-Resistance in Advanced Prostate Cancer." Molecular Cancer Therapeutics 16 (10): 2257–66.

Lombard, Alan P., Wei Lou, Cameron M. Armstrong, Leandro S. D'Abronzo, Shu Ning, Christopher P. Evans, and Allen C. Gao. 2021. "Activation of the Amplicon in Docetaxel- and Cabazitaxel-Resistant Prostate Cancer Cells." Molecular Cancer Therapeutics 20 (10): 2061–70.

Lund, Anders H., and Maarten van Lohuizen. 2004. "Epigenetics and Cancer." Genes & Development 18 (19): 2315–35.

Mahon, Kate L., Susan M. Henshall, Robert L. Sutherland, and Lisa G. Horvath. 2011. "Pathways of Chemotherapy Resistance in Castration-Resistant Prostate Cancer." Endocrine-Related Cancer 18 (4): R103–23.

Maloney, Sara M., Camden A. Hoover, Lorena V. Morejon-Lasso, and Jenifer R. Prosperi. 2020. "Mechanisms of Taxane Resistance." Cancers 12 (11). https://doi.org/10.3390/cancers12113323.

Maluf, Fernando Cotait, Felipe Moraes Toledo Pereira, Adriano Gonçalves Silva, Aldo Lourenço Abbade Dettino, Ana Paula Garcia Cardoso, André Seeke Sasse, Andrey Soares, et al. 2021. "Consensus on the Treatment and Follow-Up for Metastatic Castration-Resistant Prostate Cancer: A Report from the First Global Prostate Cancer Consensus Conference for Developing Countries (PCCCDC)." JCO Global Oncology 7 (April): 559–71.

Martin, Richard M., Lars Vatten, David Gunnell, and Pål Romundstad. 2010. "Blood Pressure and Risk of Prostate Cancer: Cohort Norway (CONOR)." Cancer Causes & Control: CCC 21 (3): 463–72.

McGuire, Shelley. 2016. "World Cancer Report 2014. Geneva, Switzerland: World Health Organization, International Agency for Research on Cancer, WHO Press, 2015." Advances in Nutrition 7 (2): 418–19.

McIlwain, David R., Thorsten Berger, and Tak W. Mak. 2013. "Caspase Functions in Cell Death and Disease." Cold Spring Harbor Perspectives in Biology 5 (4): a008656.

Mita, Alain C., Louis J. Denis, Eric K. Rowinsky, Johann S. Debono, Andrew D. Goetz, Leonel Ochoa, Bahram Forouzesh, et al. 2009. "Phase I and Pharmacokinetic Study of XRP6258 (RPR 116258A), a Novel Taxane, Administered as a 1-Hour Infusion Every 3 Weeks in Patients with Advanced Solid Tumors." Clinical Cancer Research: An Official Journal of the American Association for Cancer Research 15 (2): 723–30.

Mueller, Helen S., Colin E. Fowler, Simona Dalin, Enrico Moiso, Tee

Udomlumleart, Salil Garg, Michael T. Hemann, and Jacqueline A. Lees. 2021. “Acquired Resistance to PRMT5 Inhibition Induces Concomitant Collateral Sensitivity to Paclitaxel.” Proceedings of the National Academy of Sciences of the United States of America 118 (34). https://doi.org/10.1073/pnas.2024055118.

Nader, Rita, Joelle El Amm, and Jeanny B. Aragon-Ching. 2018. “Role of Chemotherapy in Prostate Cancer.” Asian Journal of Andrology 20 (3): 221–29.

Ong, Shao-En, Gerhard Mittler, and Matthias Mann. 2004. “Identifying and Quantifying in Vivo Methylation Sites by Heavy Methyl SILAC.” Nature Methods 1 (2): 119–26.

Oudard, Stéphane, Karim Fizazi, Lisa Sengeløv, Gedske Daugaard, Fred Saad, Steinbjørn Hansen, Marie Hjälm-Eriksson, et al. 2017. “Cabazitaxel Versus Docetaxel As First-Line Therapy for Patients With Metastatic Castration-Resistant Prostate Cancer: A Randomized Phase III Trial-FIRSTANA.” Journal of Clinical Oncology: Official Journal of the American Society of Clinical Oncology 35 (28): 3189–97.

Owens, Jake L., Elena Beketova, Sheng Liu, Samantha L. Tinsley, Andrew M. Asberry, Xuehong Deng, Jiaoti Huang, Chenglong Li, Jun Wan, and Chang-Deng Hu. 2020. “PRMT5 Cooperates with pICln to Function as a Master Epigenetic Activator of DNA Double-Strand Break Repair Genes.” iScience 23 (1): 100750.

Pal, Sharmistha, Robert A. Baiocchi, John C. Byrd, Michael R. Grever, Samson T. Jacob, and Saïd Sif. 2007. “Low Levels of miR-92b/96 Induce PRMT5 Translation and H3R8/H4R3 Methylation in Mantle Cell Lymphoma.” The EMBO Journal 26 (15): 3558–69.

Peng, Wan-Xin, Er-Meng Xiong, Lu Ge, Yan-Ya Wan, Chun-Li Zhang, Feng-Yi Du, Min Xu, Reyaz Ahmed Bhat, Jie Jin, and Ai-Hua Gong. 2016. “Egr-1 Promotes Hypoxia-Induced Autophagy to Enhance Chemo-Resistance of Hepatocellular Carcinoma Cells.” Experimental Cell Research 340 (1): 62–70.

Picus, J., and M. Schultz. 1999. “Docetaxel (Taxotere) as Monotherapy in the Treatment of Hormone-Refractory Prostate Cancer: Preliminary Results.” Seminars in Oncology 26 (5 Suppl 17): 14–18.

Pienta, K. J. 2001. “Preclinical Mechanisms of Action of Docetaxel and Docetaxel Combinations in Prostate Cancer.” Seminars in Oncology 28 (4 Suppl 15): 3–7.

Rasheed, Shayaan, Renee A. Bouley, Ryan J. Yoder, and Ruben C. Petreaca. 2023. “Protein Arginine Methyltransferase 5 (PRMT5) Mutations in Cancer Cells.” International Journal of Molecular Sciences 24 (7).

https://doi.org/10.3390/ijms24076042.

Rubio, Andres J., Alfonso E. Bencomo-Alvarez, James E. Young, Vanessa V. Velazquez, Joshua J. Lara, Mayra A. Gonzalez, and Anna M. Eiring. 2021. “26S Proteasome Non-ATPase Regulatory Subunits 1 (PSMD1) and 3 (PSMD3) as Putative Targets for Cancer Prognosis and Therapy.” Cells 10 (9). https://doi.org/10.3390/cells10092390.

Sella, Avishay, Cora Sternberg, Svetlana Kovel, Nirit Yarom, and Iwona Skoneczna. 2007. “Progression after Docetaxel-Based Chemotherapy in Androgen-Independent Prostate Cancer.” BJU International 100 (3): 533–35.

Semenas, Julius, Cinzia Allegrucci, Stephen A. Boorjian, Nigel P. Mongan, and Jenny Liao Persson. 2012. “Overcoming Drug Resistance and Treating Advanced Prostate Cancer.” Current Drug Targets 13 (10): 1308–23.

Shailesh, Harshita, Zain Z. Zakaria, Robert Baiocchi, and Saïd Sif. 2018. “Protein Arginine Methyltransferase 5 (PRMT5) Dysregulation in Cancer.” Oncotarget 9 (94): 36705–18.

Shi, Zhen-Duo, Lin Hao, Xiao-Xiao Han, Zhuo-Xun Wu, Kun Pang, Yang Dong, Jia-Xin Qin, et al. 2022. “Targeting HNRNPU to Overcome Cisplatin Resistance in Bladder Cancer.” Molecular Cancer 21 (1): 37.

Siegel, Rebecca, Elizabeth Ward, Otis Brawley, and Ahmedin Jemal. 2011. “Cancer Statistics, 2011: The Impact of Eliminating Socioeconomic and Racial Disparities on Premature Cancer Deaths.” CA: A Cancer Journal for Clinicians 61 (4): 212–36.

Sivakumar, Gayathri, "Polo-like kinase 4 at the nexus of epigenetic modifications and the DNA damage signaling network" (2014). Electronic Theses and Dissertations. 5146.

Skoufias, Dimitrios A., Salvatore DeBonis, Yasmina Saoudi, Luc Lebeau, Isabelle Crevel, Robert Cross, Richard H. Wade, David Hackney, and Frank Kozielski. 2006. “S-Trityl-L-Cysteine Is a Reversible, Tight Binding Inhibitor of the Human Kinesin Eg5 That Specifically Blocks Mitotic Progression.” The Journal of Biological Chemistry 281 (26): 17559–69.

Steinberg, G. D., B. S. Carter, T. H. Beaty, B. Childs, and P. C. Walsh. 1990. “Family History and the Risk of Prostate Cancer.” The Prostate 17 (4): 337–47.

Stopa, Nicole, Jocelyn E. Krebs, and David Shechter. 2015. “The PRMT5

Arginine Methyltransferase: Many Roles in Development, Cancer and beyond." Cellular and Molecular Life Sciences: CMLS 72 (11): 2041–59.

Strahl, B. D., and C. D. Allis. 2000. "The Language of Covalent Histone Modifications." Nature 403 (6765): 41–45.

Tarighat, S. S., R. Santhanam, D. Frankhouser, H. S. Radomska, H. Lai, M. Anghelina, H. Wang, et al. 2016. "The Dual Epigenetic Role of PRMT5 in Acute Myeloid Leukemia: Gene Activation and Repression via Histone Arginine Methylation." Leukemia 30 (4): 789–99.

Tee, Wee-Wei, Mercedes Pardo, Thorold W. Theunissen, Lu Yu, Jyoti S. Choudhary, Petra Hajkova, and M. Azim Surani. 2010. "Prmt5 Is Essential for Early Mouse Development and Acts in the Cytoplasm to Maintain ES Cell Pluripotency." Genes & Development 24 (24): 2772–77.

Toba, K., K. Kishi, T. Koike, E. F. Winton, H. Takahashi, K. Nagai, S. Maruyama, et al. 1996. "Profile of Cell Cycle in Hematopoietic Malignancy by DNA/RNA Quantitation Using 7AAD/PY." Experimental Hematology 24 (8): 894–901.

Wang, Jing-Quan, Zhuo-Xun Wu, Yuqi Yang, Qiu-Xu Teng, Yi-Dong Li, Zi-Ning Lei, Khushboo A. Jani, Neeraj Kaushal, and Zhe-Sheng Chen. 2021. "ATP-Binding Cassette (ABC) Transporters in Cancer: A Review of Recent Updates." Journal of Evidence-Based Medicine 14 (3): 232–56.

Wang, Xiudi, Peipei Li, Chenying Wang, Dagui Zhang, Linghui Zeng, Xiyong Liu, and Jiajin Lin. 2020. "DEAD-Box RNA Helicase 39 Promotes Invasiveness and Chemoresistance of ER-Positive Breast Cancer." Journal of Cancer 11 (7): 1846–58.

Wu, Licun, Diana C. Birle, and Ian F. Tannock. 2005. "Effects of the Mammalian Target of Rapamycin Inhibitor CCI-779 Used Alone or with Chemotherapy on Human Prostate Cancer Cells and Xenografts." Cancer Research 65 (7): 2825–31.

Yagoda, A., and D. Petrylak. 1993. "Cytotoxic Chemotherapy for Advanced Hormone-Resistant Prostate Cancer." Cancer 71 (3 Suppl): 1098–1109.

Yang, Yanzhong, and Mark T. Bedford. 2013. "Protein Arginine Methyltransferases and Cancer." Nature Reviews. Cancer 13 (1): 37–50.

Yip, Hon Yan Kelvin, and Antonella Papa. 2021. "Signaling Pathways in Cancer: Therapeutic Targets, Combinatorial Treatments, and New Developments." Cells 10 (3). https://doi.org/10.3390/cells10030659.

Yuen, Hiu-Fung, Ka-Kui Chan, Claire Grills, James T. Murray, Angela Platt-

Higgins, Osama Sharaf Eldin, Ken O'Byrne, et al. 2012. "Ran Is a Potential Therapeutic Target for Cancer Cells with Molecular Changes Associated with Activation of the PI3K/Akt/mTORC1 and Ras/MEK/ERK Pathways." Clinical Cancer Research: An Official Journal of the American Association for Cancer Research 18 (2): 380–91.

Zeegers, Maurice P. A., Annemarie Jellema, and Harry Ostrer. 2003. "Empiric Risk of Prostate Carcinoma for Relatives of Patients with Prostate Carcinoma: A Meta-Analysis." Cancer 97 (8): 1894–1903.

Zelivianski, Stanislav, Matthew Spellman, Mark Kellerman, Vladimir Kakitelashvilli, Xia-Wei Zhou, Esmeralda Lugo, Ming-Shyue Lee, et al. 2003. "ERK Inhibitor PD98059 Enhances Docetaxel-Induced Apoptosis of Androgen-Independent Human Prostate Cancer Cells." International Journal of Cancer. Journal International Du Cancer 107 (3): 478–85.

Zheng, Guopei, Fang Peng, Renkui Ding, Yanhui Yu, Yongmei Ouyang, Zhuchu Chen, Zhiqiang Xiao, and Zhimin He. 2010. "Identification of Proteins Responsible for the Multiple Drug Resistance in 5-Fluorouracil-Induced Breast Cancer Cell Using Proteomics Analysis." Journal of Cancer Research and Clinical Oncology 136 (10): 1477–88.

Zhu, Yiming, Chiyuan Piao, Zhe Zhang, Yuanjun Jiang, and Chuize Kong. 2022. "The Potential Role of c-MYC and Polyamine Metabolism in Multiple Drug Resistance in Bladder Cancer Investigated by Metabonomics." Genomics 114 (1): 125–37.

Zurita-Lopez, Cecilia I., Troy Sandberg, Ryan Kelly, and Steven G. Clarke. 2012. "Human Protein Arginine Methyltransferase 7 (PRMT7) Is a Type III Enzyme Forming ω-NG-Monomethylated Arginine Residues." The Journal of Biological Chemistry 287 (11): 7859–70.